

University of Southern Indiana
Pott College of Science, Engineering, and Education
Engineering Department
8600 University Boulevard
Evansville, Indiana 47712

Design and Simulation of a Heat Exchanger for a Mechanical Coffee Dryer

ENGR491 Senior Design

Joshua Botello and Russell Denton

Fall 2023

Approved by: _____

Faculty Advisor: Milad Rad, Ph.D.

Date

Approved by: _____

Department Chair: Paul Kuban, Ph.D.

Date

Acknowledgments

This project would not have been possible without the knowledge and resources from the University of Southern Indiana. A special thank you is given to Dr. Glen Kissel for his time teaching the group how to research, synthesize, and present technical/professional/engineering topics in ENGR471. We thank Mrs. Jamie Curry, who organized many events and purchase orders and kept the project on schedule. We acknowledge advisors Dr. Brandon Field and Dr. Milad Rad for their time and commitment to the project. Finally, we want to thank our family and friends who support us.

Abstract

The drying of coffee is a critical aspect of the post-harvest process and plays a crucial role in achieving high-quality coffee. The drying process requires significant energy to remove moisture from the harvested beans, emphasizing the importance of using efficient equipment and sustainable sources. The capstone project focuses on designing a heat exchanger for a mechanical coffee drying system that uses biomass combustion. This report briefly covers coffee processing, heat exchangers, and computational fluid dynamics. The project compared various heat exchangers and deemed that a shell and tube heat exchanger could meet the requirements of drying 1000 kg of coffee. The project deliverables include a validation study for SolidWorks Flow Simulation 2023, a 3D model of the heat exchanger, and heat and flow simulations. Due to time constraints, there was no constructed physical prototype. Kern's method was used to produce a thermal-hydraulic design for the first iteration of the shell and tube heat exchanger, and SolidWorks was used to adjust key geometric parameters until the drying goals were met. A validation study of conjugate heat transfer involving laminar and turbulent, incompressible flow in SolidWorks Flow Simulation 2023 was conducted with a max deviation of 3.8% from analytical results. The final heat exchanger design consisted of 19 (44 mm x 50 mm) tubes of 321 stainless steel alloy, one baffle cut 75%, and the tube bundle was 3.25 meters long with a 325.7 mm inner shell diameter. The weight of the tube bundle was 232 kg. The simulated air outlet temperature value reached 51.5°C, producing a pressure drop of 2890 Pascals. The power requirement to overcome pressure drop was calculated to be 4.9 kW, and the effectiveness of the simulated heat exchanger was 72.9%. A mesh convergence study was conducted to confirm the robustness of the simulation at 1.4 million cells.

Table of Contents

1.0 Introduction	1
1.1 Objective	2
1.2 Deliverables	2
1.3 References	3
2.0 Background	3
2.1 Coffee Production & Processing	3
2.1.1. Coffee Drying Processes	8
2.1.2 References	12
2.3 Heat Exchangers	13
2.3.1 References	22
2.4 Project Motivation	23
2.4.1 References	24
2.5 Literature Review of Previous Design Projects	25
2.5.1 References	28
2.6 Computational Fluid Dynamics	28
2.6.1 References	35
3.0 Project Requirements	35
3.1 Concept Selection	36
3.2 Factors that Impact Design Choices	36
3.3 Chosen Design	37
3.4 Professional Standards	38
3.4.1 References	38
4.0 Methodology	40
4.1 Thermal-Hydraulic Design of Shell and Tube Heat Exchangers	40
4.2 Design Methodology Phase 2: Modeling and Simulation	57
4.3 References	60
5.0 Validation of SolidWorks Flow Simulation 2023 for Conjugate Heat Transfer	61
5.1 References	73
6.0 Results	73
7.0 Conclusion	82
APPENDIX	85

A: System Hierarchy 85

B: Concept of Operations..... 86

C: ABET Outcome 2, Design Factor Considerations 87

D: Project Schedule..... 88

E: Table of Requirements 89

F: Table of Failure Modes and Effect Analysis 90

G: Kern’s Method Flow Chart 91

H: Material Properties: Alloy 321..... 92

I: MATLAB Code for First Successful Kern’s Method Iteration. 92

J: MATLAB Code for Validation Study (e-NTU Method) 95

K: SolidWorks Flow Simulation Setup for the Validation Study 97

L: SolidWorks Flow Simulation Setup for the Final Design 100

Table of Figures

Figure 1. Mechanical Coffee Drying System [3].....	1
Figure 2. A Cross-Sectional Rendering of the Final Iteration of the Senior Design Project.	3
Figure 3. A Simplified Flowchart of Coffee from Bean to Cup.	4
Figure 4. Coffee harvesting [2].....	4
Figure 5. Coffee beans layers removed in depulping, and Machinery used for depulping [3][4]. .	5
Figure 6. Coffee Processing sink tanks for fermentation [5].....	5
Figure 7. Solar Coffee Drying [6].....	6
Figure 8. Coffee beans before and after milling and Machinery for coffee beans sorting [7] [8]. .	7
Figure 9. Coffee Roasting [9]	7
Figure 10. Coffee before and after grinding process. [10].....	8
Figure 11. Solar coffee drying [6].....	9
Figure 12. Static mechanical coffee dryer parts diagram [11].....	10
Figure 13. JM Strada Static mechanical coffee dyer for 9000kg of coffee [12].....	10
Figure 14. Ecoflama Rotating bed mechanical coffee dyer [13]	11
Figure 15. Heat Exchanger working principle diagram and temperature difference diagram [3]	14
Figure 16. Shell and tube heat exchanger internal diagram [5]	16
Figure 17. Plate heat exchangers expanded diagram [6]	17
Figure 18. Air-Cooled heat exchanger with fan [7].....	17
Figure 19. Finned tube heat exchanger [8]	18
Figure 20. Double Pipe Heat Exchanger diagram [9].....	18
Figure 21. Plate-fin heat exchanger parts (expanded view) [10]	19
Figure 22. Regenerative heat exchanger diagram [11]	19
Figure 23. Spiral heat exchanger diagram and real view [12]	20
Figure 24. Heat exchanger types of flow configurations [13]	21
Figure 25. The make-up of a computational domain with a coarse mesh.	32
Figure 26. A computational domain with a fine mesh.....	32
Figure 27. Grid refinement in SolidWorks Flow Simulation 2023.	33
Figure 28. Boundary Conditions.....	34
Figure 29. Common TEMA designations for shell constructions [1]	39
Figure 30. Temperature Profiles of a counter-flow heat exchanger [3].....	44
Figure 31. Correlations to determine shell clearance (Kern's Method) [2].....	48
Figure 32. Area to determine the equivalent diameter of a square and triangular pitch tube bank [2].....	52
Figure 33. Kern's empirical correlation to determine the heat transfer factor [2].	54
Figure 34. Kern's empirical correlation to determine the friction factor [2].....	56
Figure 35. A simplified flow chart outlining the modeling and simulation design phase.	58
Figure 36. Rendering of the heat exchanger produced the first successful Kern's Method Iteration.....	58
Figure 37. Defined global variables of the heat exchanger in SolidWorks.	59
Figure 38. Diagram of a parallel-flow concentric tube heat exchanger.....	61
Figure 39. NTU correlation for a parallel flow concentric tube heat exchanger [3].	64

Figure 40. Solidworks Model of the concentric tube HXR for the validation study.	71
Figure 41. The results of the SolidWorks Flow Simulation 2023 Study.	72
Figure 42. Simulation Results of the first successful Kern's Method iteration.	74
Figure 43. Flow path of the drying air through the heat exchanger.	75
Figure 44. Addition of tubes to fill out the bundle.	75
Figure 45. Drying Air Outlet Temperature vs Geometry Changes.	76
Figure 46. Shell-side Pressure Drop vs. Geometry Changes.	77
Figure 47. Investigation of Misleading Simulation Results.	78
Figure 48. Final simulation iteration.	79
Figure 49. Drying Air Flow Within the Final Design Simulation.	79
Figure 50. Plot of Mesh Convergence of Final Design.	80
Figure 51. System Hierarchy.	85
Figure 522. Concept of Operations.	86
Figure 533. Kern's Method Flow Chart from Coulson's Chemical Engineering v6.	91

Table of Tables

Table 1. Known parameters and fluid properties involved in the coffee drying project.	42
Table 2. Overall Heat Transfer Coefficients of various applications [4].	45
Table 3. Parameters of tubes during the first Kern's Method.	46
Table 4. Empirical coefficients to determine the tube bundle diameter [2].	47
Table 5. Properties of the tube-side combustion gas.	50
Table 6. Fouling factor coefficients [2].	55
Table 7. Expressions for the effectiveness of various types of heat exchangers [2].	63
Table 8. Parameters used for the validation study.	65
Table 9. Kay and Perkins Nusselt Correlations for shell-side flow in a concentric tube HXR. ...	68
Table 10. Mesh Convergence of Final Design.	80
Table 11 Appendix C Design Factors Considered.	87
Table 12. Design Project Schedule.	88
Table 13. Table of Project Requirements.	89
Table 14. Failure Modes and Effect Analysis.	90

1.0 Introduction

Green coffee beans are typically harvested with a high moisture content; drying them is important before they can be roasted and processed for consumption. Mechanical drying is a widely used method to remove moisture from green coffee beans, which involves using hot air to evaporate water from the beans [1]. To ensure that the process is efficient and sustainable, it is crucial to consider the thermal efficiency of the drying system.

Thermal efficiency is the ratio of the energy input to the energy output of a system. In the case of mechanical drying of green coffee beans, high thermal efficiency means that the drying process can be completed with the minimum amount of energy required [2]. This is not only essential to reduce the cost of the process but also to minimize the environmental impact of the drying system. By optimizing thermal efficiency, it is possible to reduce greenhouse gas emissions that can result from the use of fossil fuels to power the drying process.

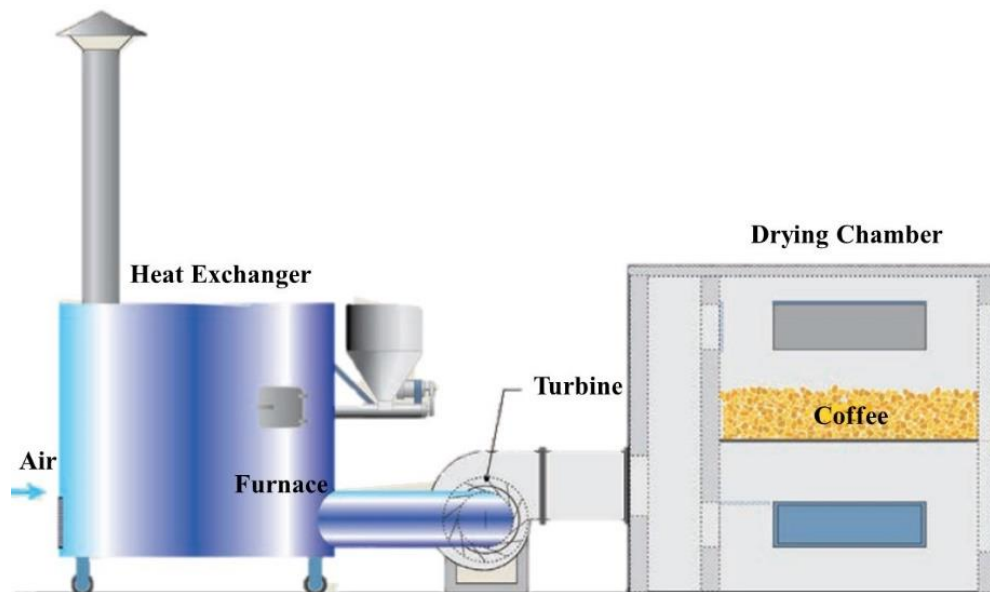


Figure 1. Mechanical Coffee Drying System [3]

This report examines various methods to enhance the thermal efficiency of heat exchangers utilized in mechanical coffee drying systems. It also includes the used approach to improve the heat exchanger and the impact that these changes had on the designed the system. The report includes a final engineering design and a computational fluid dynamics analysis of the proposed design, as well as a validation of the computational fluid design software compared to analytical

calculations. Furthermore, the report presents the results of the final design and the benefits and future improvements to the system.

Overall, this report aims to address the importance of thermal efficiency in mechanical coffee drying systems and present a feasible solution that can optimize the process's energy usage while reducing its environmental impact.

1.1 Objective

The objective of the senior design project was to:

Design and simulate a heat exchanger for a mechanical coffee drying system to demonstrate the importance of integrating simulation tools with thermal-mechanical engineering principles to understand industrial processes.

1.2 Deliverables

The deliverables for the final project will include:

- A 3D model of the heat exchanger, including material specification.
- A validation study to ascertain the feasibility and accuracy of SolidWorks Flow Simulation as an analysis tool.
- Thermal-hydraulic design of a shell and tube exchanger using Kern's Method.
- Heat and flow simulations using SolidWorks Flow Simulation 2023.
- Complete engineering calculations relating to the energy efficiency of the heat exchanger system design.

Due to the complexity and time constraints of the project, there will not be a fabricated model of the design.

This report briefly covers coffee processing, heat exchangers, and computational fluid dynamics, a comparison of conceptual designs, and an engineering analysis of the final design iteration of the heat exchanger, as shown below in Figure 2.



Figure 2. A Cross-Sectional Rendering of the Final Iteration of the Senior Design Project.

1.3 References

- [1] Isquierdo, E.P., et al. "Drying Kinetics and Quality of Natural Coffee." American Society of Agricultural and Biological Engineers, Sept. 2013. Research Gate, <http://dx.doi.org/10.13031/trans.56.9794>. Accessed 29 Jan. 2023.
- [2] Robinson, Osorio, et al. "Simulation of the Internal Environment of a Post-harvest Installation and a Solar Dryer of Coffee." Revista Brasileira de Engenharia Agrícola e Ambiental, 2016. EBSCO, discovery.ebsco.com/c/yhnfgy/viewer/pdf/fhow2m5pq5.
- [3] Parra Coronado, Alfonso, et al. Optimización Operacional de Secadores Mecánicos para Café Pergamino. Federación Nacional de Cafeteros de Colombia- Centro Nacional de Investigaciones de Café, 2017.

2.0 Background

2.1 Coffee Production & Processing

Coffee, one of the world's most consumed beverages, undergoes a process from the coffee cherry on the tree to the cup of coffee served on tables across the globe. Understanding the entire coffee production process is fundamental in appreciating the significance of efficient post-harvest steps like coffee drying, which is the focal point of our senior design project. The entirety

of the process is shown below in Figure 3; note the difference between drying and roasting and are discussed subsequently.

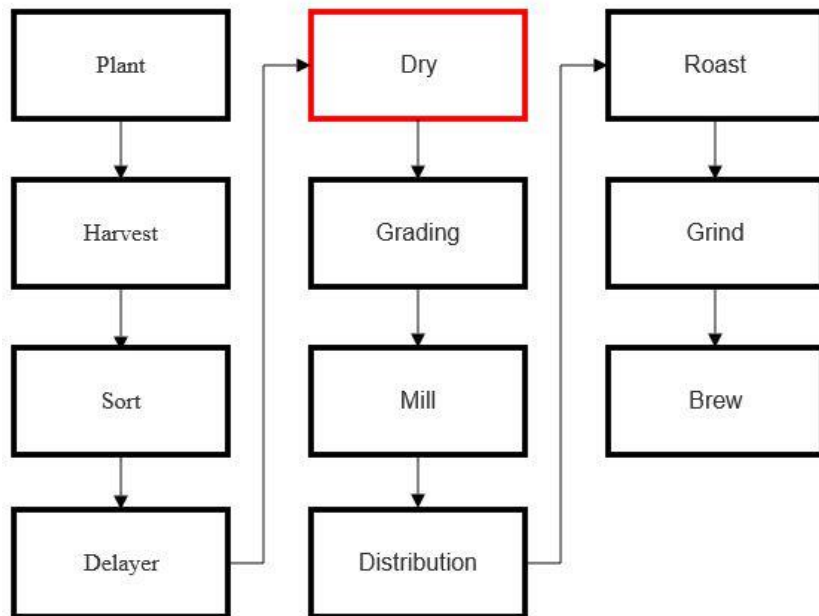


Figure 3. A Simplified Flowchart of Coffee from Bean to Cup.

Harvesting

Coffee production commences with harvesting, where skilled laborers carefully handpick ripe coffee cherries. This labor-intensive process is crucial for selecting only the cherries at their peak ripeness, ensuring the best flavor and quality of the coffee beans. Such selection contributes to the coffee's premium quality and character [1]. Figure 4 shows coffee beans being harvested from the tree as they are ready to be processed.



Figure 4. Coffee harvesting [2]

De-pulping and Fermentation

The harvested cherries undergo de-pulping, where the outer skin is removed to reveal the coffee beans [1], which can be observed in Figure 5. This is a critical step, as improper de-pulping can lead to defects in the coffee beans. This process is carried out by using a special stainless still mill that is shown below in figure 5.



Figure 5. Coffee beans layers removed in depulping, and Machinery used for depulping [3][4].

After de-pulping, the beans undergo a fermentation process, a crucial phase that influences the beans' flavor profile. The duration of fermentation is finely tuned, as prolonged fermentation can impart undesirable flavors while insufficient fermentation may not remove the mucilage completely [1] This process is performed by dumping coffee grains on water tanks and letting the beans sit in the tank for a period, this is observed in Figure 6.



Figure 6. Coffee Processing sink tanks for fermentation [5]

Drying

Once the beans have been de-pulped and fermented, they contain a high moisture content. Drying the beans is the next step, and it's pivotal in coffee production. The goal of this stage of the process involves reducing the coffee moisture content from 50% to 10%. This is where our senior design project plays a significant role. Traditional methods involve sun-drying (shown in Figure 7), but mechanical drying is increasingly favored due to its efficiency. Mechanical dryers, such as the one we are focusing on, employ hot air to evaporate the water content in the beans, contributing to a more consistent and efficient drying process [1].



Figure 7. Solar Coffee Drying [6]

Milling and Sorting

After drying, the coffee beans are hulled to remove any remaining layers. This is obtained by milling the dried coffee beans removing the yellow layer known as coffee husk which is later used as combustion fuel as a subproduct of the process. Next, coffee beans are then sorted to ensure that only beans of uniform size and quality proceed. This process is performed in a vibrating mesh sorter that uses an average grain weight to sort them according to its size. This step enhances the beans' market value and ensures uniformity in the roasting process [1]. The process and difference between the beans before and after milling are shown below in Figure 8.



Figure 8. Coffee beans before and after milling and Machinery for coffee beans sorting [7] [8].

Roasting

One of the last steps of this process is roasting. Coffee roasting is an art in itself. Beans are exposed to varying temperatures and durations to achieve the desired flavor profile, color, and aroma. The precise roasting process significantly influences the final coffee's taste, from light roasts with bright acidity to dark roasts with deep flavors and aromas. The degree of roasting is critical to the coffee's sensory qualities [1]. Figure 9 pictures coffee beans after being roasted in a semi-industrial piece of machinery.



Figure 9. Coffee Roasting [9]

Grinding and Brewing

Upon roasting, the coffee beans are ground into the desired particle size for brewing. The method of brewing, whether through espresso, drip, or other techniques, further contributes to the final coffee's unique characteristics. Variables such as water temperature, brewing time, and bean-to-water ratio are meticulously controlled by baristas and coffee enthusiasts to craft the perfect cup of coffee [1]. Figure 10 displays a comparison between coffee beans and grounded coffee.



Figure 10. Coffee before and after grinding process. [10]

2.1.1. Coffee Drying Processes

Coffee drying is an important step in the post-harvest phase that influences the coffee beans' quality and overall production efficiency. Drying methods can be categorized into two primary approaches: solar coffee drying and mechanical coffee drying, each with its own sub-methods and techniques.

Solar Coffee Drying

Solar coffee drying, also known as sun drying, is one of the oldest and most traditional methods of drying coffee beans. In this approach, freshly harvested coffee cherries are spread out in thin layers under the sun on large patios or raised beds (shown in Figure 11). Solar drying relies on the natural heat and airflow provided by the sun to evaporate the moisture content in the beans. This method is favored for its simplicity and low cost. However, it is highly weather-dependent, with drying times varying based on sunlight and climate conditions. Extended

exposure to the elements can lead to over-drying or uneven drying, affecting the final coffee quality [1].



Figure 11. Solar coffee drying [6]

Mechanical Coffee Drying

Mechanical coffee drying methods have gained prominence due to their efficiency and consistency in achieving optimal moisture levels in coffee beans. These techniques use mechanical devices and hot air to expedite the drying process, reducing dependency on weather conditions.

Static Bed

Static bed drying is a mechanical method where coffee beans are placed on a stationary bed. Hot air is circulated through the bed to facilitate the drying process. This method allows for better control of drying conditions, including temperature and humidity. Static bed drying minimizes the risk of over-drying and under-drying, ensuring consistent bean quality. It's widely used in commercial coffee processing facilities and is ideal for high-volume drying requirements. Careful monitoring and control of airflow and temperature are necessary to achieve optimal results [1]. A schematic diagram of a static bed mechanical coffee dryer is shown in Figure 12; this diagram shows a detailed list of the system's components.

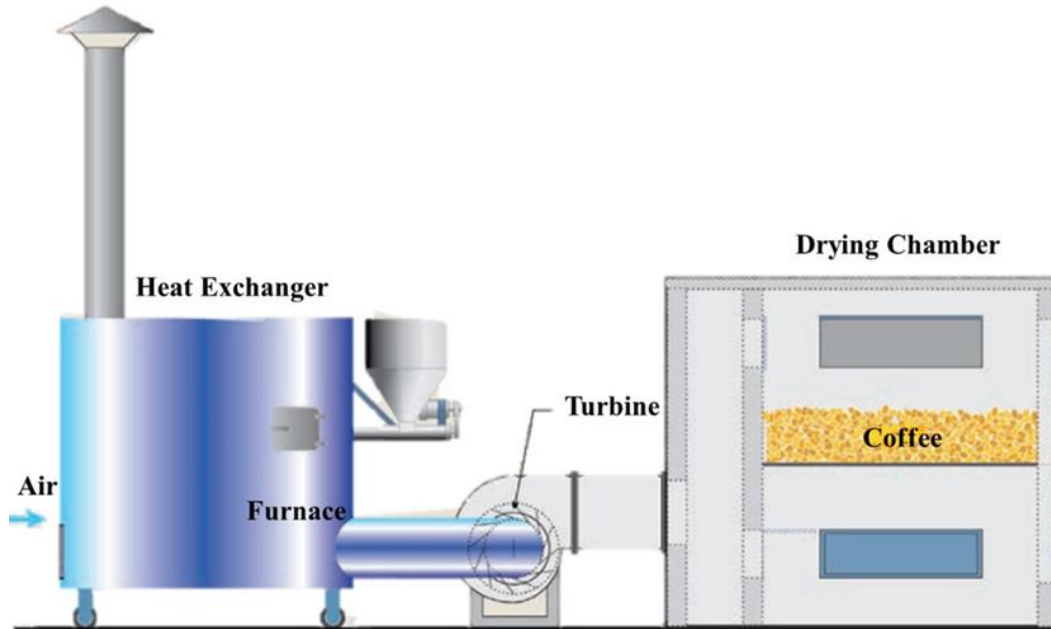


Figure 12. Static mechanical coffee dryer parts diagram [11]

However, static bed mechanical coffee dryers come in different shapes and structures. These can vary from small sizes for semi-industrial plants to large-scale systems for industrial plants.

Figure 13 shows a static bed mechanical coffee dryer produced by the manufacturer JM Strada, a commercially recognized company for producing coffee processing machines.



Figure 13. JM Strada Static mechanical coffee dryer for 9000kg of coffee [12]

Rotating Bed

Rotating bed drying is another mechanical approach that involves a rotating drum or bed where coffee beans are placed. The drum or bed rotates, ensuring an even distribution of hot air around the beans. This method is efficient, with a shorter drying time compared to static bed drying. The rotating action prevents beans from sticking together and promotes uniform drying. However, the initial cost of the equipment may be higher, making it more suitable for larger coffee processing operations. Effective heat and airflow control is critical for achieving consistent results with rotating bed drying [1]. Figure 14 shows a small rotating bed mechanical coffee dryer used in a semi-industrial plant developed by EcoFlama, a commercial manufacturer of this machinery.



Figure 14. Ecoflama Rotating bed mechanical coffee dryer [13]

Other Mechanical Coffee Drying Techniques

Apart from static and rotating bed drying, various other mechanical drying techniques have been developed to cater to specific requirements and capacities. These methods may include fluidized bed drying, column drying, and more. Each approach offers unique advantages and is chosen based on factors such as production volume, resource availability, and environmental considerations.

In summary, it is essential to select the drying method that aligns with the specific coffee production context, aiming to optimize efficiency and coffee quality. Our project focuses on optimizing a mechanical device used in a mechanical coffee drying system. By modifying this piece of equipment that works together with the system to dry coffee, an improvement in the efficiency of the system can be obtained.

2.1.2 References

- [1] Sivetz, Michael, M.S., and H. Elliot Foote, Ph.D. Coffee Processing Technology. Vol. 1, Westport, Connecticut, Avi Publishing Company, 1963. HathiTrust, babel.hathitrust.org/cgi/pt?id=mdp.39015002932617&view=1up&seq=8.
- [2] Recolectar Café. Mundo Cafeto, 8 June 2018, mundocafeto.com/beneficiado/recoleccion-de-cafe-cereza/.
- [3] Las Semillas De Café Una Vez Se Han Despulpado. Inneflable, 27 Jan. 2023, ineffablecoffee.com/cafe-proceso-lavado/.
- [4] Despulpado del Café Cereza. Mundo Cafeto, 19 May 2019, mundocafeto.com/beneficiado/despulpado-del-cafe-cereza/.
- [5] La fermentación del café. Cafe Moreno, cafesmoreno.com/la-fermentacion-del-cafe/.
- [6] Coffee Drying Guide. Zelalem Organic Coffee, Mar. 2022, zelalemcoffee.com/wp-content/uploads/2022/03/Coffee-Drying-Guide-Cover.jpg.
- [7] Ka'u Washed Green Bean. Kau Coffee Mill, kaucoffeemill.com/product/kau-washed-green-bean/.
- [8] "Machines Sorting size raw coffee beans." iStock Photo, uploaded by Lavoview, 20 Mar. 2017, www.istockphoto.com/video/machines-sorting-size-raw-coffee-beans-gm652590806-119371409.
- [9] Coffee Roasting. MTPAK Coffee, 9 Feb. 2021, mtpak.coffee/2021/02/coffee-roasting-basics-guide-to-first-second-crack/.
- [10] Coffee grinding. Kaffee Products, 23 Mar. 2023, kaffeproducts.com/blogs/blog/how-to-choose-the-best-coffee-grinder-for-your-brewing-method.

[11] Parra Coronado, Alfonso, et al. Optimización Operacional de Secadores Mecánicos para Café Pergamino. Federación Nacional de Cafeteros de Colombia- Centro Nacional de Investigaciones de Café, 2017.

[12] Secadora automática 720@. JM Strada, www.jmestrada.com/tienda/cafe/secadoras-automaticas/secadora-automatica-720/.

[13] Rotary Mechanical Coffee Dryer. Fatello Coffee, www.fratellocoffee.com/blogs/blog/coffee-drying-speeds.

2.3 Heat Exchangers

To dry coffee, a source of heat is needed as a main part of the process. In mechanical coffee drying, heat is produced in a combustion chamber by combusting some type of fuel. However, the gases produced by this process are not used to dry the coffee beans. Clean air needs to be heated using flue gases to extract humidity out of the coffee beans [1]. This heat exchange process is achieved by using a heat exchanger attached to the system.

Heat exchangers are fundamental components in a wide array of applications, serving as pivotal elements for efficient heat transfer and temperature regulation [2]. These devices are integral to diverse industries, enabling the exchange of thermal energy between two or more fluids, gases, or solids. The following section delves into the multifaceted world of heat exchangers, their working principle, their applications, types, efficiency, and more.

Working Principle of Heat Exchangers

The working principle of heat exchangers is rooted in the fundamental laws of thermodynamics, specifically the principles governing heat transfer. Heat exchangers facilitate the exchange of thermal energy between two fluids, typically at different temperatures, without the fluids coming into direct contact [2]. The process begins with one fluid, termed the hot fluid, transferring its thermal energy to the surface of the heat exchanger. Simultaneously, a second fluid, known as the cold fluid, passes over a separate surface within the exchanger. The thermal energy absorbed by the cold fluid raises its temperature [2]. This mechanism ensures efficient heat transfer without the actual mixing of the two fluids. In our design for the mechanical coffee

drying system, the heat exchanger utilizes this principle to harness thermal energy from the combustion of coffee husk, efficiently heating the air responsible for drying the coffee beans. Figure 15 shows a diagram of a common tube, a shell heat exchanger with parallel flow. The graph attached represents the temperature behavior of the fluids as they enter the system and move inside, transferring heat and exiting the system at a different temperature and with a smaller differential from the initial difference.

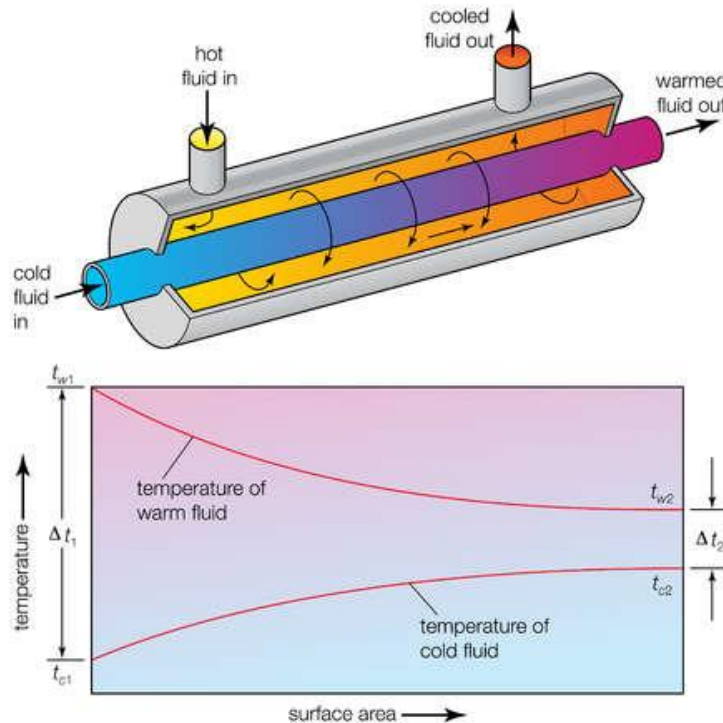


Figure 15. Heat Exchanger working principle diagram and temperature difference diagram [3]

Historical Significance

The narrative of heat exchangers unfolded over nearly 150 years, with its inception marked by the pioneering work of innovative engineers worldwide [4]. Although the concept of heat exchange machines emerged as early as the late 1800s, it was in the early 1900s that modern designs, including the ubiquitous shell and tube configuration, began to take shape.

The journey commenced in 1878 when Albrecht Dracke of Germany secured the first recorded patent for a plate heat exchanger [4]. However, the commercial applications of heat exchangers gained momentum in the early 20th century, witnessing significant developments in plate heat exchangers, particularly in pasteurizing milk. Simultaneously, the shell and tube

configuration, a hallmark in heat exchanger design, emerged in the 1920s, finding initial applications in the oil industry, including oil heaters, coolers, reboilers, and condensers.

The 1930s marked the advent of the spiral plate heat exchanger in Sweden, while the UK embraced the brazing method for crafting plate-fin heat exchangers from copper and copper alloy materials, notably in aircraft engines [4]. As the years progressed, air-cooled condensers gained traction in the 1930s, with Otto Happel and Dr. Kurt Lang contributing to their development of stationary steam turbines.

The 1940s witnessed substantial advancements in shell and tube heat exchangers, particularly in understanding shell-side pressure drop. Notably, in 1955, Babcock and Wilcox Co. filed a patent, granted in 1965 and expiring in 1982, contributing to the refinement of shell and tube heat exchanger designs [4].

While the landscape of heat exchangers continues to evolve, the fundamental forms and principles that underpin many contemporary designs were solidified between 1920 and 1950. The historical journey of heat exchangers underscores their pivotal role in diverse industries, from oil and gas to energy generation, chemical processes, defense, transport, and food and beverage. The continuous innovation and refinement of heat exchangers mirror the dynamic needs of industrial processes and technological advancements [4].

Applications of Heat Exchangers

Heat exchangers find their applications across various sectors, contributing to enhanced thermal performance, energy efficiency, and overall system functionality. These applications include, but are not limited to:

- **HVAC Systems:** Industrial heat exchangers are a cornerstone of heating, ventilation, and air conditioning (HVAC) systems. They facilitate the transfer of heat between indoor and outdoor air, helping maintain comfortable indoor temperatures while conserving energy.
- **Power Generation:** In power plants, heat exchangers play a crucial role in converting thermal energy into electrical power. They are used in steam generators, condensers, and cooling systems to manage temperature differentials efficiently.

- **Chemical Processing:** Industrial heat exchangers are extensively used in chemical processing for tasks such as distillation, evaporation, and chemical reactions. They contribute to precise temperature control and reaction efficiency.
- **Refrigeration:** Refrigeration systems rely on heat exchangers to absorb heat from the refrigerant, ensuring the controlled cooling of spaces and preservation of perishable goods.

Types of heat exchangers

Heat exchangers encompass a diverse range of types, each tailored to specific needs and applications. The primary types include:

- **Shell and Tube Heat Exchangers:** Shell and tube heat exchangers consist of a large cylindrical shell with multiple tubes inside (shown in Figure 16 below). One fluid flows through the tubes, and another fluid circulates around the tubes within the shell. Heat is transferred from one fluid to the other through the tube walls. This design allows for efficient heat transfer due to a large surface area. The shell and tube configuration are versatile and used in applications such as power plants, refineries, and HVAC systems, offering high thermal efficiency and ease of maintenance.

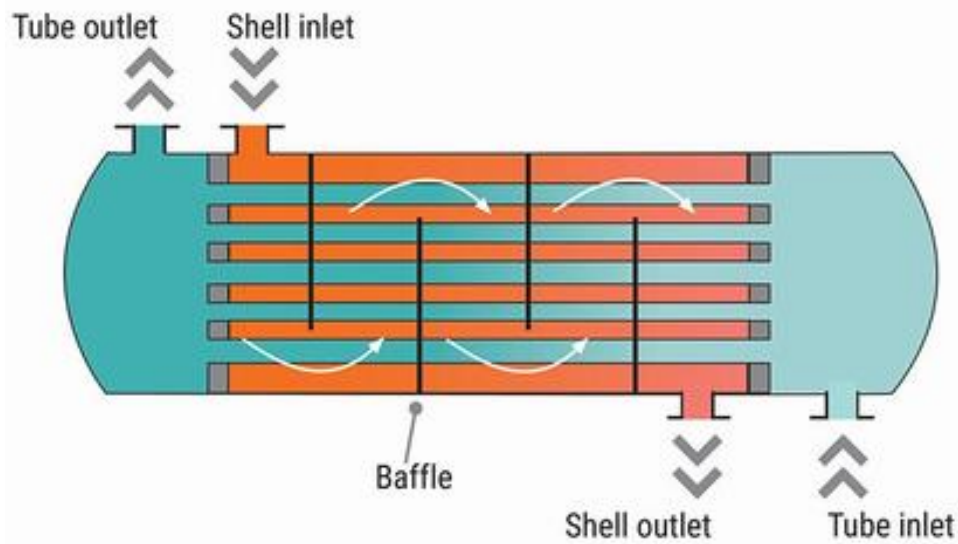


Figure 16. Shell and tube heat exchanger internal diagram [5]

- **Plate Heat Exchangers:** Plate heat exchangers comprise multiple thin plates stacked together, separated by gasket seals. Each fluid alternately flows through the channels formed by the plates, which can be observed in Figure 17 below. Heat is transferred between the fluids through the plates. This design provides a compact and efficient solution, making it ideal for applications with space constraints. The modular design allows for easy expansion, but they may be more prone to fouling.

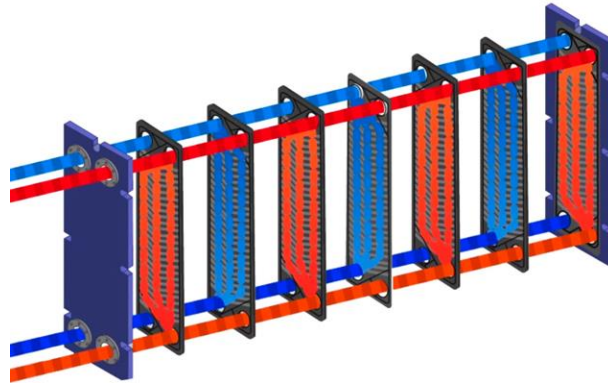


Figure 17. Plate heat exchangers expanded diagram [6]

- **Air-Cooled Heat Exchangers:** Air-cooled heat exchangers use ambient air as the cooling medium. Finned tubes, exposed to the air, dissipate heat effectively. These exchangers are employed where water cooling is impractical, such as in remote locations or industrial sites with water scarcity. Efficiency is influenced by factors like air temperature and flow. A common type of commercially available air-cooled heat exchanger is shown in Figure 18.



Figure 18. Air-Cooled heat exchanger with fan [7]

- Finned Tube Heat Exchangers:** Finned tube heat exchangers feature tubes with extended surfaces (fins). These fins increase the heat transfer surface area, improving efficiency. Commonly used in air heating and cooling systems, they are effective for applications where maximizing surface area is crucial. However, the fins may be susceptible to damage and fouling. Figure 19 shows an example of these heat exchangers.

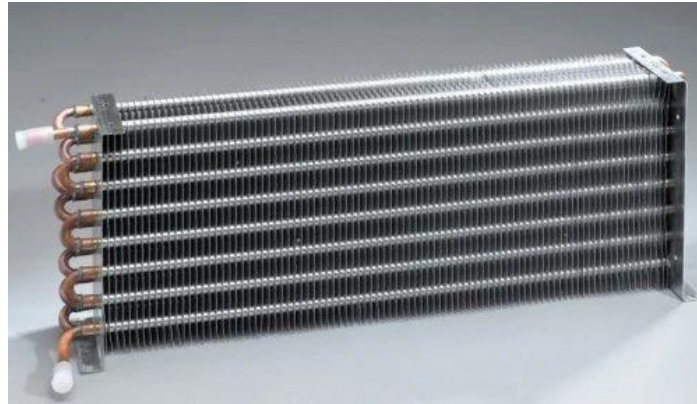


Figure 19. Finned tube heat exchanger [8]

- Double Pipe Heat Exchangers:** Double pipe heat exchangers have a simple design with one pipe inside another. One fluid flow through the inner pipe, while the other flows in the annular space between the pipes. While straightforward and easy to maintain, they may lack the efficiency of more complex designs. They are often used in small-scale applications. Figure 20 shows an example of these heat exchangers.

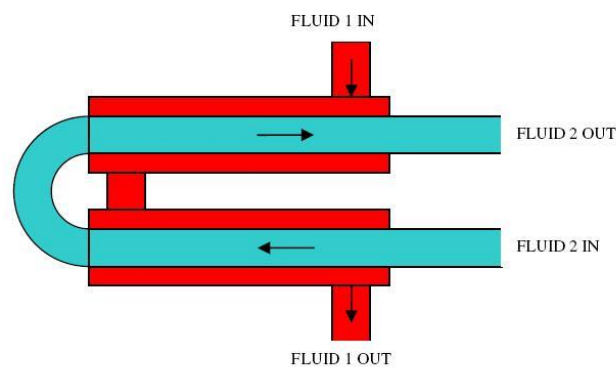


Figure 20. Double Pipe Heat Exchanger diagram [9]

- Plate-Fin Heat Exchangers:** Plate-fin heat exchangers use plates with fins to enhance surface area. Fluids flow alternatively through channels formed by the plates. This design is

compact and finds applications in aircraft and certain industrial processes. Maintenance can be challenging due to the intricate nature of the design. Figure 21 shows an example of these heat exchangers.

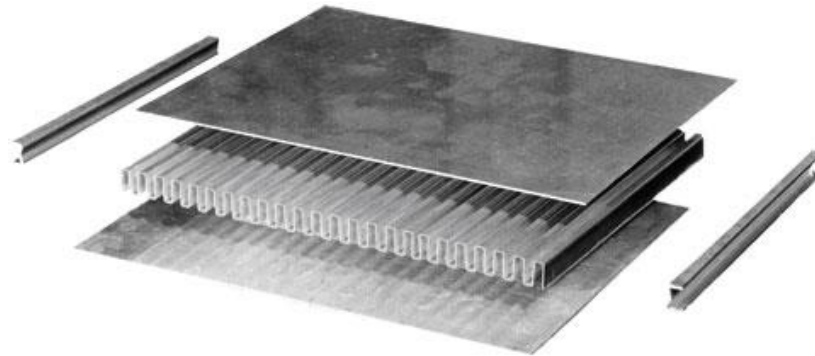


Figure 21. Plate-fin heat exchanger parts (expanded view) [10]

- **Regenerative Heat Exchangers:** Regenerative heat exchangers repeatedly switch between working and regeneration phases. They typically use a matrix (regenerator) to store and release heat. This design maximizes heat recovery, making them suitable for applications where efficiency is crucial. However, the cycling nature and complexity may require sophisticated control systems. Figure 22 shows an example of these heat exchangers.

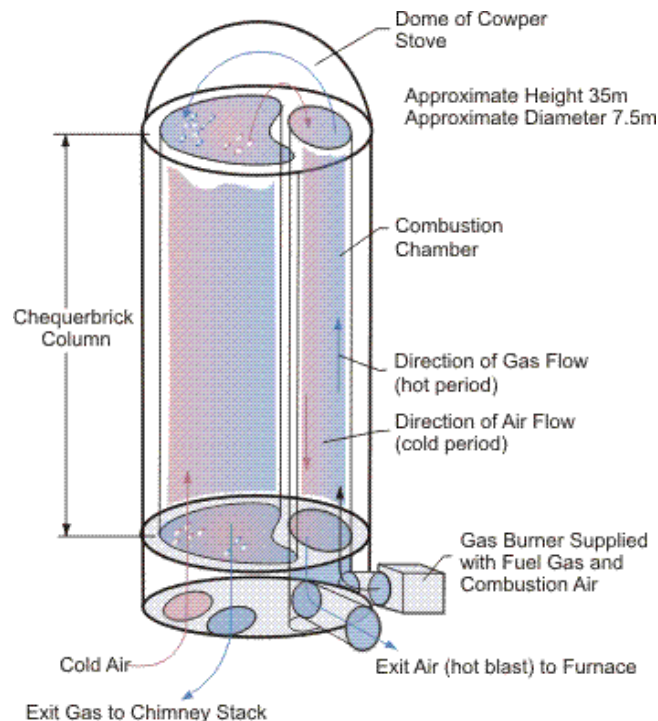


Figure 22. Regenerative heat exchanger diagram [11]

- **Spiral Heat Exchangers:** Spiral heat exchangers consist of two flat plates coiled into a spiral. Fluids follow a spiral path, enhancing heat exchange. This design offers efficient heat transfer and is used in chemical processing and wastewater treatment. The spiral configuration improves heat transfer while maintaining a relatively compact form, though construction can be intricate, affecting maintenance. Figure 23 shows an example of these heat exchangers and a working diagram.

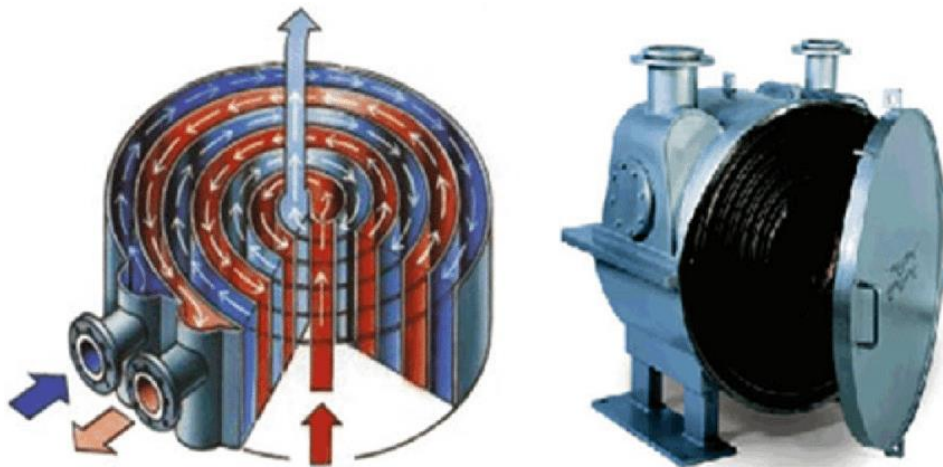


Figure 23. Spiral heat exchanger diagram and real view [12]

The choice of a heat exchanger type depends on factors like the specific application, space considerations, required efficiency, and maintenance considerations. Each type has its advantages and disadvantages, addressing different needs in various industries.

Heat Exchanger Flow Configurations

The flow configuration of the fluids involved significantly influences the efficiency and performance of heat exchangers. Different flow patterns are employed to optimize heat transfer in various applications. Understanding these configurations is essential for selecting the most suitable design for a given set of requirements. The types of flow configurations are the following:

- **Parallel Flow Configuration:** In this design, both hot and cold fluids traverse the heat exchanger in the same direction, entering at one end and exiting at the other. The simplicity of its design makes it a popular choice. However, the parallel flow configuration may exhibit

a limitation known as temperature approach, where the temperature difference between the two fluids at the exit is not maximized, affecting its overall efficiency.

- **Counterflow Configuration:** Distinguished by the movement of hot and cold fluids in opposing directions, the counterflow configuration stands out for its high thermal efficiency. As the fluids move against each other, a maximized temperature difference along the exchanger's length is achieved. Although it offers superior efficiency, its manufacturing can be more intricate than simpler configurations.
- **Crossflow Configuration:** Also referred to as transverse flow, crossflow involves fluids moving perpendicular to each other. Typically found in air coolers and some radiator designs, crossflow configurations offer moderate efficiency. They are preferred in situations where counterflow designs might be impractical due to specific spatial or operational constraints.
- **Multi-pass Flow Configuration:** Multi-pass configurations entail fluids making multiple passes through the heat exchanger before exiting. Achieved by guiding the fluids through distinct channels or passages, multi-pass designs allow for further optimization of temperature differences. While offering enhanced heat transfer, these configurations introduce increased complexity and may lead to additional pressure drop, necessitating careful consideration in design.

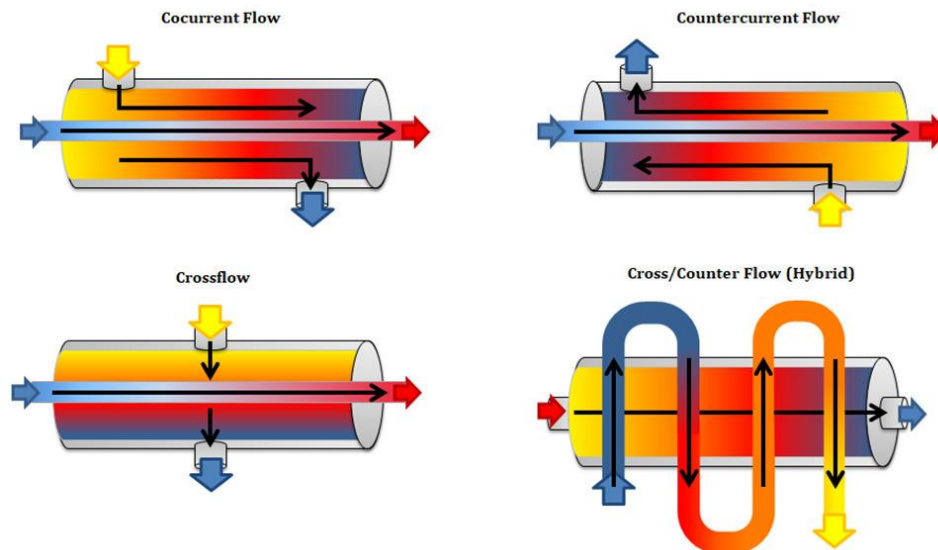


Figure 24. Heat exchanger types of flow configurations [13]

Figure 24 above shows a close comparison of the different possible types of fluid flows that can be implemented in a heat exchanger. In this case, this was represented inside a shell and tube heat exchanger. The color of the flow represents temperature, with red for hot and blue for cold temperatures.

Selecting the most suitable flow configuration depends on the interplay of factors such as temperature requirements, spatial limitations, and the characteristics of the involved fluids []. Each configuration has distinct advantages and drawbacks, and the ultimate choice is up to the unique demands of the intended application.

Fabrication

The fabrication of industrial heat exchangers involves materials selection, design, and manufacturing processes. Common materials include stainless steel, copper, and aluminum, chosen for their thermal conductivity and corrosion resistance. Advanced fabrication techniques, such as welding and brazing, are employed to assemble heat exchanger components, ensuring integrity and longevity.

In summary, heat exchangers are integral components in various applications, offering efficiency and precise temperature control. Their diverse types, efficiency considerations, historical significance, and fabrication methods underscore their importance in modern industrial processes and systems.

2.3.1 References

- [1] Sivetz, Michael, M.S., and H. Elliot Foote, Ph.D. *Coffee Processing Technology*. Vol. 1, Westport, Connecticut, Avi Publishing Company, 1963. HathiTrust, babel.hathitrust.org/cgi/pt?id=mdp.39015002932617&view=1up&seq=8.
- [2] Cengel, Yunus, et al. "Part 3: Heat Transfer." *Fundamentals of Thermal-Fluid Sciences*, 6th ed., McGraw Hill, 2021.
- [3] Britannica, The Editors of Encyclopaedia. "heat exchanger". *Encyclopedia Britannica*, 6 Oct. 2023, <https://www.britannica.com/technology/heat-exchanger>. Accessed 6 December 2023.

- [4] "Who invented the heat exchanger." Sterling Thermal Technology, 8 Nov. 2022, www.sterlingtt.com/2022/11/08/invention-of-heat-exchanger/#:~:text=In%201878%2C%20the%20first%20recorded,made%20for%20plate%20heat%20exchangers.
- [5] Shell and Tube Heat Exchanger. Saint-Gobain, 5 May 2020, www.ceramicsrefractories.saint-gobain.com/news-articles/heat-exchangers-your-questions-answered.
- [6] Plate Heat Exchanger. Savree, savree.com/en/encyclopedia/plate-heat-exchanger-phe.
- [7] Air-Cooled Heat Exchanger. Toba Energy Resources, www.tobaenergy.com/product/thermal-transfer-aoc-24-1-air-cooled-heat-exchanger/.
- [8] Finned Tube Type Heat Exchanger. Volfram, volframsystems.weebly.com/finned-tube-type-heat-exchanger.html.
- [9] Double Pipe Heat Exchanger. EnggCyclopedia, enggyclopedia.com/2023/01/double-pipe-heat-exchanger/.
- [10] Plate fin heat exchanger. Heat Exchanger Design Book, hedhme.com/content_map/?link_id=222&article_id=429.
- [11] Regenerative heat exchanger. Thermopedia, www.thermopedia.com/content/1087/.
- [12] Spiral Heat Exchanger. Research Gate, www.researchgate.net/figure/Diagram-of-spiral-heat-exchanger_fig85_308464561.
- [13] Heat Exchanger Flow Configurations. Thomas, www.thomasnet.com/articles/process-equipment/understanding-heat-exchangers/.

2.4 Project Motivation

Several factors affect the thermal efficiency of a green coffee bean mechanical drying system, including the design of the equipment, the temperature and humidity of the drying air, and the flow rate of the air [1]. The design of the drying equipment must be optimized to ensure that the beans are exposed to the hot air uniformly and that there is minimal heat loss to the surrounding environment. Additionally, the temperature and humidity of the drying air must be carefully controlled to prevent over-drying or under-drying of the beans, which can affect their

quality. Finally, the flow rate of the air must be optimized to ensure that it can remove moisture from the beans efficiently without wasting energy. Overall, by optimizing the thermal efficiency of a green coffee bean mechanical drying system, it is possible to improve the quality of the dried beans, reduce the cost of the process, and minimize its environmental impact [1]. This can be achieved by designing a heat exchanger with high thermal efficiency and low-pressure drop to increase the general system's work efficiency.

The current heat exchanger designs for mechanical coffee drying systems have several limitations that reduce their thermal efficiency. One of the main issues is that these heat exchangers are typically hand-crafted, leading to inconsistencies and variations in their design. This can result in lower heat transfer rates and less efficient energy usage. Furthermore, there has been relatively little research on the optimal design of heat exchangers for coffee drying systems, which further limits their effectiveness [2].

Another issue is the high-pressure drop that occurs throughout the system, which can further decrease thermal efficiency [2]. The pressure drop is due to the high airflow required to adequately dry the coffee beans, which results in a higher resistance to airflow through the heat exchanger. This, in turn, can lead to increased energy usage and costs associated with the mechanical drying process.

Therefore, there is a need to improve the design of heat exchangers for mechanical coffee drying systems to enhance their thermal efficiency and reduce pressure drop throughout the system. By optimizing the heat exchanger design and airflow resistance, it is possible to reduce the energy consumption required to dry coffee beans and minimize the environmental impact of the process.

2.4.1 References

- [1] Sivetz, Michael, M.S., and H. Elliot Foote, Ph.D. *Coffee Processing Technology*. Vol. 1, Westport, Connecticut, Avi Publishing Company, 1963. HathiTrust, babel.hathitrust.org/cgi/pt?id=mdp.39015002932617&view=1up&seq=8.
- [2] Oliveros Tascón, Carlos E., et al. "APROVECHAMIENTO EFICIENTE DE LA ENERGÍA EN EL SECADO MECÁNICO DEL CAFÉ." *Avances Técnicos CENICAFE*, no. 380, Feb. 2009.

2.5 Literature Review of Previous Design Projects

Diseño, Construcción y Caracterización de Secador de Granos de Café, Utilizando la Energía Térmica Contenida en Fluidos Geotérmicos [1]

(Design, Construction and Characterization of a Coffee Bean Dryer, Using the Thermal Energy Contained in Geothermal Fluids)

This report describes the design, construction, and characterization of a coffee grain dryer that utilizes thermal energy from geothermal fluids. The paper provides a detailed explanation of the design and construction process, including the selection of materials, components, and instrumentation. The authors also describe the testing and evaluation of the dryer system's performance, including measurements of drying efficiency, energy consumption, and grain quality. The study shows that the geothermal-based dryer system is efficient, cost-effective, and environmentally friendly.

This literature source can be valuable for the senior project report on designing a heat exchanger and furnace for a coffee dryer system, as it presents a unique approach to utilizing renewable energy sources for drying coffee grains. The paper provides insights into the design process, including the selection of appropriate materials and components, as well as the testing and evaluation of the system's performance. The information presented in the document can be used to inform the design and construction of the heat exchanger and furnace system, and to compare the performance of different energy sources for coffee drying. Additionally, the study's findings on the efficiency, cost-effectiveness, and environmental impact of the geothermal-based dryer system can be used to inform the overall goals and objectives of the senior project report.

Development and Validation of a Heated Drying Air Diffusion System to Optimize Rotary Dryers and Final Coffee Quality [2]

This article discusses the development and testing of a heated drying air diffusion system to optimize the performance of rotary dryers used in coffee processing. The authors describe the design and construction of the system, as well as its validation through laboratory testing and field trials. The article provides relevant information about the design and optimization of heat exchangers and furnace systems, as well as the use of computational fluid dynamics (CFD) and finite element analysis (FEA) in the evaluation of heat transfer and system performance.

This source can be used as a valuable literature source for the senior project report, as it provides insights into the design and optimization of heat exchangers and furnace systems for coffee drying. The article highlights the importance of understanding the heat transfer mechanisms involved in the drying process and the role of air velocity and temperature in achieving optimal drying conditions. The use of CFD and FEA in the evaluation of system performance can also provide useful guidance for the design and testing of the heat exchanger and furnace system in the senior project. Additionally, the article provides insights into the importance of field testing and validation in the design and optimization of such systems, which can help to ensure that the final product meets the desired performance specifications.

Hacia la Mejora del Secado Mecánico del Café en Colombia [3]

(Towards the Improvement of Mechanical Coffee Drying in Colombia)

This report aims to improve the mechanical drying process of coffee in Colombia. The report discusses the current state of coffee drying in Colombia and highlights the importance of improving the process to increase the quality and competitiveness of Colombian coffee. It explores various aspects of coffee drying, including the physics of drying, equipment, and processes used in Colombia. While the report does not focus specifically on heat exchangers or furnaces, it provides valuable information on coffee drying, which could be useful in the design of a heat exchanger and furnace system for coffee drying.

This information can be used to determine the requirements and specifications of the heat exchanger and furnace system. For instance, the report discusses the importance of controlling the drying temperature and humidity to prevent damage to the coffee beans. This information can be used to determine the design parameters of the heat exchanger and furnace system, such as the required heating capacity and airflow rate. Additionally, the report provides insights into the challenges and limitations of coffee drying, which can be considered in the design of the system to ensure its reliability and efficiency. Finally, this report presents the lack of efficiency of actual heat exchangers and how manufacturers trade between pressure drops and thermal efficiency.

Modelamiento y Diseño de un Secador Estático de Café Pergamino (Silo de Café) [4]

(Modeling and Design of a Static Parchment Coffee Dryer (Coffee Silo))

The report focuses on the design and modeling of a static coffee dryer, specifically for parchment coffee. The study discusses the technical specifications, design considerations, and modeling aspects of the dryer. Relevant information about designing a heat exchanger includes the importance of heat transfer efficiency and the need to optimize the air flow rate and temperature control. The document also highlights the use of thermal insulation materials to minimize heat loss and maximize energy efficiency.

The document provides detailed information about the technical specifications and design considerations for a static coffee dryer, which can be applied to the project. It offers insights into the importance of heat transfer efficiency, air flow rate optimization, and temperature control, which are critical aspects of designing an effective heat exchanger. Additionally, the report highlights the use of thermal insulation materials to minimize heat loss and energy waste, which can be useful in optimizing the energy efficiency of the proposed system. Finally, this report matches closely the requirements of the project proposed since it contains a detailed design and analysis of a heat exchanger for a Mechanical Coffee Drying System.

Literature Review Lessons Learned

After reviewing the previous reports on designing heat exchangers for mechanical coffee drying systems, several key lessons were learned. Firstly, it is crucial to consider the specific requirements of the system when designing a heat exchanger, as different systems may have different needs in terms of heat transfer and pressure drop. Secondly, the choice of materials for

the heat exchanger must be carefully evaluated, considering factors such as corrosion resistance and thermal conductivity. Finally, the use of computational fluid dynamics (CFD) simulations can greatly aid in the design process, allowing for more accurate predictions of the performance of the heat exchanger before construction.

Overall, the literature review highlighted the importance of a thorough and systematic approach to designing heat exchangers for mechanical coffee drying systems. By carefully considering the system requirements and materials selection and utilizing CFD simulations, it is possible to optimize the design for both thermal efficiency and sustainability.

2.5.1 References

- [1] Espinoza, Vladimir Alberto, et al. *Diseño, Construcción y Caracterización de Secador de Granos de Café, Utilizando la Energía Térmica Contenida en Fluidos Geotérmicos*. Universidad del Salvador, Mar. 2018.
- [2] Coradi, Paulo Carteri, et al. "Development and Validation of a Heated Drying Air Diffusion System to Optimize Rotary Dryers and Final Coffee Quality." PLoS ONE, 22 June 2021. PLoS ONE, <https://doi.org/10.1371/journal.pone.0251312>.
- [3] Gutiérrez Flórez, Jhony Mauricio, and Henry Copete López. *Hacia la Mejora del Secado Mecánico del Café en Colombia*. Report no. 0123-7799, Medellín, Colombia, Instituto Tecnológico Metropolitano, 23 Dec. 2009. Tecno Lógicas 23.
- [4] Lee Laverde, Jonathan Felipe, and Cesar Augusto Delgado Agudelo. *Modelamiento y Diseño de un Secador Estático de Café Pergamino (Silo de Café)*. Universidad Tecnológica de Pereira, 2013.

2.6 Computational Fluid Dynamics

Designing and analyzing engineering systems involving fluid flow involves two primary methods: experimentation and computation. The former often necessitates the development of prototypes to evaluate in testing facilities experimentally. The latter involves solving differential equations, whether analytically or with computer-based simulations. Computational fluid dynamics (CFD) is a branch of numerical techniques that, using a computer (or multiple computers), enables the modeling of fluid flow, heat transfer, and other related phenomena within complex geometries. The origins can be dated back to the 19th century when physicists and mathematicians began to develop numerical methods for solving the partial differential

equations involved in fluid flow. Notable contributions came from Louis Marie Henri Navier and Sir George Stokes, who independently formulated fluid dynamics equations that include the viscous forces of a fluid in motion, serving as CFD's foundational building blocks. Since solving these equations is computationally heavy, it was not until the advent of modern-day computing power that allowed the advancement of the technology [1].

Computational fluid dynamics software has become an important tool for engineers due to its ability to accelerate design and analysis processes. It is widely used in aerospace, chemical operations, HVAC, and large-scale power equipment sectors to increase system efficiencies and reduce development time. However, despite having the capability of delivering accurate information, it is up to the user to properly set up the model lest the results become useless and a massive waste of time and money. This section will briefly discuss the general governing equations involved in modern CFD techniques, the basic procedure of simulating CFD, and commonly used commercial software packages.

In general, the basis of CFD relies on a set of fundamental equations that describe the flow of fluids and heat transfer in a mathematical framework. The dynamic behavior of fluids can be described by three conservation laws. From Fluid-Mechanics by Çengel and Cimbala, the basic equations are [2]:

1. The conservation of mass (Continuity equation)
2. The conservation of momentum (Navier-Stoke equation)
3. The conservation of energy (First Law of Thermodynamics)

The conservation of mass is as follows:

$$\frac{D\rho}{Dt} + \rho(\nabla \cdot \vec{V}) = 0 \quad (1)$$

where ρ is the density of the fluid, the \vec{V} velocity, and the gradient operator ∇ :

$$\vec{\nabla} = \vec{i} \frac{\partial}{\partial x} + \vec{j} \frac{\partial}{\partial y} + \vec{k} \frac{\partial}{\partial z} \quad (2)$$

It states that mass in a control volume can neither be destroyed nor created and that the mass flow difference between the inlet and outlet of the system is zero. If the fluid is considered incompressible (density remains constant or the change is negligible throughout the system), then the conservation of mass equation simplifies to

$$\nabla \cdot \vec{V} = \frac{\partial u}{\partial x} + \frac{\partial v}{\partial y} + \frac{\partial w}{\partial z} = 0 \quad (3)$$

where u, v, and w are the velocity components at the point (x, y, z). Liquids can almost always be modeled as an incompressible flow. At Mach numbers less than ~0.3, gas flows can be considered incompressible due to the change of density being negligible at low velocities.

The conservation of momentum equation is also referred to as the Navier-Stokes equation and is represented as

$$\frac{\partial}{\partial t}(\rho \vec{v}) + \nabla \cdot (\rho \vec{v} \vec{v}) = -\nabla P + \nabla \cdot \vec{\tau} + \rho \vec{g} \quad (4)$$

where P is the static pressure, $\vec{\tau}$ is the viscous stress tensor, and $\rho \vec{g}$ is the gravitational force per unit volume. If the fluid is incompressible and the viscosity, μ , remains constant, the equation simplifies to

$$\rho \frac{D\vec{V}}{Dt} = -\nabla P + \rho \vec{g} + \mu \nabla^2 \vec{V} \quad (5)$$

This equation is deemed the Navier-Stokes equation, the cornerstone of fluid mechanics. The second-order partial differential equation has no known general analytical solutions; however, there are solutions for elementary flow fields and simple geometry.

The conservation of energy equation is also used in CFD when heat transfer is important. A common type of equation used is as follows [3]

$$\rho \left[\frac{\partial h}{\partial t} + \nabla \cdot (h \vec{v}) \right] = -\frac{\partial P}{\partial t} + \nabla \cdot (k \nabla T) + \phi \quad (6)$$

where $\frac{\partial h}{\partial t}$ is the time rate of energy per unit volume, $\nabla \cdot (h\vec{v})$ describes the convective transport energy, $\frac{\partial P}{\partial t}$ represents the work done by pressure, $\nabla \cdot (k\nabla T)$ is the heat conduction within the fluid, and ϕ is a source term (chemical reaction or other internal heat generation).

Most CFD software handles turbulence and the governing equations by incorporating various turbulence models that approximate turbulent flow behavior [4]. These models introduce additional equations to simulate turbulence characteristics within the computational domain, such as eddy viscosity and turbulent kinetic energy. These equations allow the code to predict how turbulence affects fluid properties like velocity and pressure. Most commercial software allows for the selection of various turbulence models, which make different assumptions about turbulence behavior, and the choice of which one to use depends on the specific application. The most used turbulence models include the Reynolds-Averaged Navier-Stokes (RANS) models, which simplify turbulent flow by averaging over time, and these include variants like the k- ϵ model and the k- ω model. The simulation involved in this project will only use the RANS k- ϵ model variant, and the details can be read in Sobachkin's Numerical Basis of CAD-Embedded CFD.

A lot of modern CFD codes use the cell-centered finite volume method (FVM) to solve the partial differential equations previously mentioned. This method will be the only one discussed and used in this project. The first step of the FVM is to define a computational domain that best encapsulates the model. The computational domain is divided into small elements called cells, as shown in Figure 25 below. The collection of cells within the computational domain is called a mesh. These individual cells can be thought of as control volumes that the mathematical models are applied to and are solved in a linear, discretized fashion. Fortunately, most software packages include automatic mesh generations using various cell geometries to best suit the desired application.

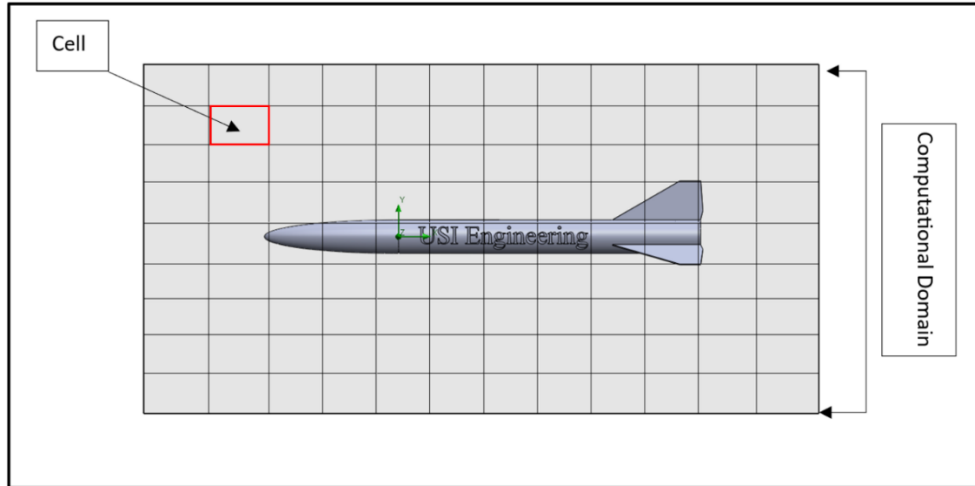


Figure 25. The make-up of a computational domain with a coarse mesh.

The number of cells within a mesh significantly impacts a simulation's accuracy and computational cost. In general, more cells in the mesh provide a finer representation of the flow field, allowing for better capture of flow details and gradients. This can result in more accurate results, especially for complex flows. However, a higher cell count requires greater computer resources, leading to longer simulation times and increased computational costs. Developing the right balance is needed, as a coarse mesh, as seen in Figure 25 above, can introduce errors. In contrast, an excessively fine mesh (see Figure 26 below) can be computationally demanding and time-consuming.

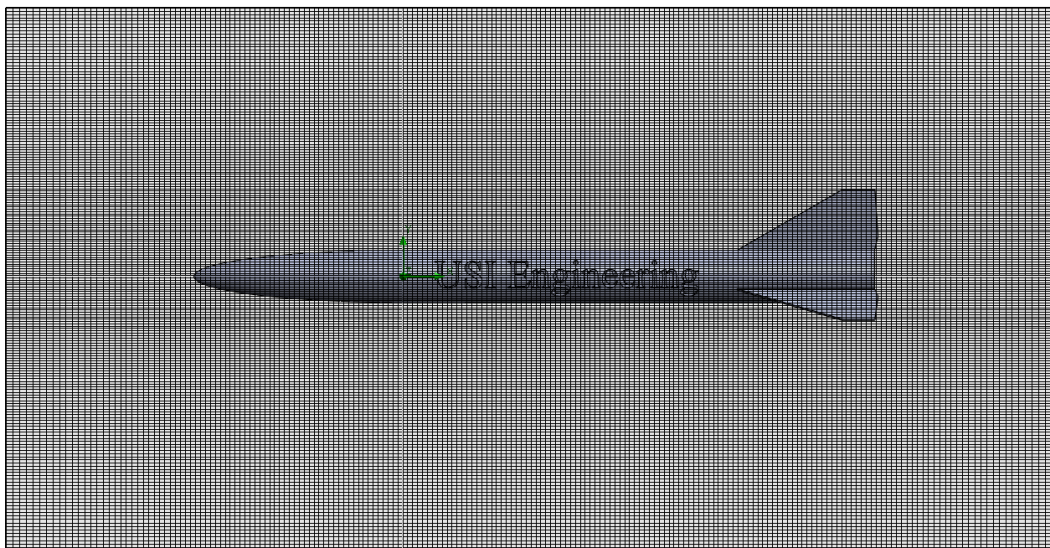


Figure 26. A computational domain with a fine mesh.

Users should refine the mesh around areas of interest through mesh adaptation, which means adjusting cell size in specific regions to capture important flow details accurately. Refining the mesh should be done in areas the user predicts will have high or complex flow gradients. This allows the user to achieve more accurate results while optimizing computational resources, ensuring that the simulation focuses its computational effort where it matters most (see Figure 27 below). The colors represent the mesh refinement level, with blue being the coarsest and red being the finest.

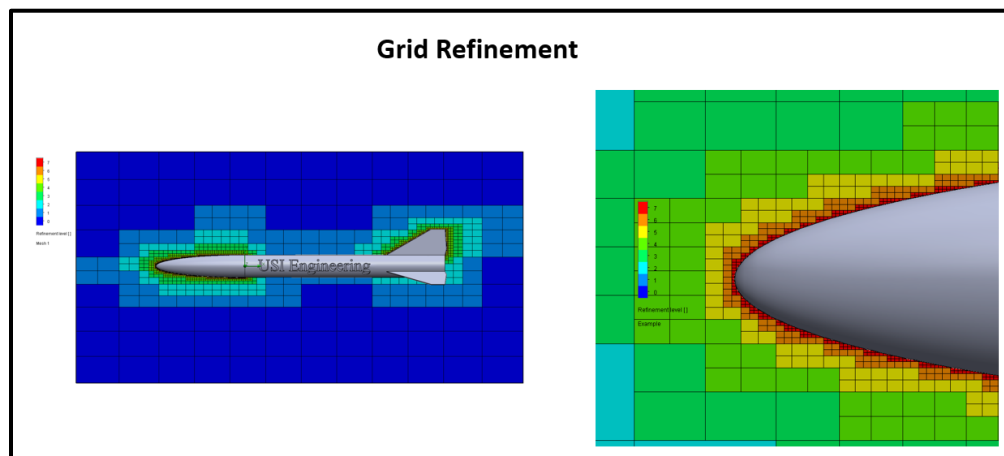


Figure 27. Grid refinement in SolidWorks Flow Simulation 2023.

After generating a confident mesh, the second step is to assign boundary conditions that describe the system around the perimeter of the computational domain. This acts as a guide for the solver to determine the solution of the simulation. Setting up appropriate boundary conditions is another crucial step to ensure the accuracy of results. There are several types of boundary conditions to consider. Inlet conditions dictate the properties of the incoming flow, such as velocity, temperature, and pressure. Outlet conditions specify how the flow exits the domain, typically regarding pressure or flow rates. Wall conditions are applied for solid surfaces, often utilizing the no-slip condition. Symmetry conditions are used in cases of symmetric geometries, while periodic conditions maintain consistency across repeating domains. Pressure inlet/outlet conditions come into consideration when pressure is known, but velocity may not be. It is necessary to know when to apply assumptions and their relevance to the physical problem to produce accurate simulation results [5].

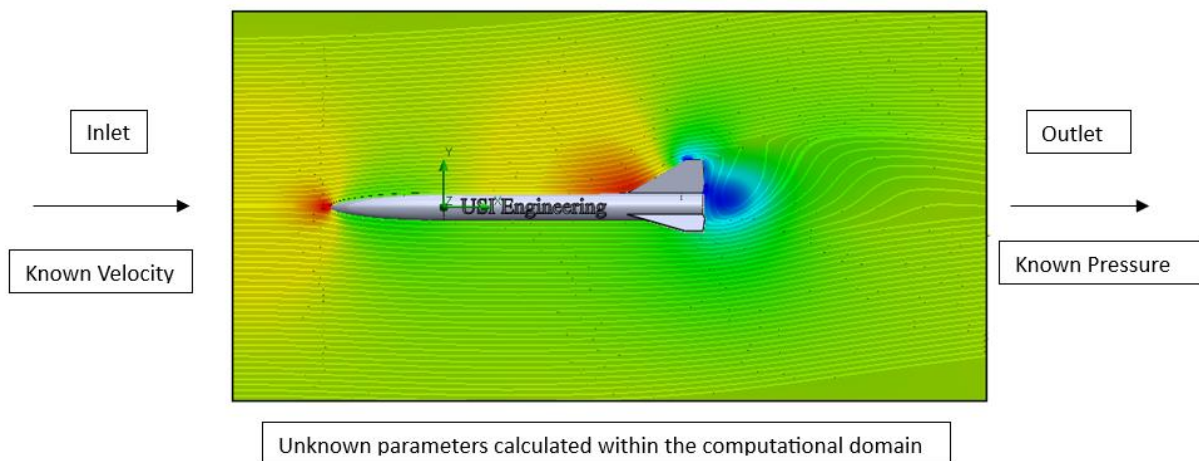


Figure 28. Boundary Conditions.

After meshing and setting up the boundary conditions that best suit a system, the final step is to check for simulation mesh convergence. Convergence occurs when refining the computational mesh no longer significantly changes the simulation results between iterations. Achieving mesh convergence is essential for ensuring simulation accuracy and conformance to real-life phenomena. It is best practice to compare results to existing experimentations, data, or measurements to validate the simulation. This process is extremely important in determining if the numerical simulation effectively displays the real-life physical behavior of the system it is attempting to represent. If the simulation results do not match the real-world data within an acceptable margin, then the model risks being a waste of effort, time, and money. Adjustments to the model, mesh, boundary conditions, or assumptions must be made, and the simulation is iterated until validation criteria are met.

Since computational fluid dynamics can be an enormous tool in expediting the design phase within various industries, it should be no surprise that commercially available software packages exist. Each package has advantages and features that can cater to a particular need. In this report, only SolidWorks Flow Simulation will be considered due to the availability and familiarity of the software.

This section covered the fundamental components of CFD simulations. To summarize, it discussed the basic governing equations used in CFD, it followed by including insights into mesh generation and boundary condition specification for accurate simulation setup. It then

emphasized the significance of convergence and validation through comparisons with experimental or analytical data to ensure the dependability of the simulations.

2.6.1 References

- [1] Wei, Yufeng. “The development and application of CFD Technology in mechanical engineering.” IOP Conference Series: Materials Science and Engineering, vol. 274, 2017, p. 012012, <https://doi.org/10.1088/1757-899x/274/1/012012>.
- [2] Cengel, Yunus A., and John M. Cimbala. “Chapter 15: Introduction to Computational Fluid Dynamics.” Fluid Mechanics: Fundamentals and Applications, 4th ed., McGraw-Hill Education, New York, NY, 2018.
- [3] “What Is CFD: What Is Computational Fluid Dynamics?” SimScale, 30 Nov. 2023, www.simscale.com/docs/simwiki/cfd-computational-fluid-dynamics/what-is-cfd-computational-fluid-dynamics/.
- [4] Sobachkin, A, and G Dumnov. Numerical Basis of CAD-Embedded CFD - Solidworks, Dassault Systemes, www.solidworks.com/sw/docs/Flow_Basis_of_CAD_Embedded_CFD_Whitepaper.pdf.
- [5] “Chapter 4: Numerical Solution Technique.” Technical Reference SolidWorks Flow Simulation 2023, Dassault Systemes, 2023.

3.0 Project Requirements

Based on the research done on the specific application of our project, the actual designs commercially available as well as previous studies realized to solve the same problem this project seeks to solve, the following requirements have been selected:

- 1.) The heat exchanger fluids shall not mix.
- 2.) The system shall have a heat exchanger effectiveness of at least 60%.
- 3.) The heat exchanger shall reduce the average batch moisture content of a layer of 0.25 [m] of 1000 kg of parchment coffee to 12%.
- 4.) The drying air shall be heated to a temperature of 51 °C (+/- 2°C) upon exiting the heat exchanger.

- 5.) The heat exchanger shall not produce a shell-side pressure drop greater than 1000 [Pa].
- 6.) The tube-side fluid shall be of combustion gases from burning coffee husks.

3.1 Concept Selection

With the objective to design an efficient heat exchanger for the mechanical drying of coffee beans, it is imperative to explore a variety of heat exchanger concepts. This section focuses on the considerations for concept selection and the rationale behind choosing a specific design for our project.

3.2 Factors that Impact Design Choices

This section delves into the key considerations that significantly impact the design process. From the precision required in managing temperature parameters to the structural implications of geometry, and the economic balance of cost considerations, every aspect is meticulously examined. The ensuing paragraphs dissect temperature requirements, pressure drop considerations, geometric intricacies, and cost dynamics, elucidating their individual roles in the intricate tapestry of the design process.

- **Temperature Requirements:** The temperature requirements represent a critical aspect influencing the design of the heat exchanger. In the context of a mechanical coffee drying system, precision in temperature control is paramount to ensure optimal drying conditions. The choice of materials and the overall design must align with the specified temperature parameters to guarantee effective heat transfer, maintain product quality, and achieve the desired efficiency in the drying process. The materials must also ensure that the design minimizes any risks to public health and safety. This involves selecting materials that are non-toxic and safe for contact with coffee beans. Thorough consideration of the temperature requirements is foundational to the reliability and success of the heat exchanger system.
- **Pressure Drop Requirements:** Pressure drop considerations are pivotal in the design of a heat exchanger, directly impacting the efficiency and performance of the system. In the case of mechanical coffee drying, understanding, and managing pressure drop requirements are crucial for optimizing airflow and, subsequently, heat transfer. Excessive pressure drops can result in increased energy consumption and operational costs. Thus, a meticulous

analysis of the pressure drop requirements guides the selection of an appropriate design, ensuring a balance between efficient heat transfer and minimal energy expenditure.

- **Geometry:** The geometry of the heat exchanger plays a significant role in determining its structural integrity, thermal efficiency, and overall effectiveness in the coffee drying process. The selection of a specific geometry, such as tube arrangements or fin designs, directly influences heat transfer characteristics. Moreover, geometric considerations extend to the spatial constraints of the system, ensuring that the chosen design aligns with the available space and installation requirements. Striking a harmonious balance between geometric configurations and functional efficiency is a key aspect in the heat exchanger design process.
- **Cost:** Cost considerations are integral to the decision-making process in designing a heat exchanger for a mechanical coffee drying system. This encompasses not only the initial investment but also operational and maintenance costs over the system's lifecycle. Balancing performance requirements with cost-effectiveness is imperative to achieve a sustainable and economically viable solution. Material selection, fabrication processes, and system complexity all contribute to the overall cost dynamics. A thorough cost analysis ensures that the chosen design aligns with budgetary constraints while delivering optimal performance and long-term reliability.

3.3 Chosen Design

After having learned the different options available for our senior design project through our background section, we have opted for a tube and shell heat exchanger design, which incorporates a tube bank. This design offers advantages in terms of heat transfer efficiency and adaptability to the unique requirements of the coffee drying process. Furthermore, our heat exchanger design will feature a cleaning mechanism to prevent fouling, ensuring sustained performance over time. This choice aligns with our objectives of optimizing energy transfer, reducing drying time, and enhancing the quality of the dried coffee beans. Throughout the concept selection process, we've been guided by insights from previous projects and a commitment to designing a heat exchanger that addresses the specific needs of coffee drying systems.

3.4 Professional Standards

Throughout the design process, careful consideration was given to Tubular Exchanger Manufacturing Association (TEMA) standards [1]. TEMA is an organization dedicated to establishing industry standards for the design and construction of shell and tube heat exchangers. The standards include the various aspects of design which include materials, fluid properties, and temperature and pressure considerations. Another contribution of TEMA includes the categorizing heat exchangers based on their shell-and-tube configurations with each designation associated with distinct construction features, allowing engineers and manufacturers to communicate and design heat exchangers more effectively. The designations typically include letters and numbers, and each character represents a specific aspect of the heat exchanger's design. Common TEMA designations for shell constructions can be found in Figure 29 on the next page. The chosen shell construction type aligns with TEMA Type 'AET,' incorporating key features such as a removable channel and cover for internal tube cleaning without unbolting the piping and a floating head due to the extreme temperature difference between the hot and cold fluid potentially causing high stresses in the axial direction of the shell and tubes. This compliance with industry-recognized standards ensures the reliability and performance of the heat exchanger in accordance with widely accepted practices.

3.4.1 References

[1] Standards of the Tubular Exchanger Manufacturers Association. Tubular Exchanger Manufacturers Association, 1988.

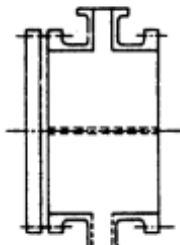
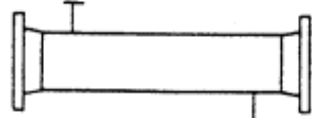
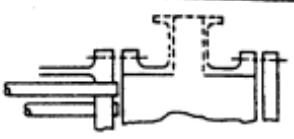
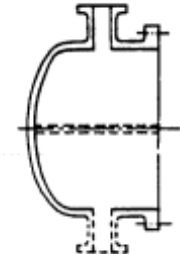
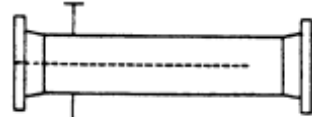
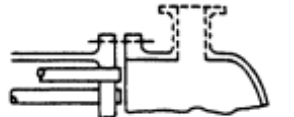
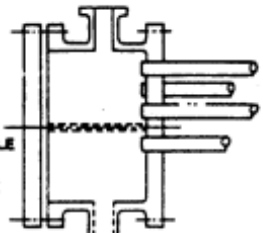
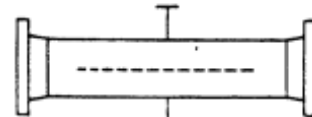
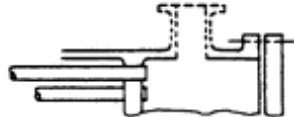
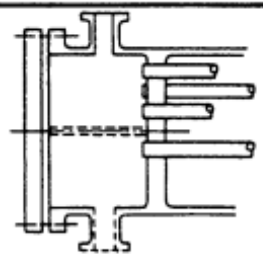
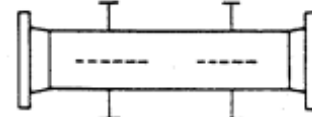
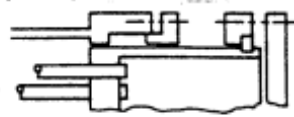
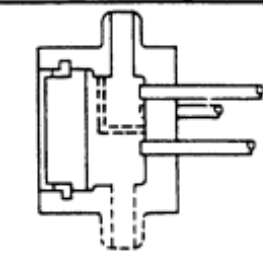
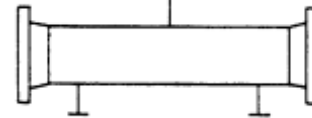

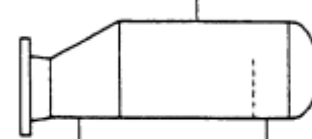

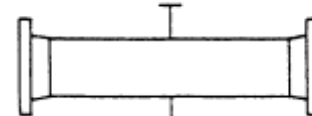
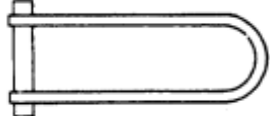
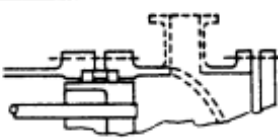
	FRONT END STATIONARY HEAD TYPES		SHELL TYPES		REAR END HEAD TYPES
A	 CHANNEL AND REMOVABLE COVER	E	 ONE PASS SHELL	L	 FIXED TUBESHEET LIKE "A" STATIONARY HEAD
B	 BONNET (INTEGRAL COVER)	F	 TWO PASS SHELL WITH LONGITUDINAL BAFFLE	M	 FIXED TUBESHEET LIKE "B" STATIONARY HEAD
C	 REMOVABLE TUBE BUNDLE ONLY CHANNEL INTEGRAL WITH TUBE- SHEET AND REMOVABLE COVER	G	 SPLIT FLOW	N	 FIXED TUBESHEET LIKE "N" STATIONARY HEAD
N	 CHANNEL INTEGRAL WITH TUBE- SHEET AND REMOVABLE COVER	H	 DOUBLE SPLIT FLOW	P	 OUTSIDE PACKED FLOATING HEAD
D	 SPECIAL HIGH PRESSURE CLOSURE	J	 DIVIDED FLOW	S	 FLOATING HEAD WITH BACKING DEVICE
		K	 KETTLE TYPE REBOILER	T	 PULL THROUGH FLOATING HEAD
		X	 CROSS FLOW	U	 U-TUBE BUNDLE
				W	 EXTERNALLY SEALED FLOATING TUBESHEET

Figure 29. Common TEMA designations for shell constructions [1].

In our chosen heat exchanger design for the coffee drying system, we are distinctively harnessing the combustion of coffee husk as the energy source. Coffee husks are a byproduct of coffee processing and are readily available. By utilizing this biomass waste as fuel for the heat exchanger, we not only contribute to sustainability by reducing waste but also address the energy needs of the drying process. The combustion of coffee husk offers an eco-friendly and cost-effective alternative to traditional energy sources.

In the following sections, we will get into the details of our chosen heat exchanger design, including its specifications, simulation approach, and validation studies. This will provide a comprehensive understanding of how our design solution meets the project's goals and objectives, ultimately contributing to the optimization of the mechanical coffee drying process operating conditions.

4.0 Methodology

4.1 Thermal-Hydraulic Design of Shell and Tube Heat Exchangers

Designing an effective heat exchanger involves basic knowledge of heat transfer, thermodynamics, and engineering principles. The process is often split between thermo-hydraulic and mechanical/structural designs. This project will focus on the thermo-hydraulic aspect, which will help determine the overall heat transfer coefficient, pressure drop, heat duty, and total heat transfer area. However, mechanical parameters like shell diameter, tube diameter, and baffle spacing are required to complete the process. This section of the report uses Kern's Method to design a shell and tube heat exchanger with parameters guided by those found in a biomass-fueled mechanical coffee dryer system. The method was developed by the American chemical engineer Donald Kern, who made significant contributions to the field of heat exchangers. Kern's work, particularly his book "Process Heat Transfer," has provided the general guidelines for modern heat exchanger design principles and engineering practices [1]. Along with the presentation of the method, this section also gives step-by-step calculations of the first iteration for the reader. This section follows Coulson and Richardson's Chemical Engineering Version 6 [2].

Kern's Method of Shell and Tube Heat Exchanger Design

1. Identify application parameters.
2. Select the type of heat exchanger.
3. Evaluate the heat transfer rate (\dot{Q}) and Log-Mean-Temperature-Difference (LMTD).
4. Determine heat exchanger configuration and dimensions by assuming an overall heat transfer coefficient, U .
5. Evaluate the convective heat transfer coefficient on the tube side.
6. Evaluate the convective heat transfer coefficient on the shell side.
7. Calculate the overall heat transfer coefficient, U .
8. If the calculated U value \neq the assumed U value, use the calculated U value to determine new dimensions and continue from step 4 (iterate).
9. Check power consumption and pressure drops until within specifications(iterate).

A design procedure flowchart can be seen in Appendix F. This method assumes that the system is in a steady state. It also assumes the fluid properties remain constant and are evaluated at the arithmetic mean for each fluid. Combustion gases can be assumed to resemble properties of air. All heat being lost by the combustion gas is being received by the drying air.

1.) Identifying application parameters.

To begin, the application parameters must be identified. These parameters include the properties of the hot and cold fluids, inlet and outlet temperatures, flow rates, required outlet temperatures, pressure conditions, phase of the fluids (if dealing with multiphase flows), operating environment, and relevant regulatory requirements. These parameters are the basis for calculating the necessary heat transfer area and ensuring that the heat exchanger effectively meets the application's specific operational conditions and constraints. Table 1 below defines the known parameters and fluid properties involved in the coffee dryer system.

Table 1. Known parameters and fluid properties involved in the coffee drying project.

Symbol	Value	Unit	Description
\dot{m}_c	1.8	$\frac{\text{kg}}{\text{s}}$	The mass flow rate of drying air
$T_{c,i}$	22	°C	Inlet temperature of drying air from the environment
$T_{c,o}$	50	°C	The outlet temperature of drying air to the dryer
$T_{h,i}$	820	°C	The inlet temperature of combustion gas
$T_{h,o}$	200	°C	Outlet temperature of combustion gas to stack

Symbol	Value	Unit	Description
ρ_c	1.145	$\frac{\text{kg}}{\text{m}^3}$	Density of air
$C_{p,c}$	1007	$\frac{\text{J}}{\text{kg} - \text{K}}$	Specific heat of air at a constant pressure
k_c	0.02625	$\frac{\text{W}}{\text{m} - \text{K}}$	Thermal conductivity of air
Pr_c	0.727	--	Prandtl Number
<i>Properties of air evaluated at 36 °C (1 atm)</i>			

Symbol	Value	Unit	Description
ρ_h	0.70	$\frac{\text{kg}}{\text{m}^3}$	Density of CO_2
$C_{p,h}$	1148	$\frac{\text{J}}{\text{kg} - \text{K}}$	Specific heat of CO_2 at a constant pressure
k_h	0.0548	$\frac{\text{W}}{\text{m} - \text{K}}$	Thermal conductivity of CO_2
Pr_h	0.724	--	Prandtl Number
<i>Properties of combustion gas (assumed CO_2) evaluated at 500 °C (1 atm)</i>			

2.) Select the type of heat exchanger.

As mentioned in Section 2, selecting the right type of heat exchanger is an important decision because it directly affects the system's performance. The various heat exchanger configurations have unique features that suit specific operating conditions. Factors like space availability, fluid properties, heat transfer needs, maintenance requirements, and pressure restrictions should be carefully considered to ensure efficient heat transfer while meeting operational standards. This project uses a fixed head, counterflow shell-and-tube heat exchanger with a single tube pass. The tube bundle will be oriented in a triangular-pitched manner.

3.) Evaluate the required heat transfer rate (\dot{Q}) and the Log-Mean-Temperature-Difference (LMTD)

With the assumption that all heat energy is being completely transferred from the hot fluid to the colder fluid, the heat transfer rate is calculated by,

$$\dot{Q} = \dot{m}_c C_{p,c} (T_{c,o} - T_{c,i}) = \dot{m}_h C_{p,h} (T_{h,i} - T_{h,o}) \quad (7)$$

The required heat transfer rate can be determined by substituting in known values and will be used to estimate the size of the heat exchanger.

$$\dot{Q} = \dot{m}_c C_{p,c} (T_{c,o} - T_{c,i}) = 1.8 \frac{\text{kg}}{\text{s}} (1007) \frac{\text{J}}{\text{kg} \cdot \text{K}} (50^\circ\text{C} - 22^\circ\text{C}) = 50.8 \text{ kW}$$

One way to analyze and design a heat exchanger is by using the logarithmic mean temperature difference (LMTD) to estimate the required geometry and heat transfer area of a heat exchanger. This is especially useful when both fluids' inlet and outlet temperatures are known. Another method called the effectiveness-NTU, is discussed and applied in Section 5. Figure 30 below shows the hot and cold fluids' temperatures as they travel through a counter-flow heat exchanger. Since the fluids may be cooling/heating at different rates due to flow conditions and the properties changing it is best practice to use the logarithmic mean temperature difference. It is calculated through the use of the equation

$$\Delta T_{lm} = \frac{\Delta T_2 - \Delta T_1}{\ln \frac{\Delta T_2}{\Delta T_1}} \quad (8)$$

where for a counter-flow heat exchanger

$$\Delta T_1 = T_{h,i} - T_{c,o} = 820 \text{ }^\circ\text{C} - 50 \text{ }^\circ\text{C} = 770 \text{ }^\circ\text{C}$$

$$\Delta T_2 = T_{h,o} - T_{c,i} = 200 \text{ }^\circ\text{C} - 22 \text{ }^\circ\text{C} = 178 \text{ }^\circ\text{C}$$

, therefore

$$\Delta T_{lm} = 404.2 \text{ }^\circ\text{C} = 404.2 \text{ K}$$

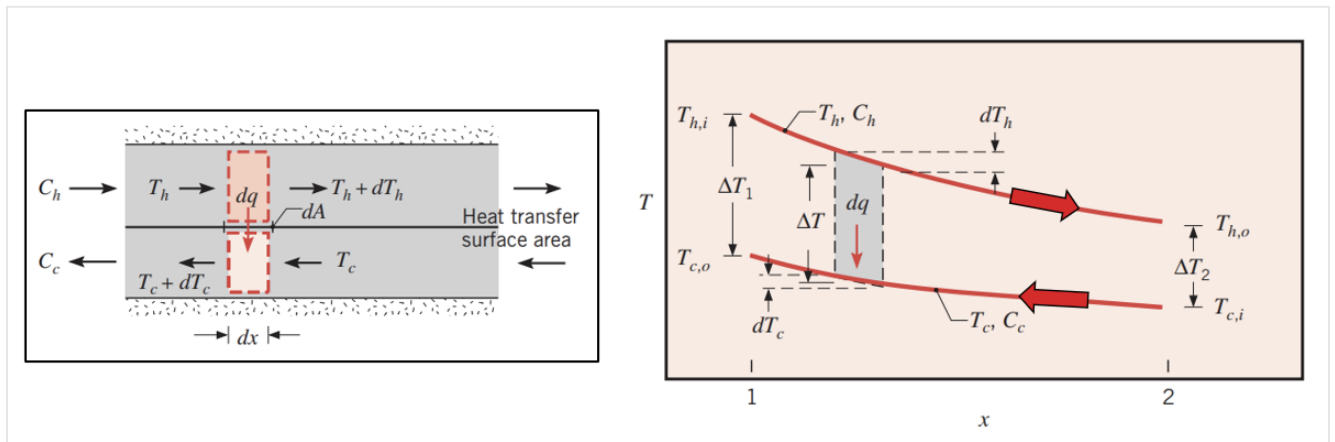


Figure 30. Temperature Profiles of a counter-flow heat exchanger [3].

4.) Determine heat exchanger configuration and dimensions.

For the first iteration of this method, there must be reasonable approximations on the dimensions of the shell and tube heat exchanger or the overall heat transfer coefficient, U . This is usually based on experience or previous designs. Table 2 below lists the overall heat transfer coefficients for various applications and common heat exchanger types. This iteration will use a common U value found in gas-to-gas applications to determine an estimation of the required heat transfer area using Equation 9 below.

$$U_{est} = 25 \frac{W}{m^2 \cdot K}$$

$$A_{s,est} = \frac{\dot{Q}}{U_{est} \cdot \Delta T_{lm}} = \frac{50.8 \times 10^3 W}{25 \frac{W}{m^2 \cdot K} \cdot 404.2 K} = 5.03 \text{ m}^2 \quad (9)$$

The estimated required heat transfer surface area is around 5 square meters. This will be the targeted total area of the tube bundle. For this first iteration a single-pass, triangular tube layout will be used with arbitrary selection of tube diameter, tube thickness, tube length, and total number of tubes. The exchanger will be of the fixed tube sheet design.

Table 2. Overall Heat Transfer Coefficients of various applications [4].

Typical Overall Heat Transfer Coefficients in Heat Exchangers			
Type	Application and Conditions	U	
		W/(m².K)	Btu/(hr.ft².°F)
Tubular, heating or cooling	Gases at atmospheric pressure inside and outside tubes	5 - 35	1 - 6
	Gases at high pressure inside and outside tubes	150 - 500	25 - 90
	Liquid outside (inside) and gas at atmospheric pressure inside (outside) tubes	15 - 70	3 - 15
	Gas at high pressure inside and liquid outside tubes	200 - 400	35 - 70
	Liquids inside and outside tubes	150 - 1200	25 - 200
	Steam outside and liquid inside tubes	300 - 1200	50 - 200
Tubular, condensation	Steam outside and cooling water inside tubes	1500 - 4000	250 - 700
	Organic vapors or ammonia outside and cooling water inside tubes	300 - 1200	50 - 200
Tubular, evaporation	Steam outside and high-viscous liquid inside tubes, natural circulation	300 - 900	50 - 150
	Steam outside and low-viscous liquid inside tubes, natural circulation	600 - 1700	100 - 300
	Steam outside and liquid inside tubes, forced circulation	900 - 3000	150 - 500
Air-cooled heat exchangers	Cooling of water	600 - 750	100 - 130
	Cooling of liquid light hydrocarbons	400 - 550	70 - 95
	Cooling of tar	30 - 60	5 - 10
	Cooling of air or flue gas	60 - 180	10 - 30
	Cooling of hydrocarbon gas	200 - 450	35 - 80
	Condensation of low pressure steam	700 - 850	125 - 150
	Condensation of organic vapors	350 - 500	65 - 90
Plate heat exchanger	Liquid to liquid	1000 - 4000	150 - 700
Spiral heat exchanger	Liquid to liquid	700 - 2500	125 - 500
	Condensing vapor to liquid	900 - 3500	150 - 700

The following parameters in Table 3 will be used to calculate the number of tubes required to fulfill the estimated required area.

Table 3. Parameters of tubes during the first Kern's Method.

Symbol	Value	Unit	Description
$D_{t,o}$	50.6	mm	Outer diameter of a single tube.
t_t	3.1625	mm	Thickness of a single tube.
$D_{t,i}$	44.275	mm	Inner diameter of a single tube.
L_t	1500	mm	Length of tubes.
A_t	0.238	m ²	Surface area of a single tube ($L_t \times D_{t,o} \times \pi$)

The number of tubes, N_t , required can be calculated from the following,

$$N_t = \frac{A_{s,est}}{A_t} = \frac{5.03 \text{ m}^2}{0.238 \text{ m}^2} = 21.13 \approx 22 \text{ tubes} \quad (10)$$

After determining the number of tubes, the bundle diameter, D_B , can be estimated by applying an empirical equation based on tube layouts. From Kern,

$$D_B = D_{t,o} \left(\frac{N_t}{K_1} \right)^{\frac{1}{n_1}} \text{ mm} \quad (11)$$

Where K_1 and n_1 are empirical coefficients and can be found using Table 4 below. Recall that this iteration is based on a triangular pitch with a single pass.

Table 4. Empirical coefficients to determine the tube bundle diameter [2].

Triangular pitch, $p_t = 1.25d_o$					
No. passes	1	2	4	6	8
K_1	0.319	0.249	0.175	0.0743	0.0365
n_1	2.142	2.207	2.285	2.499	2.675
Square pitch, $p_t = 1.25d_o$					
No. passes	1	2	4	6	8
K_1	0.215	0.156	0.158	0.0402	0.0331
n_1	2.207	2.291	2.263	2.617	2.643

Thus, the tube bundle diameter is

$$D_B = 50.6 \text{ mm} \left(\frac{22}{0.319} \right)^{\left(\frac{1}{2.142} \right)} = 365 \text{ mm}$$

The shell clearance in a shell and tube heat exchanger is the gap between the outer shell and the tube bundle. It's important to size the shell diameter to allow maintenance and restrict the flow from bypassing the tube bundle. It can be determined by Figure 31 from Coulson and Richardson's Chemical Engineering Volume 6,

HEAT-TRANSFER EQUIPMENT

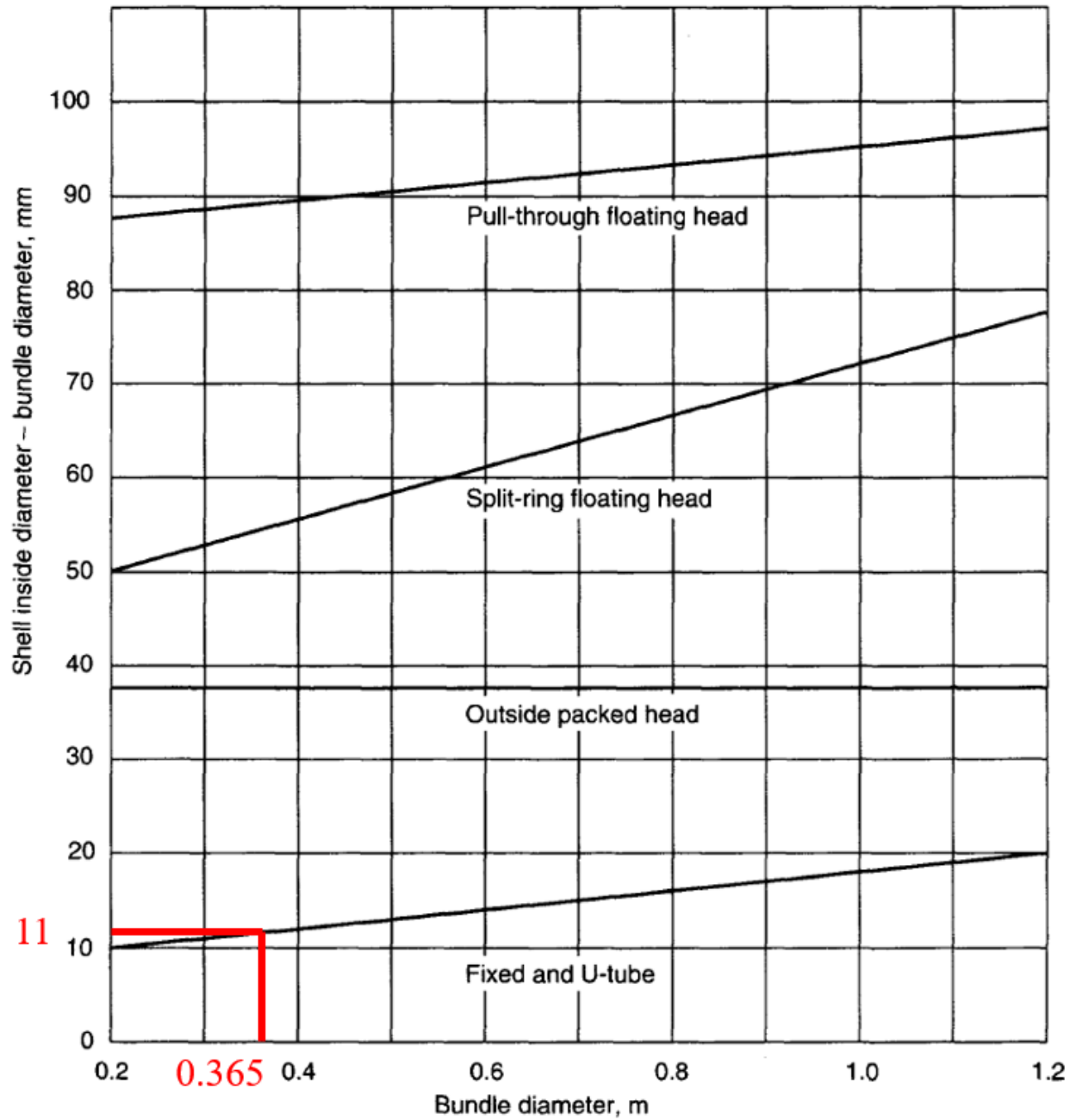


Figure 31. Correlations to determine shell clearance (Kern's Method) [2].

Thus, the inner shell diameter,

$$D_s = \text{Clearance} + D_B = 11 \text{ mm} + 365 \text{ mm} = 376 \text{ mm}$$

5.) Evaluate the convective heat transfer coefficient on the tube side.

The next step requires the determination of the convective heat transfer coefficient on the tube side, h_i . This coefficient quantifies the exchange rate of heat between the combustion gases flowing inside the tubes and the tube wall. To calculate h_i , the first step is to compute the Reynolds number (Re_i) for the fluid within the tubes, considering fluid properties, flow conditions, and geometrical factors. Subsequently, the Nusselt number (Nu_i) is established using empirical correlations that consider the flow regime. With the Nusselt number and the fluid's thermal conductivity, the convective heat transfer coefficient is then calculated.

Table 5 below lists useful properties of the combustion gas flowing through the tubes. This gas will be assumed to take on properties of CO_2 due to the size of the molecule and a proximate and ultimate analysis done on coffee husk [5].

Table 5. Properties of the tube-side combustion gas.

Symbol	Value	Unit	Description
ρ_h	0.70	$\frac{\text{kg}}{\text{m}^3}$	Density of CO ₂
$C_{p,h}$	1148	$\frac{\text{J}}{\text{kg} - \text{K}}$	Specific heat of CO ₂ at a constant pressure
k_h	0.0548	$\frac{\text{W}}{\text{m} - \text{K}}$	Thermal conductivity of CO ₂
Pr_h	0.724	--	Prandtl Number
μ_h	34.2 (10 ⁻⁶)	$\frac{\text{N} - \text{s}}{\text{m}^2}$	Dynamic viscosity of CO ₂
\dot{m}_h	0.0713	$\frac{\text{kg}}{\text{s}}$	Mass flow rate of combustion gas. Calculated from $\dot{m}_h = \frac{\dot{Q}}{C_{p,h}\Delta T_h}$
<i>Properties of combustion gas (assumed CO₂) evaluated at 500 °C (1 atm)</i>			

The average velocity, \bar{V}_t , within the tubes must first be calculated to determine the Reynolds number. It is done by the dividing the volumetric flow rate, \dot{V}_t , by the total cross-sectional area of the tubes, $A_{x,t,total}$ ($A_{x,t}$ is the cross-sectional area of a single tube).

$$\dot{V}_t = \frac{\dot{m}_h}{\rho_h} = \frac{0.0713 \frac{\text{kg}}{\text{s}}}{0.70 \frac{\text{kg}}{\text{m}^3}} = 0.1019 \frac{\text{m}^3}{\text{s}} \quad (12)$$

$$A_{x,t,total} = N_t \times A_{x,t} = N_t \times \frac{\pi D_{t,i}^2}{4} = 22 \times \frac{\pi (44.275 \text{ mm}^2)}{4} = 0.033871 \text{ m}^2 \quad (13)$$

$$\bar{V}_t = \frac{\dot{V}_t}{A_{x,t,total}} = \frac{0.1019 \frac{\text{m}^3}{\text{s}}}{0.033871 \text{ m}^2} = 3.01 \frac{\text{m}}{\text{s}} \quad (14)$$

$$Re_i = \frac{\rho_h \bar{V}_t D_{t,i}}{\mu_h} = \frac{0.70 \frac{\text{kg}}{\text{m}^3} (3.01 \frac{\text{m}}{\text{s}}) (0.044275 \text{ m})}{34.2 (10^{-6}) \frac{\text{N} \cdot \text{s}}{\text{m}^2}} = 2728 \quad (15)$$

It is important to notice that this Reynolds number correlates to a flow in the transitional region, or where there is a mix of laminar and turbulent flow occurring. This region ($2000 < Re < 4000$) contributes to unpredictable flow behavior and uncertainties. Typically, designs avoid having flows within this range, and it is common to adjust geometry or to incorporate turbulence-inducing material surfaces. This iteration will continue; however, this could be a point for design iteration until the Reynolds number lies in the purely laminar or purely turbulent regions. The heat transfer coefficient will be evaluated using both Nusselt correlations for both turbulent and laminar and the lesser value will be used.

The presented correlation for laminar flow was introduced by Sieder and Tate in 1936. It is a well-established and widely used empirical relationship for predicting forced convection heat transfer in circular tubes [6].

$$\text{Laminar: } Nu_{i,lam} = 1.86 \left(\frac{Re_i Pr_h D_{t,i}}{L} \right)^{0.33} = 1.86 \left(\frac{2728 (0.724) 44.275 \text{ mm}}{1500 \text{ mm}} \right)^{0.33} = 7.115 \quad (16)$$

The Dittus-Boelter is an extension of the Sieder-Tate correlation and is another well-known empirical correlation used to estimate the Nusselt number for forced convection heat transfer in circular tubes [7]. This is more accurate for turbulent flow regimes and is expressed as:

$$\text{Turbulent: } Nu_{i,turb} = 0.023 Re_i^{0.8} Pr_h^{0.33} = 0.023 (2728^{0.8}) (0.724^{0.33}) = 11.591 \quad (17)$$

The correlation associated with laminar flow will be used to calculate the heat transfer coefficient within the tubes ($Nu_i = Nu_{i,lam}$).

$$Nu_i = \frac{h_i D_{t,i}}{k_h} \quad (18)$$

Rearranging for h_i ,

$$h_i = \frac{k_h \text{Nu}_i}{D_{t,i}} = \frac{0.0548 \frac{\text{W}}{\text{m} \cdot \text{K}} (7.115)}{0.044275 \text{ m}} = 8.806 \frac{\text{W}}{\text{m}^2 \cdot \text{K}}$$

6.) Evaluate the convective heat transfer coefficient on the shell side.

Kern's method for calculating the shell-side heat transfer coefficient is a similar process to that of the tube-side. The main difference is the calculation of fluid velocity through the tube bank which depends on tube bundle arrangement, baffle spacing, and shell diameter. As the fluid flows through the tube bank, the linear and mass velocities will vary. The velocity used to calculate the Reynolds number will be based on the velocity occurring in the section of the tube bank with the maximum area for crossflow. This is done by simplifying the geometry into an equivalent diameter, D_e . Figure 32 below shows the shaded flow area to be used to calculate D_e for a square and triangular pitch configuration.

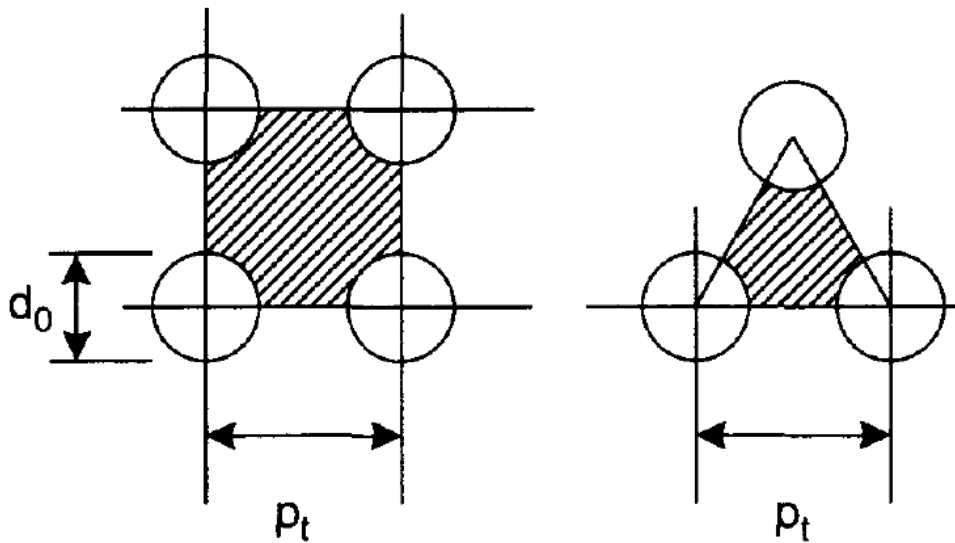


Figure 32. Area to determine the equivalent diameter of a square and triangular pitch tube bank [2].

The calculation for the equivalent diameter of the equilateral triangular pitch configuration used in this iteration is as follows (Recall $p_t = 1.25D_{t,o} = 63.25 \text{ mm}$ for this iteration)

$$D_e = \frac{1.10}{D_{t,o}} (p_t^2 - 0.917D_{t,o}^2) \quad (19)$$

$$D_e = \frac{1.10}{50.6 \text{ mm}} ((1.25 \times 50.6 \text{ mm})^2 - (0.917 \times (50.6 \text{ mm})^2))$$

$$D_e = 35.9 \text{ mm} = 0.0359 \text{ m}$$

The crossflow area between the tubes is a function of the baffle spacing, B_s , within the shell. From TEMA, the common values of baffle spacings range from 20 – 100% of shell diameters. A close (lower value) baffle spacing will result in a higher heat transfer coefficient due to increased turbulence; however, this comes at the cost of pressure drop. For this iteration, a baffle spacing of $B_s = 0.33 \times D_s = 124.08 \text{ mm}$ will be considered. The crossflow area is given by

$$A_{cf} = \frac{p_t - D_{t,o}}{p_t} D_s B_s \quad (20)$$

$$A_{cf} = \frac{63.25 \text{ mm} - 50.6 \text{ mm}}{63.25 \text{ mm}} (376 \text{ mm})(124.08 \text{ mm}) = 9330.82 \text{ mm}^2 = 0.00933082 \text{ m}^2$$

With the crossflow area and equivalent diameter, the mass and linear velocities can be calculated to determine the shell-side Reynolds number.

$$V_m = \frac{\dot{m}_c}{A_{cf}} = \frac{1.8 \frac{\text{kg}}{\text{s}}}{0.009331 \text{ m}^2} = 192.91 \frac{\text{kg}}{\text{s} \cdot \text{m}^2}$$

$$\bar{V}_s = \frac{V_m}{\rho_c} = \frac{192.91 \frac{\text{kg}}{\text{s} \cdot \text{m}^2}}{1.145 \frac{\text{kg}}{\text{m}^3}} = 168.48 \frac{\text{m}}{\text{s}}$$

$$\text{Re}_o = \frac{\rho_c \bar{V}_s D_e}{\mu_c} = \frac{1.145 \frac{\text{kg}}{\text{m}^3} (168.48 \frac{\text{m}}{\text{s}})(0.0359 \text{ m})}{18.9 (10^{-6}) \frac{\text{N} \cdot \text{s}}{\text{m}^2}} = 4.1 \times 10^5$$

Kern developed correlations based on data collected from heat exchangers with various baffle cuts. A baffle cut is the space that allows the flow to progress through the shell. The larger value of baffle cut, the lesser amount of pressure drop occurs. The Nusselt correlation is defined by

$$\text{Nu}_s = j_n \text{Re}_o \text{Pr}_c^{0.33} \quad (21)$$

where j_n is a heat transfer factor for the shell-side flow within a single shell pass exchanger. It can be found using Figure 33 below that is based on data collected from Kern. This iteration will assume a 25% baffle cut. In other words, the baffle will be 75% of the shell diameter.

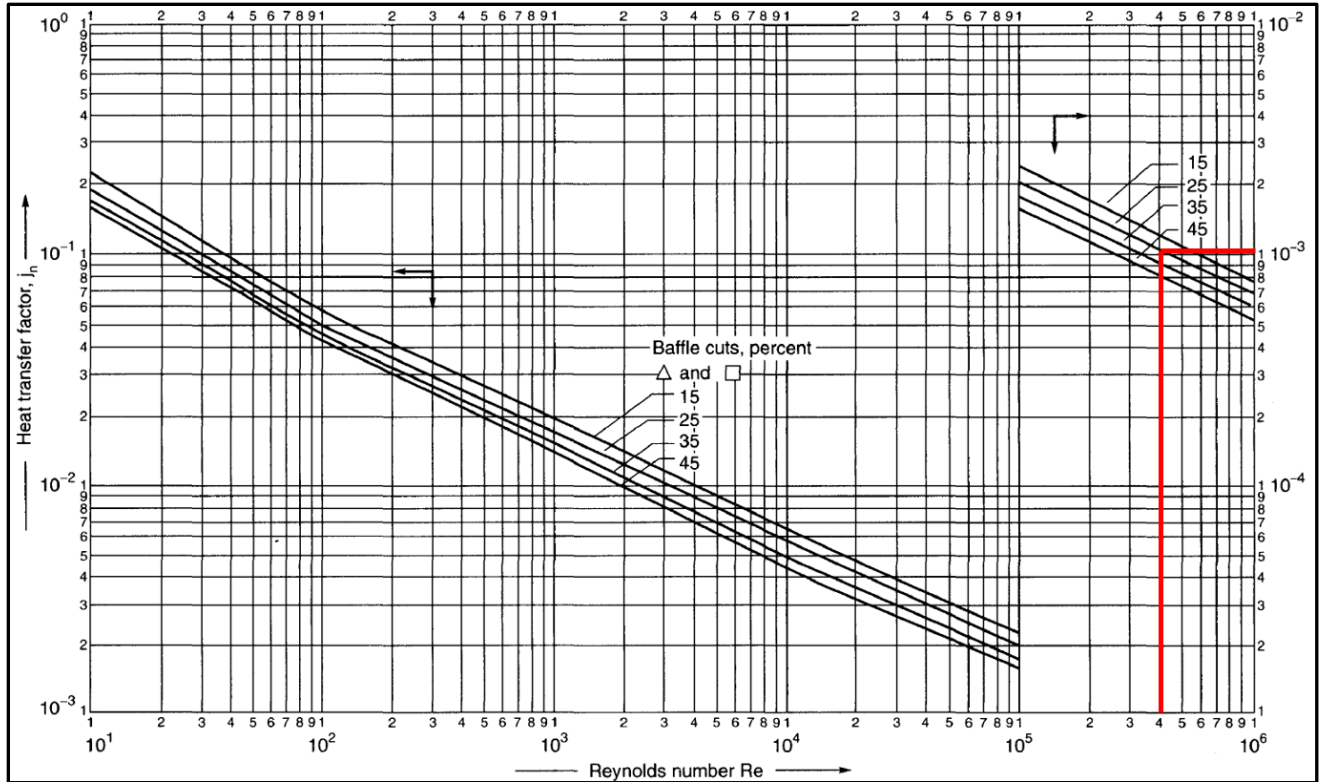


Figure 33. Kern's empirical correlation to determine the heat transfer factor [2].

From the figure $j_n \approx 1 \times 10^{-3}$ thus the Nusselt number of the shell-side flow is

$$Nu_o = (1 \times 10^{-3})(4.1 \times 10^5)(0.727)^{0.33} = 329.75$$

Which now can be used to determine the heat transfer coefficient,

$$h_o = \frac{k_c Nu_o}{D_e} = \frac{0.02625 \frac{W}{m \cdot K} (329.75)}{0.0359 \text{ m}} = 240.925 \frac{W}{m^2 \cdot K}$$

7.) Calculate the overall heat transfer coefficient, U.

The overall heat transfer coefficient, U_{calc} , is the inverse of the sum of overall resistances to heat transfer. The value of U depends on the physical properties and flow rates of the fluids, the tube material, and fouling factors. Fouling occurs when matter within the fluids is deposited on the heat exchange surfaces. This accumulation has a resistance to thermal conductivity and should be accounted for. The following equation is for the overall heat transfer

$$\frac{1}{U_{calc}} = \frac{1}{h_o} + \frac{1}{h_{o,f}} + \frac{D_{t,o} \ln \left(\frac{D_{t,o}}{D_{t,i}} \right)}{2k_t} + \frac{D_{t,o}}{D_{t,i}} \times \frac{1}{h_{i,f}} + \frac{D_{t,o}}{D_{t,i}} \times \frac{1}{h_i} \quad (22)$$

where $h_{o,f}$ and $h_{i,f}$ are the fouling factor coefficients on the outside and inside of the tubes. Typical values found in Table 6 below will be used to estimate the overall heat transfer coefficient. k_t is the thermal conductivity of the tube material. For this iteration, the material chosen is to be 321 stainless steel due to its corrosion resistance and high temperature applications.

Table 6. Fouling factor coefficients [2].

Fouling factors (coefficients), typical values		
Fluid	Coefficient (W/m ² °C)	Factor (resistance) (m ² °C/W)
River water	3000–12,000	0.0003–0.0001
Sea water	1000–3000	0.001–0.0003
Cooling water (towers)	3000–6000	0.0003–0.00017
Towns water (soft)	3000–5000	0.0003–0.0002
Towns water (hard)	1000–2000	0.001–0.0005
Steam condensate	1500–5000	0.00067–0.0002
Steam (oil free)	4000–10,000	0.0025–0.0001
Steam (oil traces)	2000–5000	0.0005–0.0002
Refrigerated brine	3000–5000	0.0003–0.0002
Air and industrial gases	5000–10,000	0.0002–0.0001
Flue gases	2000–5000	0.0005–0.0002
Organic vapours	5000	0.0002
Organic liquids	5000	0.0002
Light hydrocarbons	5000	0.0002
Heavy hydrocarbons	2000	0.0005
Boiling organics	2500	0.0004
Condensing organics	5000	0.0002
Heat transfer fluids	5000	0.0002
Aqueous salt solutions	3000–5000	0.0003–0.0002

$$\frac{1}{U_{calc}} = \frac{1}{240.925} + \frac{1}{10000} + \frac{0.0503 \ln \left(\frac{0.0503}{0.0443} \right)}{2(21.5)} + \frac{0.0503}{0.0443} \times \frac{1}{5000} + \frac{0.0503}{0.0443} \times \frac{1}{8.806}$$

$$U_{calc} = 7.44 \frac{W}{m^2 - K}$$

8.) If the calculated U value \neq the assumed U value, use the calculated U value to determine new dimensions and continue from step 4 (iterate).

Since $\frac{|U_{calc}-U_{est}|}{U_{calc}} > 30\%$ this first design iteration is unacceptable. There must be a new iteration where the new $U_{est} = 7.44 \frac{W}{m^2-K}$ in step 4 and repeated until the condition is satisfied. It is advised to have a computer code to speed this process up due to the possibility of many iterations. For illustrative purposes, the calculated U-value will be considered satisfactory to demonstrate the next steps. The iterations have been completed and can be seen in the results section of this report, Section 5.

9.) Check power consumption and pressure drops until within specifications(iterate).

Once the overall heat transfer coefficient is satisfied, the calculated pressure drops should be compared to the allowable limits. The shell-side pressure drop requires the use of a friction factor, j_f , determined from Figure 34 below. Using Re_o ,

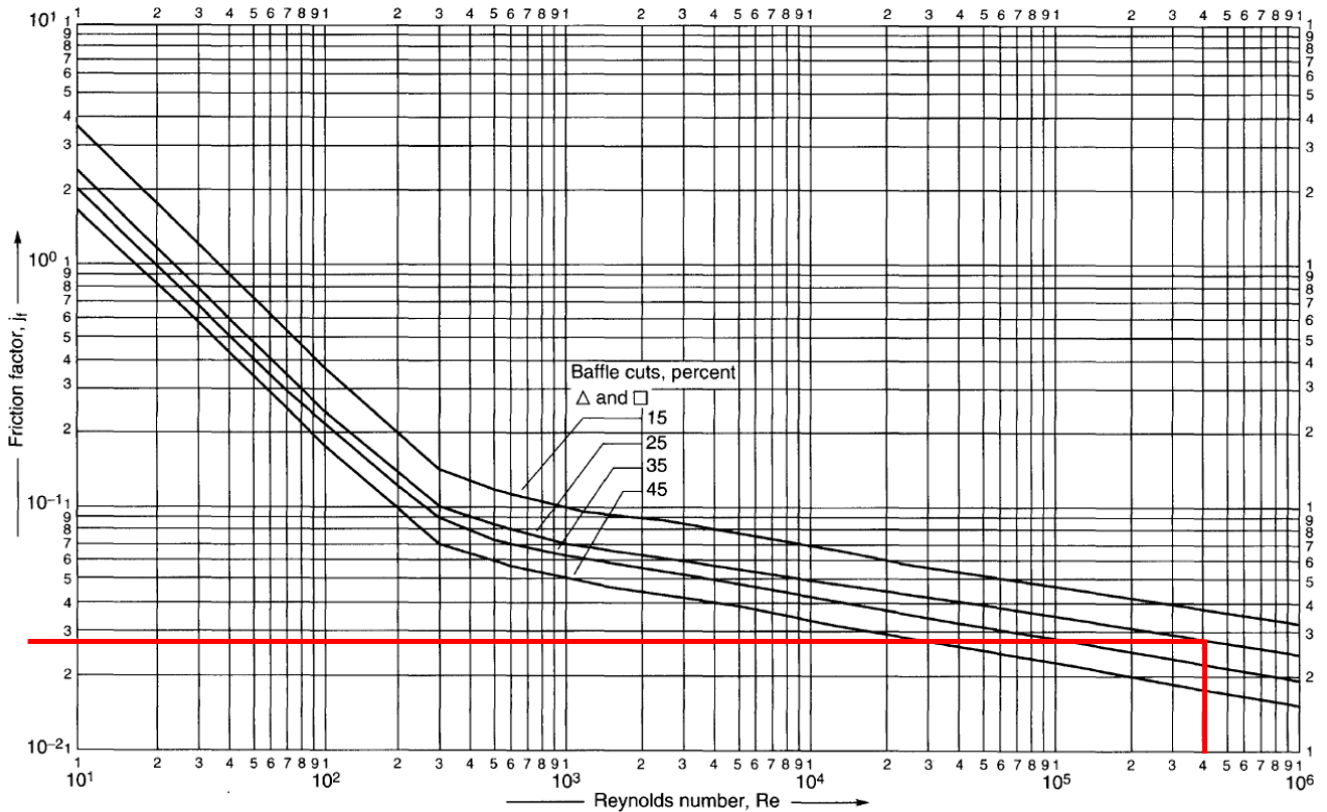


Figure 34. Kern's empirical correlation to determine the friction factor [2].

$$j_f = 2.8 \times 10^{-2}$$

The equation for the shell-side pressure drop,

$$\Delta P_s = 8j_f \left(\frac{D_s}{D_e}\right) \left(\frac{L}{B_s}\right) \left(\frac{\rho_c \bar{V}_s^2}{2}\right) \quad (23)$$

$$\Delta P_s = 8(2.8 \times 10^{-2}) \left(\frac{0.376 \text{ m}}{0.040165 \text{ m}}\right) \left(\frac{1.500 \text{ m}}{0.1241 \text{ m}}\right) \left(\frac{1.145 \frac{\text{kg}}{\text{m}^3} (168.48 \frac{\text{m}}{\text{s}})^2}{2}\right)$$

$$\Delta P_s = 412 \text{ kPa}$$

Which far exceeds the project requirement of 1000 Pa.

To conclude, the initial design of the shell and tube heat exchanger using Kern's Method gave insights into the component's performance. To restate, it is important to acknowledge that the first iteration did not align with the initially estimated U value, and the calculated pressure drop significantly deviated from expectations. This disparity between the predicted and actual performance emphasizes the iterative nature of this technique. In all, the following results section will present the refined design based. The MATLAB code solving the successful iteration can be found in Appendix H. The code shows which adjustments have been made to improve the heat exchanger and align the performance parameters closer to the requirements of coffee drying.

4.2 Design Methodology Phase 2: Modeling and Simulation

This section outlines the steps taken to model and simulate the heat exchanger using SolidWorks and SolidWorks Flow Simulation. The primary objectives of the simulation were to analyze the temperatures and pressure drops within the shell and tube heat exchanger. These details provided insights into the effectiveness of the design under different operating conditions.

A simplified flow chart is shown in Figure 35 below.

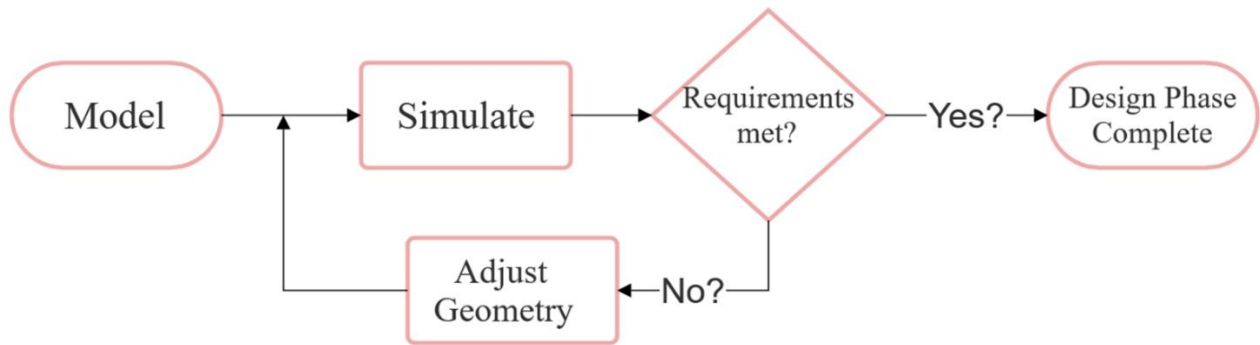


Figure 35. A simplified flow chart outlining the modeling and simulation design phase.

Using the dimensions obtained through Kern's Method in the previous section, a detailed 3D model of the shell and tube heat exchanger was created in SolidWorks (Figure 36). The model aimed to accurately represent the tube arrangement, shell geometry, baffles, and other features as defined by Kern.

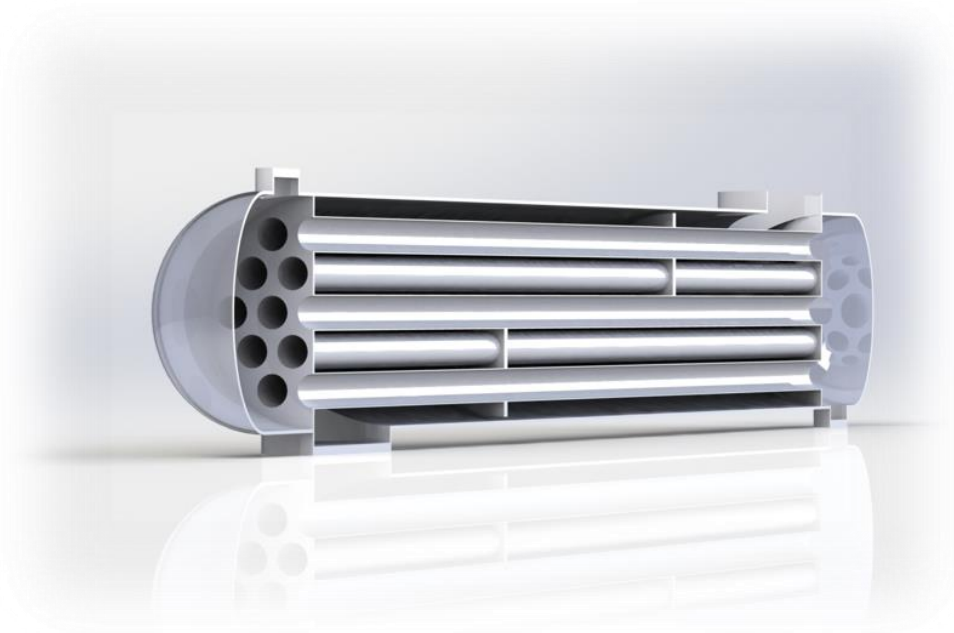


Figure 36. Rendering of the heat exchanger produced the first successful Kern's Method Iteration.

SolidWorks' equation tool allowed the assignment of global variables to key dimensions within the heat exchanger model. These global variables served as placeholders for geometric

parameters such as tube diameter, tube length, baffle spacing, and other relevant design factors, see Figure 37.

Equations, Global Variables, and Dimensions

Filter All Fields

Name	Value / Equation	Evaluates to	Comments
Global Variables			
"Outer Tube Diameter"	= 50.6	50.60	
"Inner Tube Diameter"	= 44.3	44.30	
"Tube Pitch"	= 1.25 * "Outer Tube Diameter"	63.25	
"Tube Bundle Diameter"	= "Outer Tube Diameter" * (16 / 0.319) ^ (1	314.74	
"Shell Inner Diameter"	= 325.7	325.70	
"Length"	= 3250	3250.00	
"Baffle Cut Percent"	= 75	75.00	
"Length Baffle From Left"	= 620	620.00	
"Length Baffle From Right"	= 666.6666667	666.67	
"Nozzle Air Outlet"	= "Shell Inner Diameter"	325.70	
<i>Add global variable</i>			
Features			
<i>Add feature suppression</i>			
Equations			
"D3@Sketch2"	= "Tube Pitch"	63.25mm	
"D1@Sketch4"	= "Length"	3250mm	
"D1@Sketch5"	= "Tube Bundle Diameter" * (100 - "Baffle Cut	78.69mm	
"D1@Sketch8"	= "Tube Bundle Diameter" * (100 - "Baffle Cut	78.69mm	
"D3@Sketch4"	= "Length Baffle From Left"	620mm	
"D4@Sketch4"	= "Length Baffle From Right"	666.67mm	
"D1@Sketch2"	= "Outer Tube Diameter"	50.6mm	
"D2@Sketch2"	= "Inner Tube Diameter"	44.3mm	
"D1@Sketch3"	= "Tube Bundle Diameter"	314.74mm	
"D2@Sketch3"	= "Shell Inner Diameter"	325.7mm	
"D1@Sketch17"	= "Nozzle Air Outlet"	325.7mm	
"D2@Sketch17"	= "D1@Sketch17" / 2 + 5	167.85mm	
"D2@Sketch18"	= "Nozzle Air Outlet"	325.7mm	
"D1@Sketch18"	= "D2@Sketch18" / 2 + 5	167.85mm	

Automatically rebuild Angular equation units: Degrees Automatic solve order
 Link to external file:

OK
 Cancel
 Import...
 Export...
 Help

Figure 37. Defined global variables of the heat exchanger in SolidWorks.

This approach made simulating various design configurations quick and easy, as adjustments to the global variables were seamlessly applied throughout the model. The decision to use global variables was driven by the need for a flexible, iterative design process that could be rapidly modified to meet the criteria of coffee drying. As the simulation results were obtained, adjustments to the global variables became a streamlined means of refining the model without the need for manual, time-consuming inputs to individual dimensions.

After modeling, the simulation setup was initialized and configured to represent the operating conditions of the coffee-drying heat exchanger. The boundary conditions included inlet and outlet specifications for both the shell and tube sides that followed the requirements for the drying of coffee. The comprehensive setup can be found in Appendix K.

Next, the mesh generation process was initiated to ensure reliable simulation results. The initial mesh consisted of 200,000 cells to provide accurate yet quick simulations. Following the completion of the first simulation run post-processing tools within SolidWorks Flow Simulation were used to analyze key goals such as outlet temperatures and pressure drops within the heat exchanger. If the goals were not met, key geometric parameters were adjusted until they were.

The parametric study feature in SolidWorks Flow Simulation was utilized to expedite the iterative design process. The parametric study feature uses the global variables established earlier, allowing for an automatic simulation of various design configurations. The geometric parameters subjected to this project included baffle positions, baffle cut percentage, and the heat exchanger length, all while collecting data on their impact on the heat exchanger. The collected data was analyzed to select the configurations that made the most sense in the context of the project requirements. Finally, after choosing the configuration, the final simulations were then tested for mesh convergence. SolidWorks Flow Simulation's built-in meshing options were used to generate a fine mesh that captured the complexities of fluid flow and heat transfer within the heat exchanger.

4.3 References

- [1] Kern, Donald Q. *Process Heat Transfer*. McGraw-Hill, 1950.
- [2] Coulson, John Metcalfe, et al. "Chapter 12: Heat-Transfer Equipment." *Chemical Engineering*, vol. 6, Butterworth-Heinemann, Oxford Etc., 2005.
- [3] Incropera, Frank P., and David P. DeWitt. "Chapter 11: Heat Exchangers." *Introduction to Heat Transfer*, Wiley, Hoboken, NJ, 2009.
- [4] "Overall Heat Transfer Coefficients." *Engineering ToolBox*, www.engineeringtoolbox.com/heat-transfer-coefficients-exchangers-d_450.html.
- [5] Manrique, Raiza, et al. "Evaluation of the energy density for burning disaggregated and Pelletized Coffee Husks." *ACS Omega*, vol. 4, no. 2, 8 Feb. 2019, pp. 2957–2963, <https://doi.org/10.1021/acsomega.8b02591>.
- [6] Sieder, E. N., and G. E. Tate. "Heat transfer and pressure drop of liquids in tubes." *Industrial & Engineering Chemistry*, vol. 28, no. 12, Dec. 1936, pp. 1429–1435, <https://doi.org/10.1021/ie50324a027>.
- [7] Incropera, Frank P., and David P. DeWitt. "Chapter 8: Internal Flow." *Introduction to Heat Transfer*, Wiley, Hoboken, NJ, 2009.

5.0 Validation of SolidWorks Flow Simulation 2023 for Conjugate Heat Transfer

CFD can be a powerful tool for the simulation and analysis of fluid flow dynamics and heat transfer. However, the accuracy and reliability of CFD computer codes depend on the validation of numerical models against experimental or analytical data. The validation is an important role in the simulation process as it provides a way to assess the accuracy of simulation results and ensure they can represent real-world phenomena. This section provides a validation study focused on the conjugate heat transfer within a concentric tube heat exchanger, utilizing SolidWorks Flow Simulation as the CFD tool. Figure 38 below shows the type of heat exchanger in question.

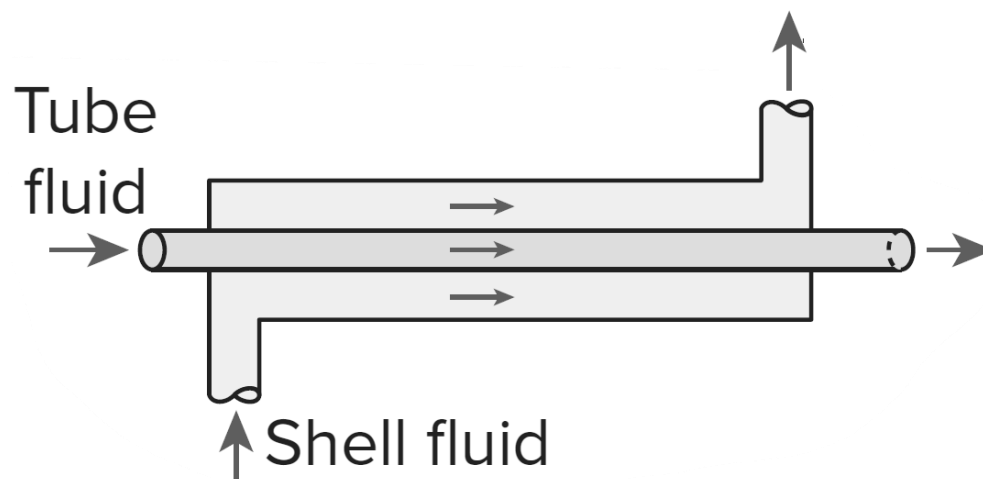


Figure 38. Diagram of a parallel-flow concentric tube heat exchanger

In the validation study done in this project, the effectiveness-Number of Transfer Units (e-NTU) method was used to assess how well the SolidWorks Flow Simulation models heat transfer in a parallel-concentric tube heat exchanger. The LMTD method of analyzing heat exchangers is best utilized when fluid inlet and outlet temperatures are known or can easily be acquired by energy balance. If only the inlet temperatures are known, it is recommended to use an alternative approach called the effectiveness-NTU, or just NTU, method [1]. The use of NTU compares the actual amount of heat transfer to the maximum amount of heat transfer possible by the dimensionless effectiveness, ϵ .

$$\varepsilon = \frac{Q_{actual}}{Q_{max}} \quad (24)$$

where

$$Q_{max} = C_{min}(T_{h,i} - T_{c,i}) \quad (25)$$

C_{min} is the minimum heat capacity rate of the two fluids. The heat capacity rate is defined by $C_1 = \dot{m}_1 c_{p,1}$. In theory, the maximum amount of heat transfer in a counterflow configuration would be equal to the product of the minimum heat capacity rate and the maximum temperature differential if the heat exchanger was of infinite length.

For any heat exchanger, the effectiveness can be described as a function of a dimensionless parameter called the number of transfer units (NTU) and the ratio of minimum to maximum rates of heat capacity, C_R .

$$\varepsilon = f(\text{NTU}, C_R)$$

$$\text{NTU} = \frac{UA}{C_{min}} \quad (26)$$

and

$$C_R = \frac{C_{min}}{C_{max}} \quad (27)$$

The expressions for effectiveness are derived through analysis of the heat exchanger performance. The derivation involves solving the energy balance equations for a heat exchanger subjected to different flow configurations, such as parallel flow and counterflow. Some expressions can be viewed in Table 7 from Incropera, below. The parallel flow arrangement was considered during the validation study.

Table 7. Expressions for the effectiveness of various types of heat exchangers [2].

Heat Exchanger Effectiveness Relations	
Flow Arrangement	Relation
Parallel flow	$\varepsilon = \frac{1 - \exp[-NTU(1 + C_r)]}{1 + C_r}$
Counterflow	$\varepsilon = \frac{1 - \exp[-NTU(1 - C_r)]}{1 - C_r \exp[-NTU(1 - C_r)]} \quad (C_r < 1)$ $\varepsilon = \frac{NTU}{1 + NTU} \quad (C_r = 1)$
Shell-and-tube	
One shell pass (2, 4, . . . tube passes)	$\varepsilon_1 = 2 \left\{ 1 + C_r + (1 + C_r^2)^{1/2} \times \frac{1 + \exp[-(NTU)_1(1 + C_r^2)^{1/2}]}{1 - \exp[-(NTU)_1(1 + C_r^2)^{1/2}]} \right\}^{-1}$
n shell passes ($2n, 4n, . . .$ tube passes)	$\varepsilon = \left[\left(\frac{1 - \varepsilon_1 C_r}{1 - \varepsilon_1} \right)^n - 1 \right] \left[\left(\frac{1 - \varepsilon_1 C_r}{1 - \varepsilon_1} \right)^n - C_r \right]^{-1}$
Cross-flow (single pass)	
Both fluids unmixed	$\varepsilon = 1 - \exp \left[\left(\frac{1}{C_r} \right) (NTU)^{0.22} \{ \exp[-C_r(NTU)^{0.78}] - 1 \} \right]$
C_{\max} (mixed), C_{\min} (unmixed)	$\varepsilon = \left(\frac{1}{C_r} \right) (1 - \exp \{ -C_r [1 - \exp(-NTU)] \})$
C_{\min} (mixed), C_{\max} (unmixed)	$\varepsilon = 1 - \exp(-C_r^{-1} \{ 1 - \exp[-C_r(NTU)] \})$
All exchangers ($C_r = 0$)	$\varepsilon = 1 - \exp(-NTU)$

Most textbooks on heat transfer and fluid mechanics provide expressions and graphs for the NTU relation for various flow styles. Figure 39 below from Cengel shows the relation used to obtain the NTU value for the parallel flow concentric tube heat exchanger being analyzed for the validation study.

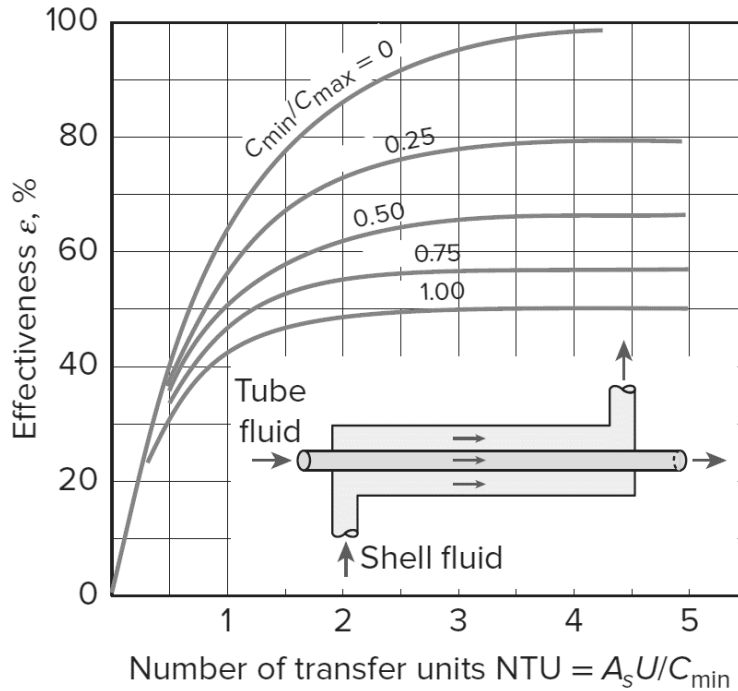


Figure 39. NTU correlation for a parallel flow concentric tube heat exchanger [3].

In summary, the Number of Transfer Units method is a valuable tool for analyzing and predicting the performance of heat exchangers. The NTU method provides a straightforward means of characterizing heat exchanger efficiency by quantifying the relationship between the heat exchanger size, heat transfer rate, and fluid properties. With the method and its components defined, the process of utilizing it to compare to simulation results is shown below in the following passage. This validation study will examine and compare results stemming from laminar, turbulent, and transition regions – all possible flow patterns which may occur in the project’s heat exchanger design.

Table 8. Parameters used for the validation study.

Parameters	Value	Units	Description
\dot{m}_s	0.01	$\frac{\text{kg}}{\text{s}}$	Mass flow rate of the air in the shell.
$T_{t,in}$	75	$^{\circ}\text{C}$	Initial temperature of the shell-side air entering the heat exchanger.
$c_{p,s}$	1.005	$\frac{\text{kJ}}{\text{kg} - \text{K}}$	Specific heat capacity of air.
\dot{m}_t	0.1	$\frac{\text{kg}}{\text{s}}$	Mass flow rate of water in the tube.
$T_{s,in}$	14	$^{\circ}\text{C}$	Initial temperature of the tube-side water entering the heat exchanger.
$c_{p,t}$	4.194	$\frac{\text{kJ}}{\text{kg} - \text{K}}$	Specific heat capacity of water.
$D_{i,shell}$	64	mm	Inner diameter of the shell.
$D_{i,tube}$	38	mm	Inner diameter of the tube.
t_t	5	mm	Thickness of the tube.
L	1500	mm	Length of the heat exchanger.
k_{302SS}	16.3	$\frac{\text{W}}{\text{m} - \text{K}}$	Thermal conductivity of 302 Stainless Steel.
k_{H_2O}	0.663	$\frac{\text{W}}{\text{m} - \text{K}}$	Thermal conductivity of water at 75 $^{\circ}\text{C}$.
k_{air}	0.0267	$\frac{\text{W}}{\text{m} - \text{K}}$	Thermal conductivity of air at the film temperature of 30 $^{\circ}\text{C}$.
ρ_{H_2O}	974.8	$\frac{\text{kg}}{\text{m}^3}$	Density of water at 75 $^{\circ}\text{C}$.
μ_{H_2O}	0.0003765	$\frac{\text{N} - \text{s}}{\text{m}^2}$	Dynamic viscosity of the water at 75 $^{\circ}\text{C}$.
Pr_t	6.904	--	Prandtl number of tube-side water.
ρ_{air}	1.164	$\frac{\text{kg}}{\text{m}^3}$	Density of air at the film temperature of 30 $^{\circ}\text{C}$.
μ_{air}	1.872×10^{-5}	$\frac{\text{N} - \text{s}}{\text{m}^2}$	Dynamic viscosity of the shell-side air at the film temperature of 30 $^{\circ}\text{C}$.
Pr_s	0.728	--	Prandtl number of shell-side air at 30 $^{\circ}\text{C}$.

For the validation study, a stainless-steel heat exchanger was considered with the tube side flow being hot water and the shell side being air. The dimensions and parameters are defined above in Table 8. First, the heat capacity rates of the shell and tube heat exchanger was determined.

$$C_s = \dot{m}_s c_{p,s} = 0.01 \frac{\text{kg}}{\text{s}} \times 1.005 \frac{\text{kJ}}{\text{kg} - \text{K}} = 10.05 \frac{\text{W}}{\text{K}} \quad (28)$$

and for tube side,

$$C_t = \dot{m}_t c_{p,t} = 0.1 \frac{\text{kg}}{\text{s}} \times 4.194 \frac{\text{kJ}}{\text{kg} - \text{K}} = 419.4 \frac{\text{W}}{\text{K}}$$

$$C_{min} = C_s = 10.05 \frac{\text{W}}{\text{K}}$$

Therefore, the maximum heat transfer rate possible with this heat exchanger is calculated using Equation 25.

$$Q_{max} = C_{min}(T_{h,i} - T_{c,i}) = 10.05 \frac{\text{W}}{\text{K}} (75 \text{ }^\circ\text{C} - 14 \text{ }^\circ\text{C}) = 613.05 \text{ W}$$

The next step is to calculate the UA value to obtain the NTU value. This requires the determination of the Reynolds number of the tube side and shell side flow to obtain the overall heat transfer coefficient. The Reynolds number can predict whether the flow will behave in a turbulent, laminar, or combined manner. For laminar flow, $Re < 2000$, the flow is smooth and orderly. Fluid elements move in parallel layers with minimal mixing between them. The motion is characterized by a well-defined flow pattern and low levels of turbulence. Transitional flow ranges from $2000 < Re < 4000$. In this range, the flow is transitioning from laminar to turbulent. It may exhibit some characteristics of both laminar and turbulent flow, and the flow pattern can be unstable. Turbulent flow occurs at $Re > 4000$. In this range, the flow is chaotic and characterized by random fluctuations and mixing of fluid elements. Turbulent flow is more energetic and can result in increased heat and mass transfer compared to laminar flow. However, these ranges are approximations and depend on surface roughness, geometry, and disturbances.

The tube side Reynolds numbers depends on the velocity of the fluid and is obtained as follows:

$$V_t = \frac{4\dot{m}_t}{\pi D_{i,tube}^2 \rho_{H_2O}} = \frac{4(0.1 \frac{kg}{s})}{\pi \times 0.064^2 m^2 \times (974.8 \frac{kg}{m^3})\pi} = 0.0904 \frac{m}{s} \quad (29)$$

$$Re_t = \frac{\rho_{H_2O} V_t D_{i,tube}}{\mu_{H_2O}} = \frac{974.8 \frac{kg}{m^3} (0.0904 \frac{m}{s}) (0.038 m)}{0.0003765 \frac{N \cdot s}{m^2}} = 8900 \quad (30)$$

Since $Re_t = 8900 > 4000$, the flow within tube is turbulent. A correlation developed by Gnielinski, Nu_{tube} , is valid for smooth tubes over a large range of Reynolds number and depends on a friction factor, f_t , of a smooth tube which is determined by the Petukhov equation [4]. Both are expressed by:

$$f_t = \frac{1}{(0.790 \ln(Re_{tube}) - 1.64)^2} = \frac{1}{(0.790 \ln(8900) - 1.64)^2} = 0.0325 \quad (31)$$

$$Nu_{tube} = \frac{(f_t/8)(Re_{tube} - 1000)Pr_t}{1 + 12.7 \left(\frac{f_t}{8}\right)^{\frac{1}{2}} (Pr_t^{\frac{2}{3}} - 1)} \quad (32)$$

$$Nu_{tube} = \frac{(0.0325/8)(8900 - 1000)(6.904)}{1 + 12.7 \left(\frac{0.0325}{8}\right)^{\frac{1}{2}} (6.904^{\frac{2}{3}} - 1)} = 70.94$$

The tube-side convection heat transfer coefficient is calculated from

$$h_i = \frac{k_{H_2O} Nu_{tube}}{D_{i,tube}} = \frac{0.663 \frac{W}{m \cdot K} (70.94)}{0.038 \text{ m}} = 1237.7 \frac{W}{m^2 \cdot K} \quad (33)$$

Repeating for the shell-side air,

$$V_s = \frac{4\dot{m}_s}{(D_{i,shell}^2 - D_{o,tube}^2)\rho_{air}\pi} = \frac{4(0.01 \frac{kg}{s})}{\pi \times (0.064^2 \text{ m}^2 - 0.048^2 \text{ m}^2)(1.164 \frac{kg}{m^3})} = 6.104 \frac{m}{s}$$

$$Re_{shell} = \frac{\rho_{air} V_s (D_{i,shell} - D_{o,tube})}{\mu_{air}} = \frac{1.164 \frac{kg}{m^3} (6.104 \frac{m}{s})(0.064 \text{ m} - 0.048 \text{ m})}{1.872 \times 10^{-5} \frac{N \cdot s}{m^2}} = 6073$$

Therefore, the shell-side flow is also considered turbulent. According to Kays and Perkins, if the shell-side flow is laminar, then the Nusselt correlation depends on the ratio of the outer tube diameter and the inner shell diameter [4]. Table 9 below lists some values and can be interpolated.

Table 9. Kay and Perkins Nusselt Correlations for shell-side flow in a concentric tube HXR.

$\frac{D_{o,tube}}{D_{i,shell}}$	Nu_{shell}	Nu_{tube}
0	--	3.66
0.05	17.46	4.06
0.10	11.56	4.11
0.25	7.37	4.23
0.50	5.74	4.43
1.00	4.86	4.86

Continuing similarly to the tube-side calculations:

$$f_s = \frac{1}{(0.790 \ln(Re_{shell}) - 1.64)^2} = \frac{1}{(0.790 \ln(6073) - 1.64)^2} = 0.0364$$

$$Nu_{shell} = \frac{(f_s/8)(Re_s - 1000)Pr_s}{1 + 12.7 \left(\frac{f_s}{8}\right)^{\frac{1}{2}} (Pr_s^{\frac{2}{3}} - 1)} = \frac{(0.0364/8)(6073 - 1000)(0.728)}{1 + 12.7 \left(\frac{0.0364}{8}\right)^{\frac{1}{2}} (0.728^{\frac{2}{3}} - 1)} = 20.08$$

The shell-side convection heat transfer coefficient is then

$$h_o = \frac{k_{air} Nu_{shell}}{D_{i,shell} - D_{o,tube}} = \frac{0.0267 \frac{W}{m \cdot K} (20.08)}{(0.064 \text{ m} - 0.048 \text{ m})} = 33.5 \frac{W}{m^2 \cdot K}$$

Finally for the overall heat transfer coefficient,

$$\frac{1}{UA} = \frac{1}{h_i D_{i,tube} \pi L} + \frac{\ln\left(\frac{D_{o,tube}}{D_{i,tube}}\right)}{2\pi L k_{302SS}} + \frac{1}{h_o D_{o,tube} \pi L} \quad (34)$$

$$\frac{1}{UA} = \frac{1}{1237.8(0.038)\pi(1.5)} + \frac{\ln\left(\frac{0.048}{0.038}\right)}{2\pi(1.5)(16.3)} + \frac{1}{33.5(0.048)\pi(1.5)} = 0.1380 \frac{K}{W}$$

$$UA = 7.25 \frac{W}{K}$$

For a parallel flow concentric heat exchanger,

$$\varepsilon = \frac{1 - e^{-NTU(1+C_R)}}{1 + C_R} \quad (35)$$

where (from Equation 27)

$$C_R = \frac{C_{min}}{C_{max}} = \frac{10.05 \frac{W}{K}}{419.4 \frac{W}{K}} = 0.0240$$

and

$$NTU = \frac{UA}{C_{min}} = \frac{7.25 \frac{W}{K}}{10.05 \frac{W}{K}} = 0.7212$$

The effectiveness of this heat exchanger is

$$\varepsilon = \frac{1 - e^{-0.7212(1+0.024)}}{1 + 0.024} = 0.51$$

The actual amount of heat being transferred within the parallel flow heat exchanger can be determined by

$$\dot{Q} = \varepsilon * \dot{Q}_{max} = 0.51 * 613.05 W = 312.6 W$$

Finally, the outlet temperatures of each fluid can be determined from the energy equation from the heat exchanger

$$\dot{Q} = \dot{m}c_p(T_{in} - T_{out})_t = \dot{m}c_p(T_{out} - T_{in})_s$$

The shell-side temperature will be considered for the validation study. Solving for the outlet temperature:

$$T_{out,s} = \frac{\dot{Q}}{\dot{m}_s c_{p,s}} + T_{in,s} = \frac{312.6 W}{0.01 \frac{kg}{s} \times 1005 \frac{J}{kg - K}} + 14^\circ C = 45.1052^\circ C$$

This calculated outlet temperature value of the shell-side fluid was compared with the results of SolidWorks Flow Simulation.

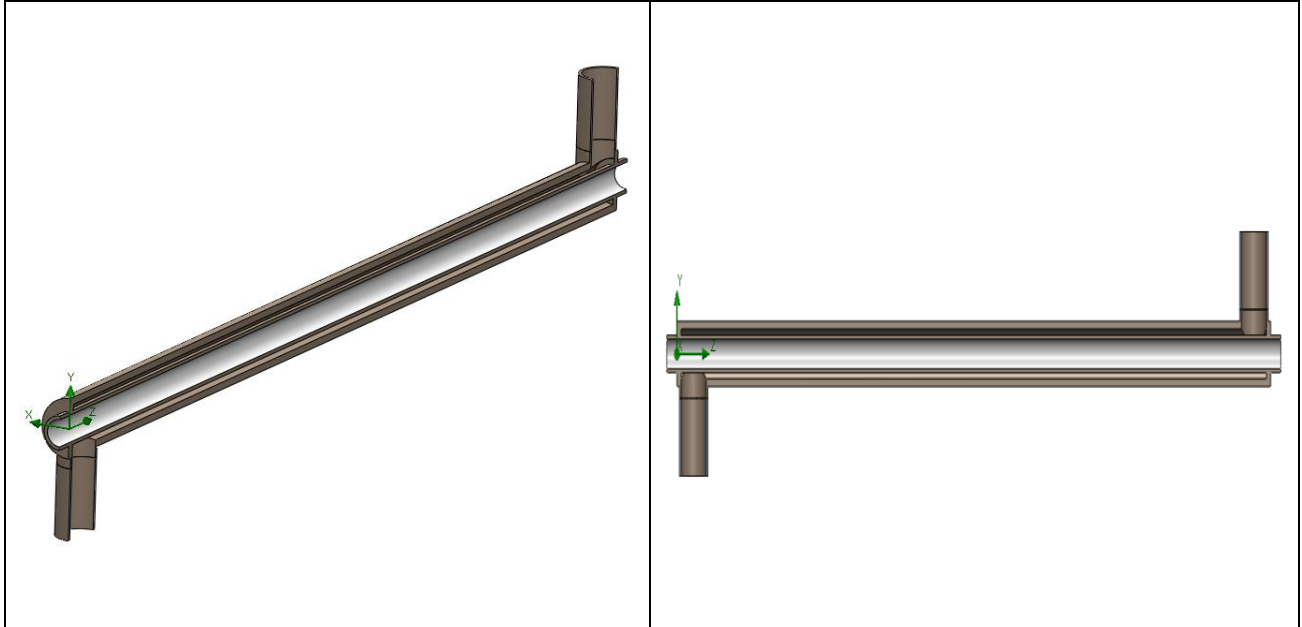


Figure 40. Solidworks Model of the concentric tube HXR for the validation study.

A 3D model in SolidWorks was developed for the heat exchanger as shown in the Figure 40 above. The 3D model was set up using the exact parameters as shown in the analytical discussion. The SWFS settings and MATLAB code for the validation can be found in Appendices I & J respectively. Simulations were performed using the parameters defined in the analytical section above. The mass flow rate on the shell side varied from 0.001 to 0.01 and the outlet temperature of the fluid was documented. Figure 41 below illustrates a comparative analysis between simulation results and analytical predictions. The data captured spans a spectrum of shell side fluid flow regimes, ranging from laminar, mixed, and turbulent flow.

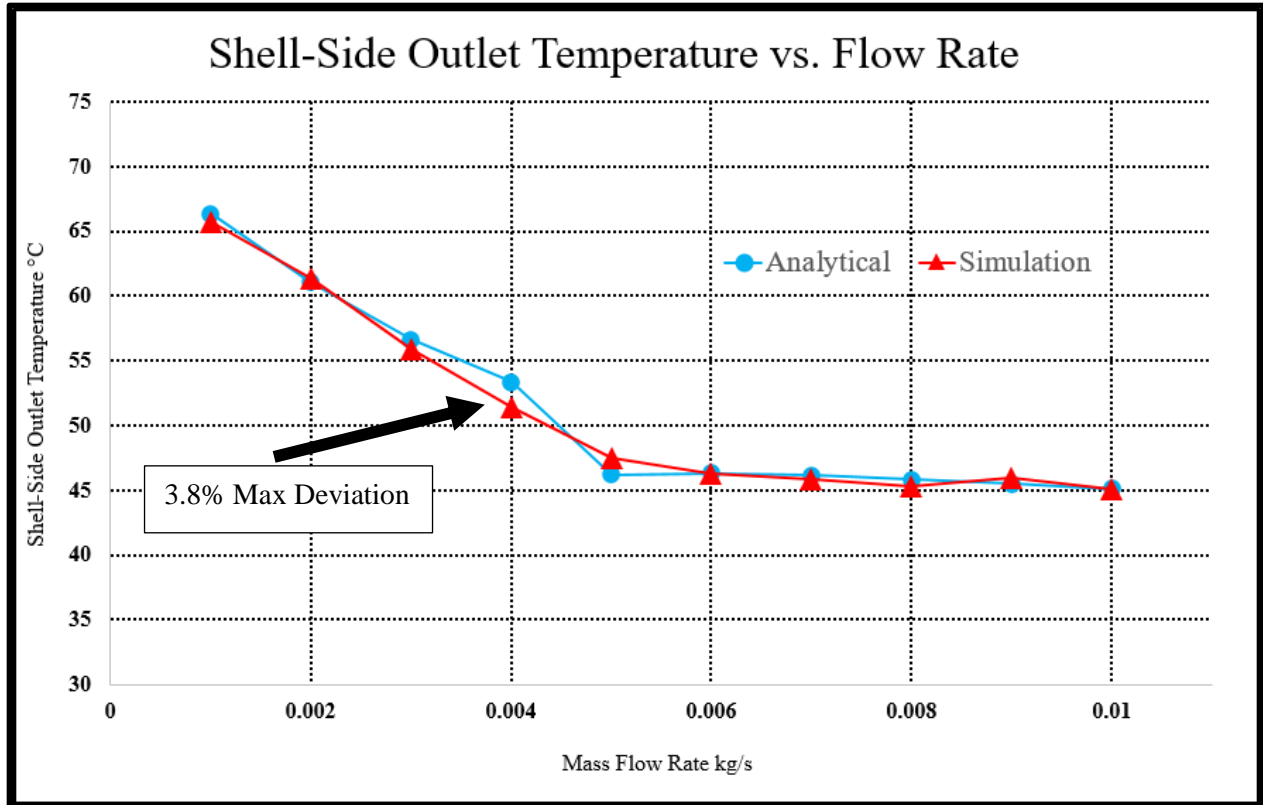


Figure 41. The results of the SolidWorks Flow Simulation 2023 Study.

The Nusselt correlations used for the different flow patterns are listed below

$Nu = 5.6$	$Re_s < 1200$	(Kays and Perkins)
$Nu = 0.26Re_s^{0.5}Pr_s^{0.37}$	$1200 < Re_s < 4000$	(Zukauskas [5])
$Nu = \frac{(f_s/8)(Re_s - 1000)Pr_s}{1 + 12.7\left(\frac{f_s}{8}\right)^{\frac{1}{2}}(Pr_s^{\frac{2}{3}} - 1)}$	for $Re_s > 4000$	(Gnielinski)

The most significant deviation between simulation and analytical results occurred in the mixed flow region, with a percent difference of 3.8%. The transition region poses challenges in analysis due to its inherent uncertainties that occur within that style of flow. Despite this, the overall comparison indicates that the simulation and analytical results are generally within a reasonable range, with deviations consistently below 10%. This validation was deemed acceptable and strengthened the project's confidence in the suitability of SolidWorks Flow Simulation for the simulation of the heat exchanger being designed.

5.1 References

- [1] W. M. Kays and H. C. Perkins. In Handbook of Heat Transfer, W. M. Rohsenow and J. P. Hartnett, eds. New York: McGraw-Hill, 1972, Chap. 7.
- [2] Incropera, Frank P., and David P. DeWitt. "Chapter 11: Heat Exchangers." Introduction to Heat Transfer, Wiley, Hoboken, NJ, 2009.
- [3] Çengel, Yunus A., et al. "Chapter 22: Heat Exchangers." Fundamentals of Thermal-Fluid Sciences, McGraw-Hill Higher Education, New York, 2012.
- [4] Matsson, John. "Chapter 8: Heat Exchanger." An Introduction to SOLIDWORKS Flow Simulation 2022, SDC Publications, 2022.
- [5] A. Zukauskas. Heat Transfer from Tubes in Crossflow. Advances in Heat Transfer, 8:93-160, 1972.

6.0 Results

The section provides a comprehensive summary of the outcomes obtained through Kern's approach. Then, it presents an analysis of the SolidWorks Flow Simulation conducted on the shell and tube heat exchanger. The parametric study and simulation results are thoroughly examined and discussed, highlighting the key performance indicators of the heat exchanger.

The first successful iteration from Kern's method was modeled and simulated. The results are shown below in Figure 42.

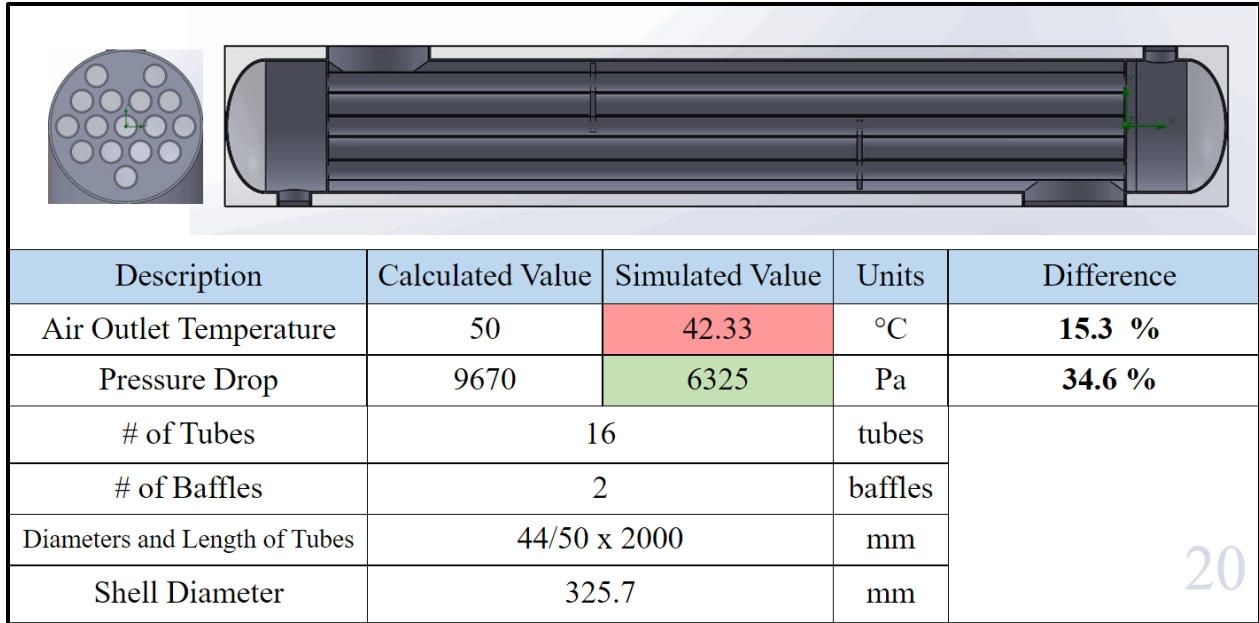


Figure 42. Simulation Results of the first successful Kern's Method iteration.

The heat exchanger consisted of 16 (44 mm x 50 mm) tubes and two baffles, and the tube bundle was 2,000 mm long with a 325.7 mm inner shell diameter. The simulated air outlet temperature value was 15.3% less than the target 50 °C at 42.33 °C. However, the simulation demonstrated a notable improvement in pressure drop performance. The simulated pressure drop surpassed Kern's Method predictions by 34.6%, improving from 9670 to 6325 pascals. This difference suggests that while the initial design, guided by Kern's Method, did not meet the desired temperature criterion, it showed a more favorable pressure drop. However, it was still a considerable difference from the 1000 Pa goal. The larger discrepancy in the pressure drop coincides with the disadvantage of the method mentioned in the Methodology section of this report, as it does not include the stream leaks of the shell-side fluid. The difference between the predicted and simulated results denotes the importance of design through simulations.

From this first model and simulation, geometric changes were made to reach the requirements set by coffee drying. Figure 43 below shows the flow pattern of drying air as it moves through the heat exchanger.

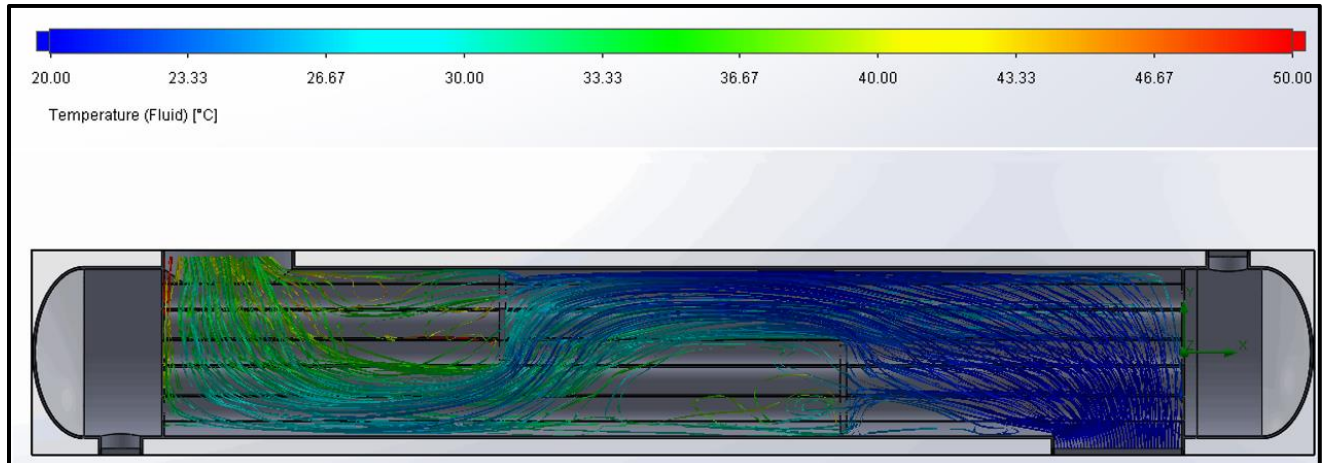


Figure 43. Flow path of the drying air through the heat exchanger.

Upon evaluation, it was noticeable that the baffle on the air inlet side of the heat exchanger provided little to no benefit to heat transfer, contributing needlessly to the pressure drop. For this reason, the decision to remove the baffle was made. Another decision was to fill in the tube bundle to increase the number of tubes from 16 to 19, as shown in Figure 44 below. This was done to improve the heat transfer surface area and to induce more turbulence. However, these changes did not affect the simulation results enough to satisfy the requirements of coffee drying. Further studies were conducted.

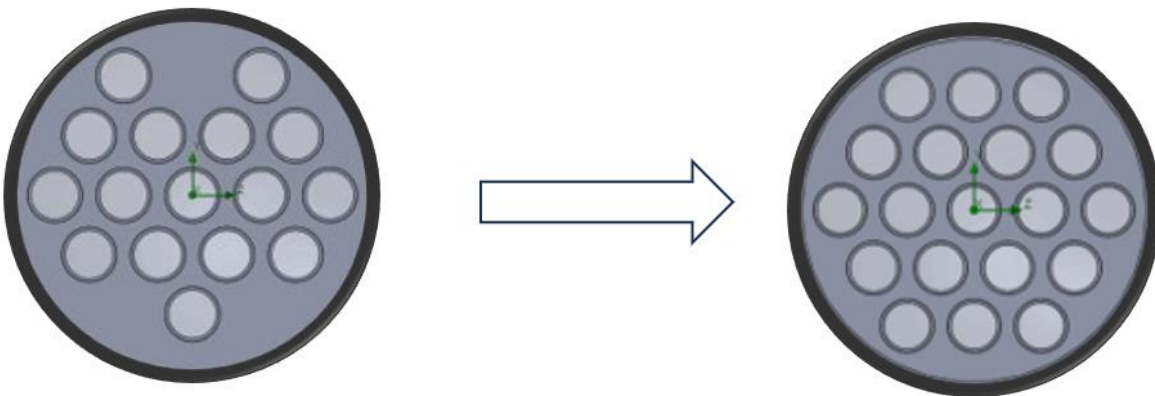


Figure 44. Addition of tubes to fill out the bundle.

As mentioned in the methodology section, a parametric study was conducted to systematically investigate the influence of key design parameters on the performance of the heat exchanger. This study utilized the global variables established in the SolidWorks model, specifically targeting variations in baffle positions, baffle cut percentage, and the length of the heat exchanger. The results of the parametric study are presented in Figures 45 & 46 below. A total of 108 configurations were observed. The data includes outlet temperatures of both fluids, pressure drop within the shell side, and trends seen across the different configurations.

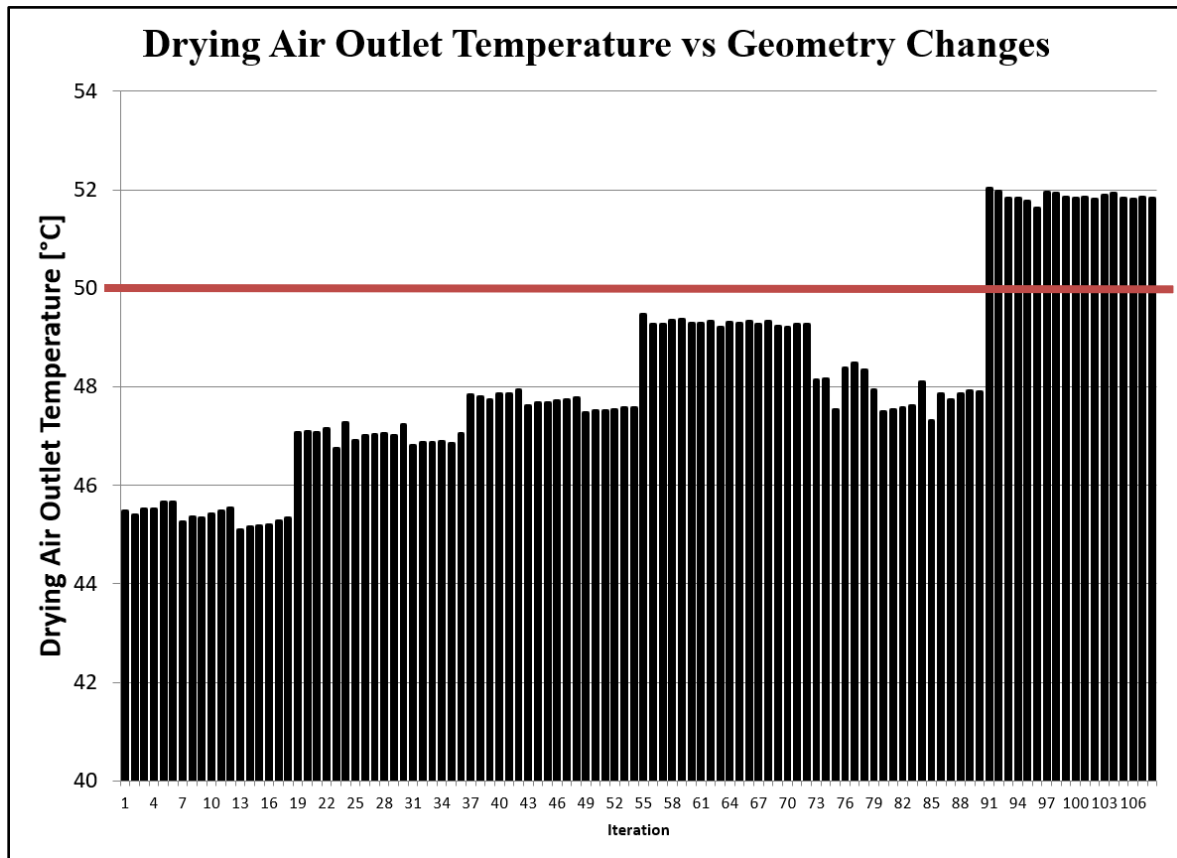


Figure 45. Drying Air Outlet Temperature vs Geometry Changes.

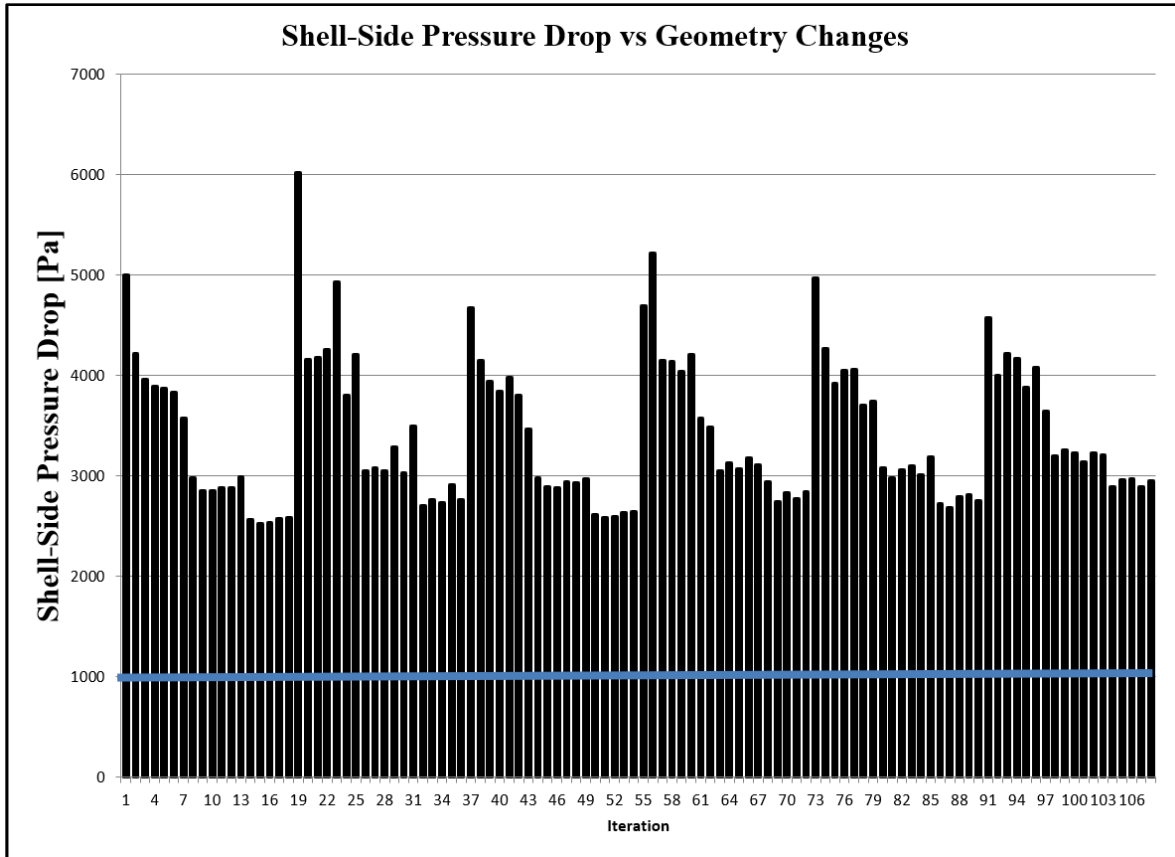


Figure 46. Shell-side Pressure Drop vs. Geometry Changes.

The parametric study provided valuable insights into the sensitivity of the heat exchanger's performance to variations in these design parameters. The trend in the data showed that the heat exchanger length was the most influential factor affecting the drying air outlet temperature, with longer configurations exhibiting notable improvements in achieving the targeted temperature. The data shows the length being extended from 2.25 to 3.25 meters in iterative order. The drying air outlet temperature increased linearly until reaching 3.05 meters (~iteration #75 in Figure 45), where the outlet temperature output was less than the shorter heat exchanger. This raised concerns, and a study was conducted in this section to determine whether the simulation produced false results. Possible reasons for these discrepancies were explored, including potential interactions between design parameters not adequately captured in the parametric study. The investigation confirmed that the results from the parametric study were misleading. Figure 47 below shows a difference between the individual simulation at length at 3.05 meters and the results produced by the parametric analysis. The outlet temperature in the parametric study was ~ 48 °C; the individual study produced a temperature of 50 °C.

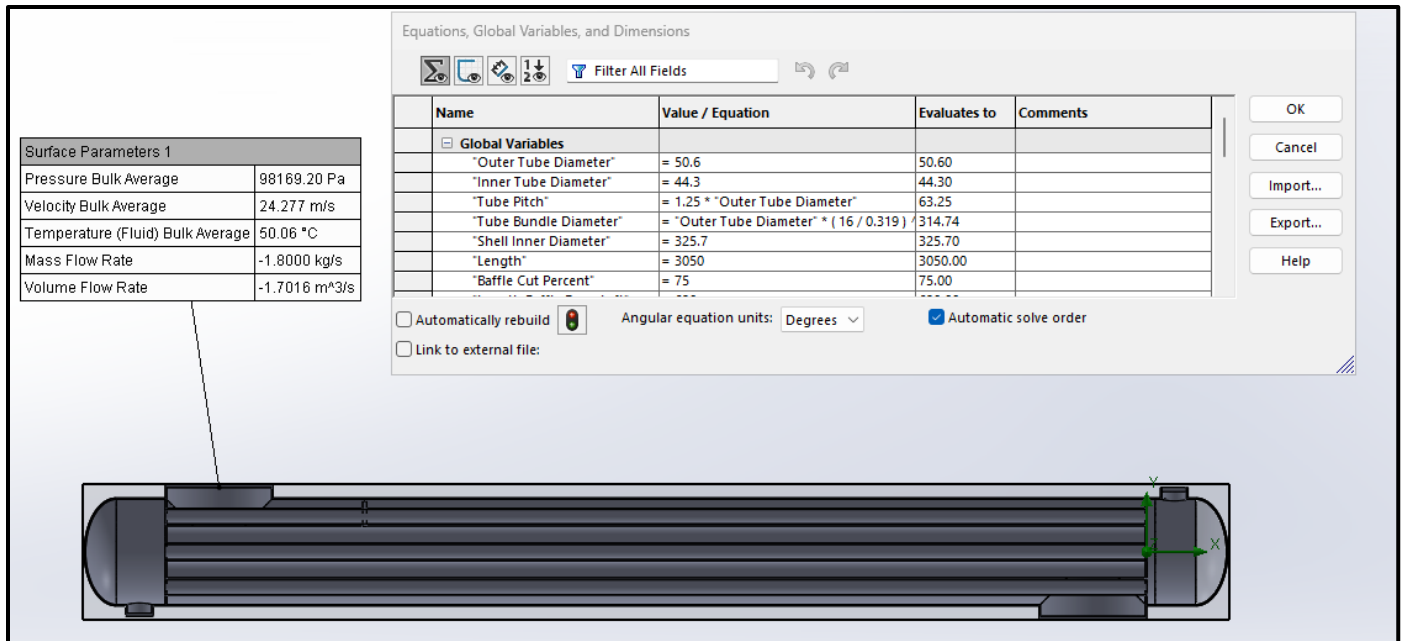


Figure 47. Investigation of Misleading Simulation Results.

This was a reminder of the importance of predicting outcomes with sound engineering principles. It was a reminder of how engineering judgment plays a crucial role in interpreting the results, identifying anomalies, and validating the modifications rather than relying solely on the numerical outputs of the simulation.

For the pressure drop on the shell-side flow, it was shown that baffle spacing, and baffle percent cut were deemed the most influential. Adjustments to these parameters resulted in noticeable changes in pressure drop. This helped in optimizing baffle arrangements for operational efficiency.

The optimal configuration was selected through the parametric study iteration that hit the 50 °C outlet temperature target while keeping the pressure drop at its lowest. However, the pressure drop goal of less than 1000 pascals was never met. The reasoning is that heat exchangers in coffee drying practice involve combustion and radiation that was out of this project's scope. Figure 48 below shows the final design characteristics.

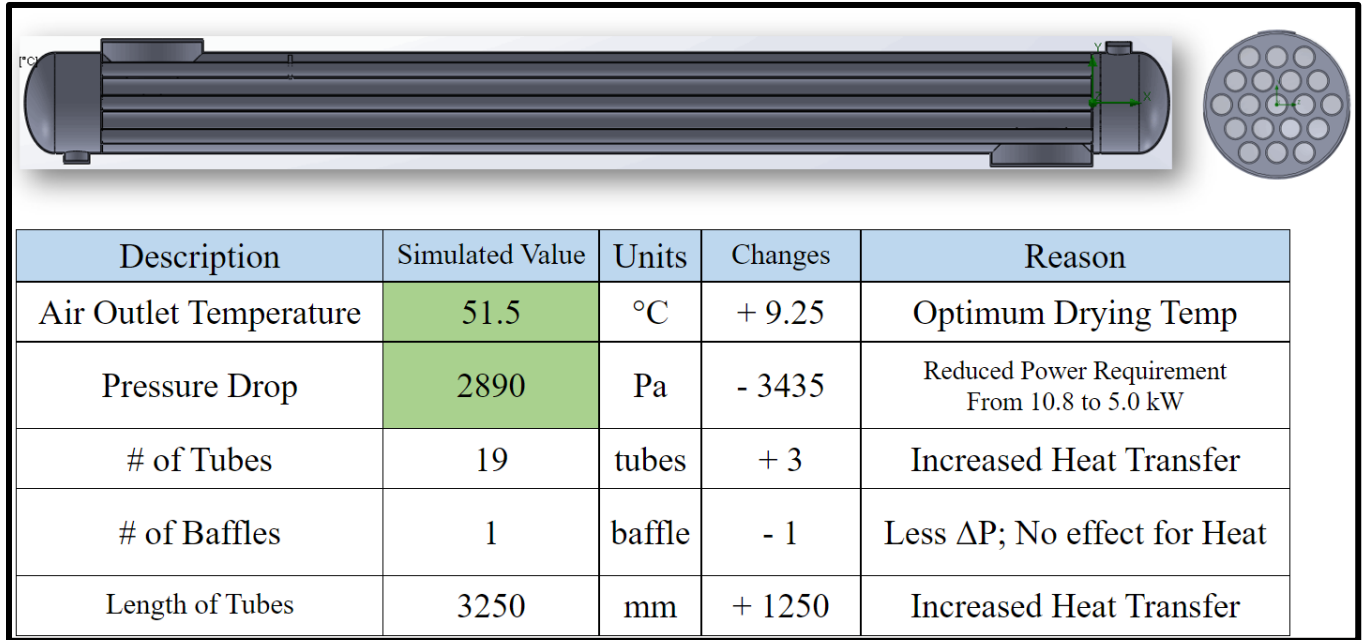


Figure 48. Final simulation iteration.

The final heat exchanger design consisted of 19 (44 mm x 50 mm) tubes, one baffle cut 75%, and the tube bundle was 3.25 meters long with a 325.7 mm inner shell diameter. The simulated air outlet temperature value reached 51.5°C, producing a pressure drop of 2890 Pascals. The results are compared to the initial design from Kern's method. The number and tube lengths were increased by three tubes and 1.25 meters to increase the heat transfer area. Removing the baffle reduced the pressure drop within the heat exchanger by 3435 pascals. Figure 49 below shows the behavior of the air temperature as it flows through the heat exchanger.

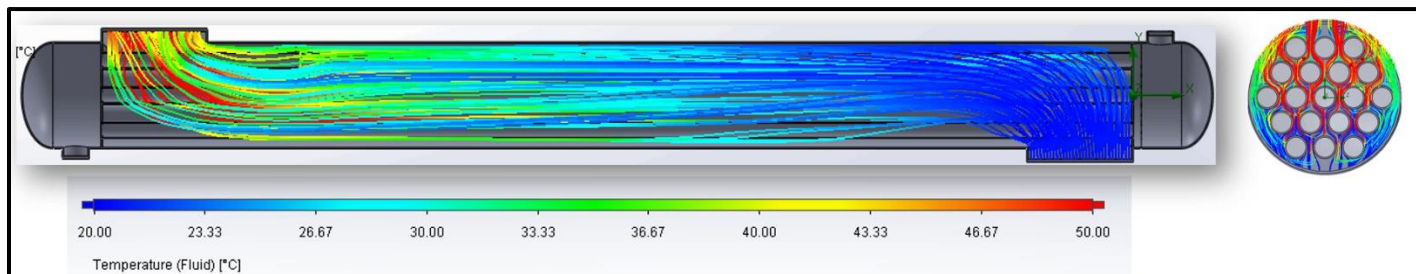


Figure 49. Drying Air Flow Within the Final Design Simulation.

The final evaluation of the designed heat exchanger will be based on several key metrics to assess its efficiency and practicality. The first metric, mesh convergence, ensures the reliability of simulation results by observing the stability of key parameters with increasing mesh resolution. This validation process is crucial to confirm that the outcomes are robust and not overly influenced by the mesh settings. Table 10 and Figure 50 below shows how the simulation results behave as the final model mesh increases.

Table 10. Mesh Convergence of Final Design

	Design Point 1	Design Point 2	Design Point 3	Design Point 4	Design Point 5
Total cells	58395	111260	244352	577352	1407601
Air Outlet Temp [°C]	51.2010584	50.95374879	50.56029141	50.865567	50.65448325
Shell-Side Pressure [Pa]	96231.07798	97530.24776	97975.25565	98369.43742	98416.57645

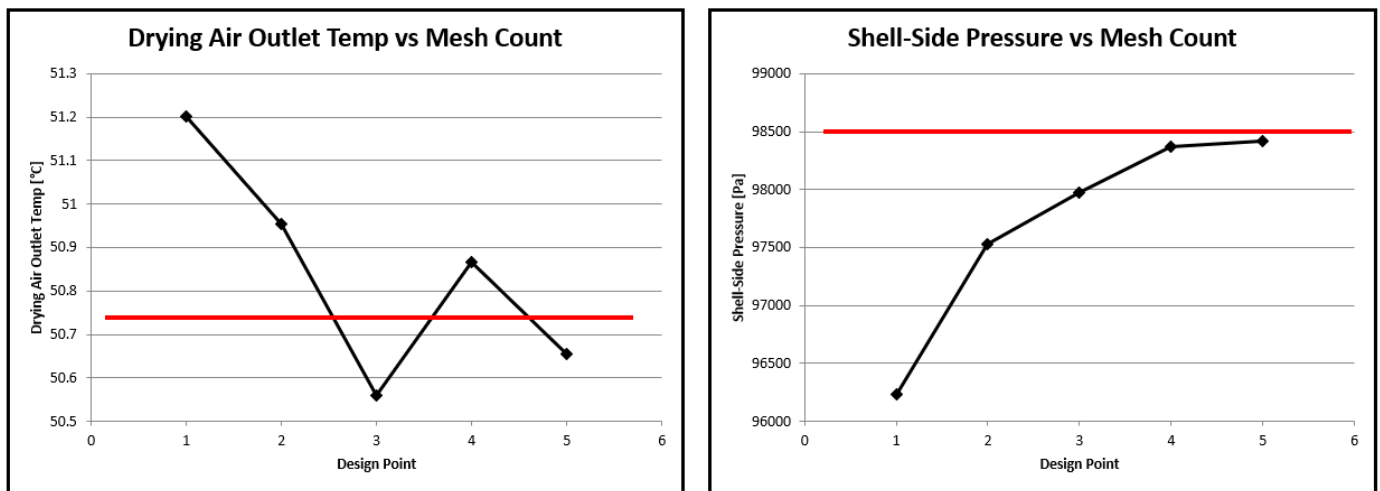


Figure 50. Plot of Mesh Convergence of Final Design.

As the cell count increases (from design point 1 to 5), the outlet air temperature converges alternately towards 50.75 °C, and the shell-side pressure converges towards 98500 pascals. This reinforces the simulation results as they are shown to be mesh independent.

Another important consideration is the power requirement to overcome pressure drop within the heat exchanger. Calculating the energy consumption associated with moving the fluid through the system helps plan for fan selection and overall energy efficiency. This metric directly addressed the operational costs tied to the pressure drop. The power requirement to overcome pressure drop in a system can be calculated using the following formula, which is

based on the fundamental relationship between power (P), pressure, and volumetric flow rate (\dot{V}) in a fluid system

$$P = \Delta P \times \dot{V} \quad (36)$$

$$P = 2890 \frac{\text{N}}{\text{m}^2} \times 1.702 \frac{\text{m}^3}{\text{s}} = 4.9 \text{ kW}$$

This power requirement, along with losses from piping/ductwork and the drying chamber and fan efficiency, would be used to determine the fan size for the entire system.

A simple cost analysis based on tube weight provides a preliminary estimation of the economic implications associated with the materials used in the heat exchanger, particularly focusing on the weight of tubes. This analysis contributes to a basic understanding of the economic considerations tied to material selection. Manufacturing costs to form the tubes are acknowledged but not quantified. The most common manufacturing method is to use a tube mill. A flat strip of 6mm thick 321 stainless steels would be passed through a series of rollers to form it into a 3.25-meter cylinder. The edges of the strip are then welded together to create a continuous tube. Post processes would be applied to achieve the desired properties. The final weight of the 19 tubes of 321 stainless steel is 232 kilograms (513 pounds).

The final performance metric will be the effectiveness of the heat exchanger. This is the same effectiveness that was discussed in the validation section. Calculating this offers a measure of performance relative to the idealized model which helps assessing the overall efficiency of the heat exchanger. For the reader's convenience, it is presented again below

$$\varepsilon = \frac{Q_{simulation}}{Q_{max}} = \frac{1.8 \frac{\text{kg}}{\text{s}} (1007 \frac{\text{J}}{\text{kg} - \text{K}})(51.5^\circ\text{C} - 22^\circ\text{C})}{0.08 \frac{\text{kg}}{\text{s}} (1148 \frac{\text{J}}{\text{kg} - \text{K}})(820^\circ\text{C} - 22^\circ\text{C})} = 0.729$$

7.0 Conclusion

Economic Analysis

While conventional economic analyses with direct cost evaluations may not apply to this research-oriented project, its potential economic impact on industrial operations is substantial. As a proof-of-concept endeavor, the current phase serves as an initial exploration into the design and simulation of an innovative heat exchanger system. The envisioned implementation of this technology in industrial plants could yield remarkable cost reductions. By optimizing energy consumption, reducing man-hours through increased efficiency, and enhancing waste management practices, the long-term economic benefits are exponential. This forward-looking perspective underscores the transformative potential of the designed heat exchanger system in contributing to the financial sustainability and competitiveness of industries reliant on similar thermal processes.

Future Work

In contemplating future trajectories for this project, several critical aspects warrant attention.

- **Different Software Simulation:** In the pursuit of advancing the project's reliability and applicability, future work should include an in-depth exploration of various simulation software platforms. While SolidWorks Flow Simulation has been instrumental in the current phase, cross-validating results with alternative software can provide a more comprehensive understanding. The comparative analysis of different simulations, perhaps using platforms like ANSYS Fluent or COMSOL Multiphysics, aims to enhance result accuracy and reliability. Each software package may have unique strengths and specialties, contributing to a more nuanced comprehension of the heat exchanger's performance under diverse conditions. This approach addresses the inherent uncertainties in simulation outcomes and ensures that conclusions drawn are robust and applicable across different computational environments.
- **Model Built:** Although constructing a physical model was not feasible within the current project's constraints, its realization stands as a critical step in the project's progression. Future endeavors should prioritize the construction of a scaled or prototype model of the heat exchanger system. This model will serve as a tangible representation of the theoretical design, offering insights into its practical functionality. Through

experimentation and testing, the model can validate the precision of the simulations and design assumptions. This hands-on approach is invaluable for identifying potential challenges, optimizing the design for real-world conditions, and ensuring the seamless integration of the heat exchanger system into industrial processes. The construction of a model is an indispensable phase in the transition from theoretical concepts to tangible, practical applications.

Lessons Learned

Engineering Design

The journey through this senior design project has been a profound learning experience in the realm of engineering design. It exposed the intricacies of conceptualizing, refining, and validating a complex system like a heat exchanger for a mechanical coffee drying system. Navigating through the design process unveiled the importance of meticulous attention to details, iterative improvements, and a deep understanding of interdisciplinary principles. Challenges encountered provided opportunities for creative problem-solving, honing skills in simulation tools, material selection, and system optimization. Also, in this project we were able to apply lessons learned from previous classes' content as heat transfer and fluid thermal design giving us an insight into a real-life application that could be implemented in the future. We also were able to utilize software tools and applications that were not taught in class, but through self-learning we are able to manage and produce an engineering final design of the project.

Teamwork Experience

Collaboration within a diverse team has been a cornerstone of this senior design project.

To develop the different tasks needed to complete this project, different sections were assigned to team members in order to maximize the amount of work produced in the reduced time frame available. After the assigned tasks were completed, the team members met on a weekly basis to discuss the results and findings and propose any desired changes or further work needed.

Microsoft teams were used to create a Team chat where files were shared, and also files were modified in real time being able to observe the advances done by the others team members. Also, Microsoft Outlook was used as an official way of communication with the faculty advisor and

team members, also being able to create appointments and schedule group meetings to complete tasks in the desired time frames.

The intricacies of designing a heat exchanger demanded cohesive teamwork, where the strengths of each team member were harnessed for the project's success. This experience underscored the importance of effective communication, shared responsibility, and mutual respect. Managing diverse perspectives, harnessing individual expertise, and aligning efforts towards a common goal were key lessons. Going through challenges as a team reinforced the notion that collective intelligence often surpasses individual brilliance in tackling complex engineering problems. The teamwork experience in this project is a small reflection of real-world engineering projects, emphasizing the interpersonal and organizational skills essential for professional success.

Final Thoughts

In conclusion, the senior design project focused on the design and simulation of a heat exchanger for a mechanical coffee drying system has been an enriching endeavor. Through rigorous engineering design processes and collaborative efforts, the project aimed not only to create an efficient system but also to instill critical skills in problem-solving, decision-making, and interdisciplinary collaboration. The design considerations, simulation results, and proposed improvements reflect the culmination of theoretical knowledge into a practical application. The final heat exchanger design consisted of 19 (44 mm x 50 mm) tubes, one baffle cut 75%, and the tube bundle was 3.25 meters long with a 325.7 mm inner shell diameter. The simulated air outlet temperature value reached 51.5°C, producing a pressure drop of 2890 Pascals. Therefore, this project achieved the desired thermal efficiency of the system as well as the desired outlet temperature needed for the application of the project, however, the pressure requirements were not met due to the nature of the mechanical equipment used, which will need further studies in order to improve its performance.

This project serves as a testament to the multifaceted nature of engineering challenges and the continuous pursuit of innovation and excellence in addressing them. While the current design represents a significant milestone, it also lays the groundwork for future iterations, improvements, and the eventual realization of efficient and sustainable mechanical coffee drying systems.

APPENDIX

A: System Hierarchy

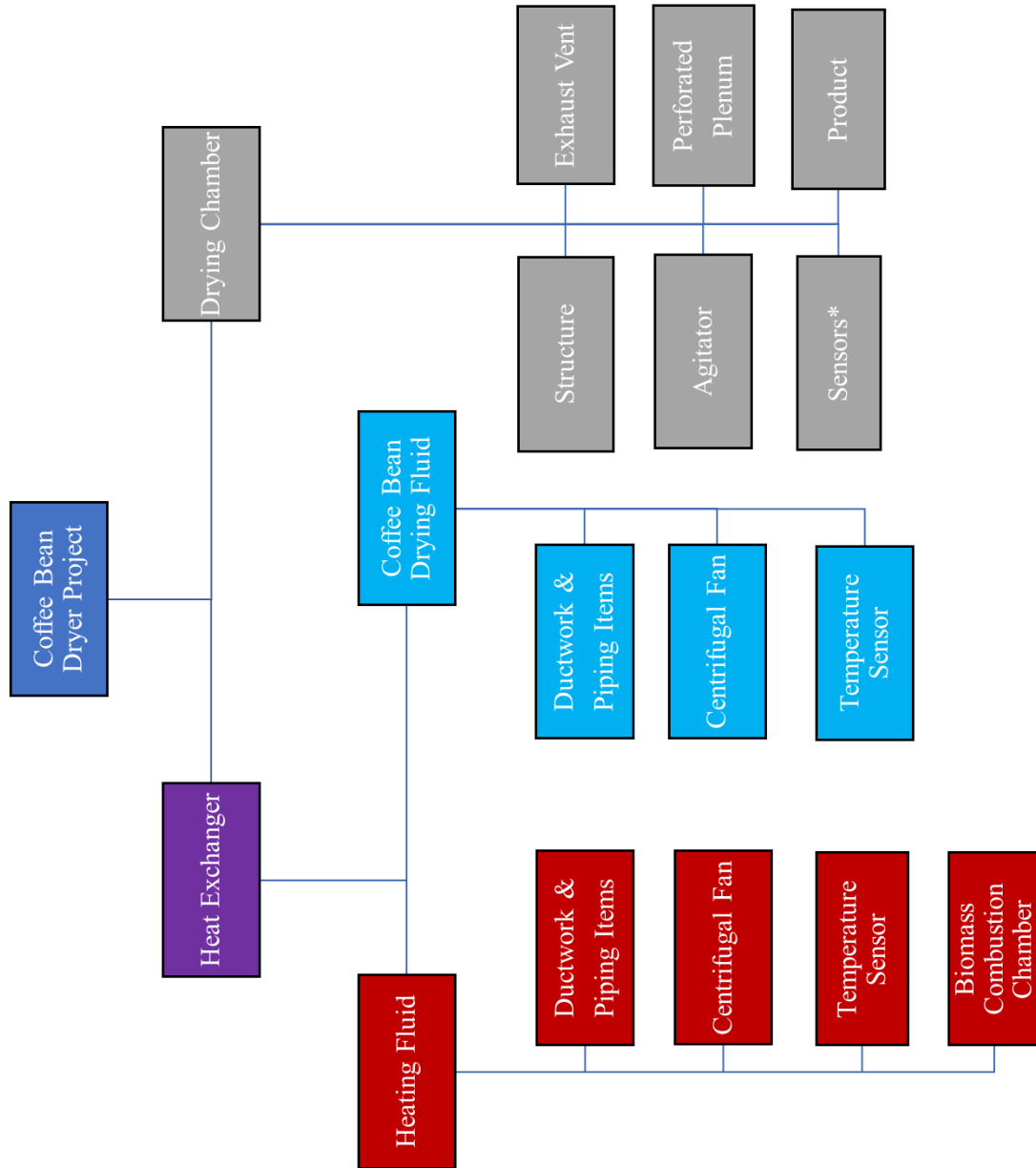


Figure 51. System Hierarchy.

B: Concept of Operations

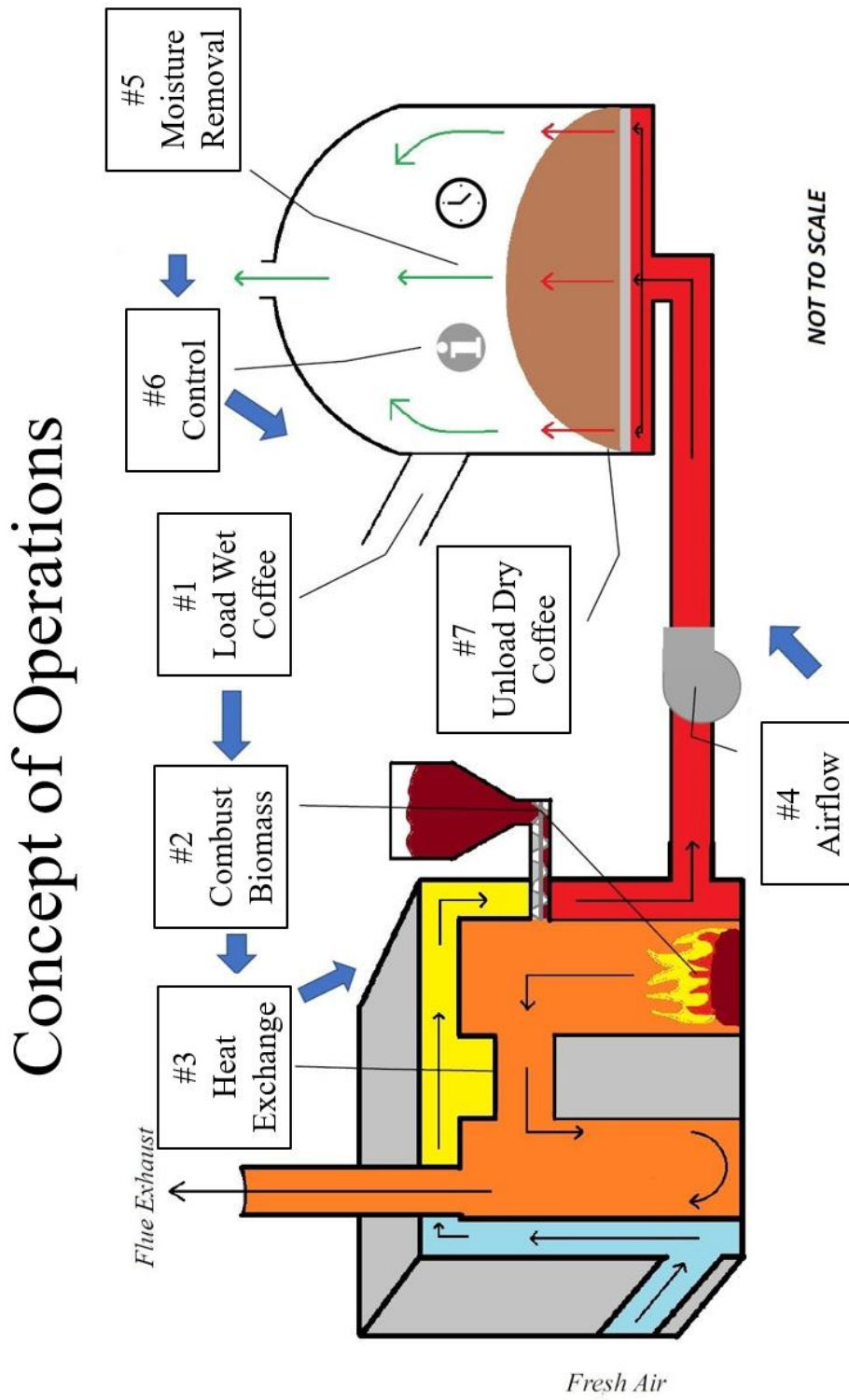


Figure 522. Concept of Operations

C: ABET Outcome 2, Design Factor Considerations

Table 11 Appendix C Design Factors Considered

Design Factor	Page number, or reason not applicable
Public health safety, and welfare	Page 36
Global	Page 24
Cultural	Page 3
Social	Page 3
Environmental	Page 24
Economic	Page 24
Ethical & Professional	While the early design phase of our project primarily focused on developing a heat exchanger for a mechanical coffee drying system, explicit ethical and professional factors were not addressed in this specific context. However, ethical considerations will be paramount in subsequent project phases, ensuring alignment with industry standards and regulations during fabrication, testing, and potential real-world applications.
Reference for Standards	Page 38

D: Project Schedule

Table 12. Design Project Schedule.

Design Project Schedule	
Task	Due Date
Spring Semester 2023	
Proposal	February 24, 2023
Begin Weekly Team Meeting	March 1, 2023
Proposal Presentation	March 13, 2023
Obtain Data from Current System	March 17, 2023
Mathematical Model/Thermal Analysis	March 31, 2023
Preliminary Design Review Presentation	April 10, 2023
Final Pre-Design Report	April 26, 2023
Fall Semester 2023	
Begin Weekly Advising	August 21, 2023
Team Review of Heat Transfer Topics and Relevant Industry Standards	August 23, 2023
Current System Analysis	August 30, 2023
Proposed System 3D Modeling	September 8, 2023
Critical Design Review	September 21, 2023
Structural Analysis	October 6, 2023
CFD and Analysis	October 20, 2023
Presentation Reviews	November 10, 2023
Draft of Report to Advisor	November 15, 2023
Final Presentation	December 1, 2023
Poster Session	December 7, 2023
Final Senior Design Report	December 8, 2023
Final Report Submitted to SOAR	December 15, 2023

E: Table of Requirements

Table 13. Table of Project Requirements.

1.) The heat exchanger fluids shall not mix.
2.) The system shall have a heat exchanger effectiveness of at least 60%.
3.) The heat exchanger shall reduce the average batch moisture content of a layer of 0.25 [m] of 1000 kg of parchment coffee to 12%.
4.) The drying air shall be heated to a temperature of 51 °C (+/- 2°C) upon exiting the heat exchanger.
5.) The heat exchanger shall not produce a shell-side pressure drop greater than 1000 [Pa].
6.) The tube-side fluid shall be of combustion gases from burning coffee husks.

F: Table of Failure Modes and Effect Analysis

Table 14. Failure Modes and Effect Analysis.

Item	Failure Mode	Cause of Failure	Possible Effects	Likelihood of Occurrence	Severity	Possible Action to Reduce Failure Effects
Heat Exchanger	Rupture (Mechanical)	Mechanical erosion, vibration, thermal/expansion fatigue. Improper use of the dryer.	Longer drying times, tainted drying air. Decreased pressures across flows.	Low	High	Maintaining proper flow velocities associated with heat exchanger materials. Isolated or attenuated from vibrational machinery. Materials must be selected to operate in drying temperatures.
Heat Exchanger	High-Pressure Difference (Design)	Impeding the flow of air through the heat exchanger.	Long dry times or insufficient drying. Decreased fan efficiency.	Medium	High	Removing heat exchanger tubes or baffles. Selecting a fan capable of overcoming pressure loss.

G: Kern's Method Flow Chart

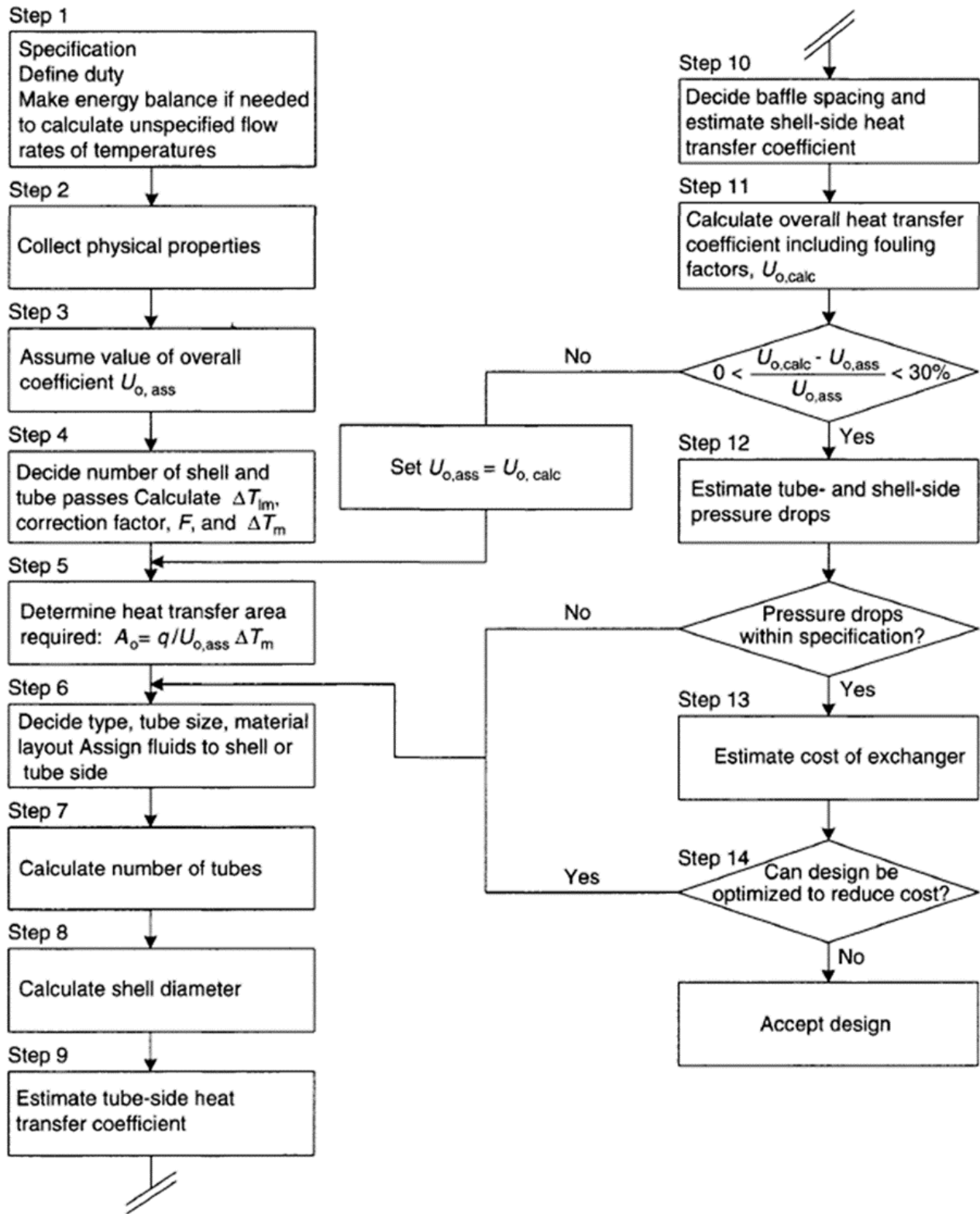



Figure 533. Kern's Method Flow Chart from Coulson's Chemical Engineering v6

H: Material Properties: Alloy 321



Alloy 321

APPLICATIONS

- Aircraft piston engine manifolds
- Expansion joints
- Thermal oxidizers
- Refinery equipment
- High temperature chemical process equipment

ABOUT ALLOY 321

Alloy 321 stainless is a titanium stabilized grade commonly used for service in the 538-870°C temperature range. For service temperatures up to about 870°C, a stabilizing treatment at 842-899°C air cool, may be used to provide optimum resistance to intergranular corrosion in the heat affected zone (HAZ), and to polythionic acid stress corrosion cracking. Alloy 321 stainless is readily welded by all common methods including submerged arc. Appropriate weld fillers are AWS ER347 bare wire and E347 covered electrodes. Alloy 321 stainless has good machinability and is readily fabricated.

MECHANICAL & PHYSICAL PROPERTIES

MECHANICAL & PHYSICAL PROPERTIES	20°C	93°C	204°C	316°C	427°C	538°C	649°C	760°C	871°C
Coefficient of Thermal Expansion, $\mu\text{m}/\text{m}^\circ\text{C}$	-	16.7	16.9	-	18	18.5	19.1	19.6	20
Thermal Conductivity/ kcal/(hr.m.°C)	-	13.1	14.4	-	17	18	-	-	-
Modulus of Elasticity, Dynamic/ $\times 10^5$ MPa	-	1.93	1.83	-	1.64	1.55	1.46	1.36	-
Ultimate Tensile Strength/ MPa	579.2	-	427.5	427.5	427.5	410.2	110.3	96.5	-
0.2% Yield Strength/ MPa	262	-	141.3	124.1	117.2	113.8	110.3	96.5	-

I: MATLAB Code for First Successful Kern's Method Iteration.

Kern's Iterative Method for the preliminary design of a S&T HXR

```

Uest = 20.8;
Dto = 50.6;
Dti = 50.6-12.7/2;
L = 2000;
pt = 1.25*Dto;

shell_clearance = 11; % Figure_ in report based on DB.
Nb = 3; % Number of time flow crosses tube bank
jn = 1.7*10^-3; % Shellside HXF Co. Based on Reo Figure _
jf = 2.5*10^-2; % Shellside pressure drop. Based on Reo Figure _
    
```

Application Parameters

```

mdotc = 1.8;
Tci = 22;
Tco = 50;
Thi = 820;
Tho = 300;
    
```

Properties evaluated at film temp $(i + o)/2$

```

filmTc = (Tco+Tci)/2;
pc = 1.145;
    
```

```

Cpc = 1007;
kc = 0.02625;
Prc = 0.727;
muc = 18.9*10^-6;

filmTh = (Tho+Thi)/2;
ph = 0.70;
Cph = 1148;
kh = 0.0548;
Prh = 0.724;
muh = 34.2*10^-6;

kt = 21.5;

```

LMTD

```

QDuty = mdotc*Cpc*(Tco-Tci);

delT1 = Thi-Tco;
delT2 = Tho-Tci;
LMTD = (delT2-delT1)/(log(delT2/delT1));
mdoth = QDuty/(Cph*(Thi-Tho));

```

Heat Exchanger Configuration

```

Aest = QDuty/(Uest*LMTD)
Dto = Dto/1000;
Dti = Dti/1000;
L = L/1000;
At = L*Dto*pi;
pt = pt/1000;

Nt = ceil(Aest/At);

```

Aest =

5.0525

Bundle Diameter from Coulson & Richardson's CHEM ENGINEERING V6

```

K1 = 0.319;
n1 = 2.142;
DB = Dto*(Nt/K1)^(1/n1)
Ds = Shell_Clearance/1000+DB;

```

DB =

0.3147

Heat Transfer Coefficient Tube Side

```
Vo1doth = mdoth/ph;  
Axt = Nt*pi/4*Dti^2;  
Vtube = Vo1doth/Axt  
Rei = ph*Vtube*Dti/muh  
  
if Rei < 3999.999  
    Nui = 1.86*(Rei*Prh*Dti/L)^0.33;  
else  
    Nui = 0.023*Rei^0.8*Prh^0.33;  
end  
  
hi = kh*Nui/Dti
```

Vtube =

4.9361

Rei =

4.4706e+03

hi =

21.3109

Heat Transfer Coefficient Shell Side

```
De = 1.10/Dto*(pt^2-0.917*Dto^2);  
BS = L/(Nb+1);  
Acf = (pt-Dto)/pt*Dc*BS;  
Vm = mdotc/Acf;  
  
Vs = Vm/pc;  
Reo = pc*Vs*De/muc  
Nuo = jn*Reo*PrC^0.33;  
ho = kc*Nuo/De
```

Reo =

1.0505e+05

ho =

117.4414

Overall Heat Transfer U

```
hof = 10000;  
hif = 5000;  
  
Uinv = ho^-1 + hof^-1 + (Dto*log(Dto/Dti)/(2*kt)) + (Dto/Dti*1/hif) + (Dto/Dti*1/hi);  
  
Ucalc = Uinv^-1  
  
Upcdiff = abs(Uest-Ucalc)/Ucalc*100
```

Ucalc =

15.9593

Upcdiff =

30.3319

Pressure Drop in Shell

```
delPs = 8*jf*(Ds/De)*(L/BS)*(pc*Vs^2)/2
```

delPs =

9.6713e+03

Published with MATLAB® R2023a

J: MATLAB Code for Validation Study (e-NTU Method)

Validation Study Set-Up of a Parallel Flow Annulus

```
ms = 0.01;  
simTsout = 45.129;  
  
Tsin = 14;  
cps = 1005;  
  
mt=0.1;  
Ttin = 75;  
cpt= 4194;
```

```

Dis = 0.064;
Dit = 0.038;
tt = 0.005;
Dot = 2*tt+Dit;
L = 1.5;

kss = 16.3;
kh2o = 0.663;
kair = 0.0267;
ph2o = 974.8;
uh2o = 0.0003765;
Prt = 6.904;

pair = 1.164;
uair = 1.872*10^-5;
Prs = 0.728;

Cs = ms*cps;
Ct = mt*cpt;

Cmin = min(Cs,Ct);
Cmax = max(Cs,Ct);

Qmax = Cmin*(Ttin-Tsin);

Vt = 4*mt/(pi*Dit^2*ph2o);
Ret = ph2o*Vt*Dit/uh2o;
ft = (0.79*log(Ret)-1.64)^-2;
Nut = ((ft/8)*(Ret-1000)*Prt)/(1+12.7*(ft/8)^(0.5)*(Prt^(2/3)-1));
hi = kh2o*Nut/Dit;

Vs = 4*ms/(pi*pair*(Dis^2-Dot^2));
Res = pair*Vs*(Dis-Dot)/uair;
fs = (0.79*log(Res)-1.64)^-2;
if Res < 1200
    Nus = 5.3;
elseif 1200<Res && Res<3000
    Nus = 0.26*Res^0.5*Prs^0.37; % Zukauskas flow over cylinder
else
    Nus = ((fs/8)*(Res-1000)*Prs)/(1+12.7*(fs/8)^(0.5)*(Prs^(2/3)-1));
end
ho = kair*Nus/(Dis-Dot);

R = 1/(pi*L)*(1/(hi*Dit)+log(Dot/Dit)/(2*kss)+1/(ho*Dot));
UA = 1/R;

NTU = UA/Cmin;
CR = Cmin/Cmax;

e = (1-exp(-NTU*(1+CR)))/(1+CR);

simTtout = 74.1;

```



```
Q = e*Qmax;

Ttout = Ttin - Q/(mt*cpt);

Tsout = Q/(ms*cps)+Tsin

PErrorts = (abs(Ttout-simTtout)/Ttout)*100;
PErrorss = (abs(Tsout-simTsout)/Tsout)*100

esim = (simTsout-Tsin)/(Ttin-Tsin);

PErrore = (abs(e-esim)/e)*100;
```

Tsout =

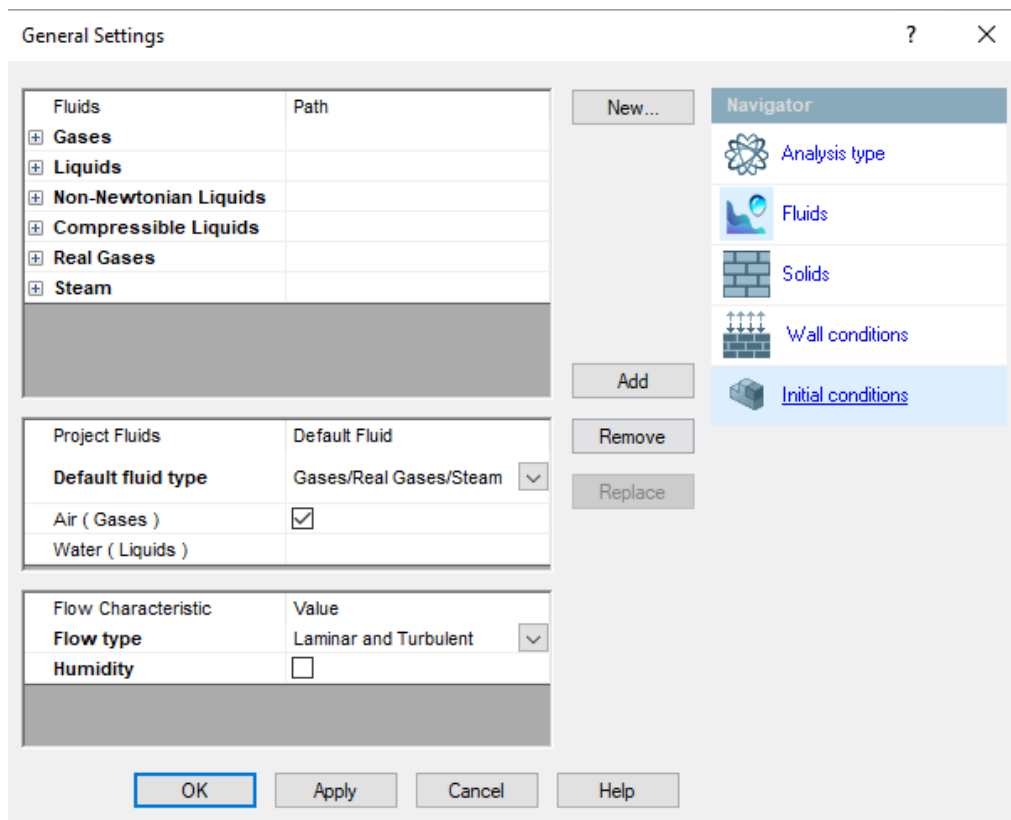
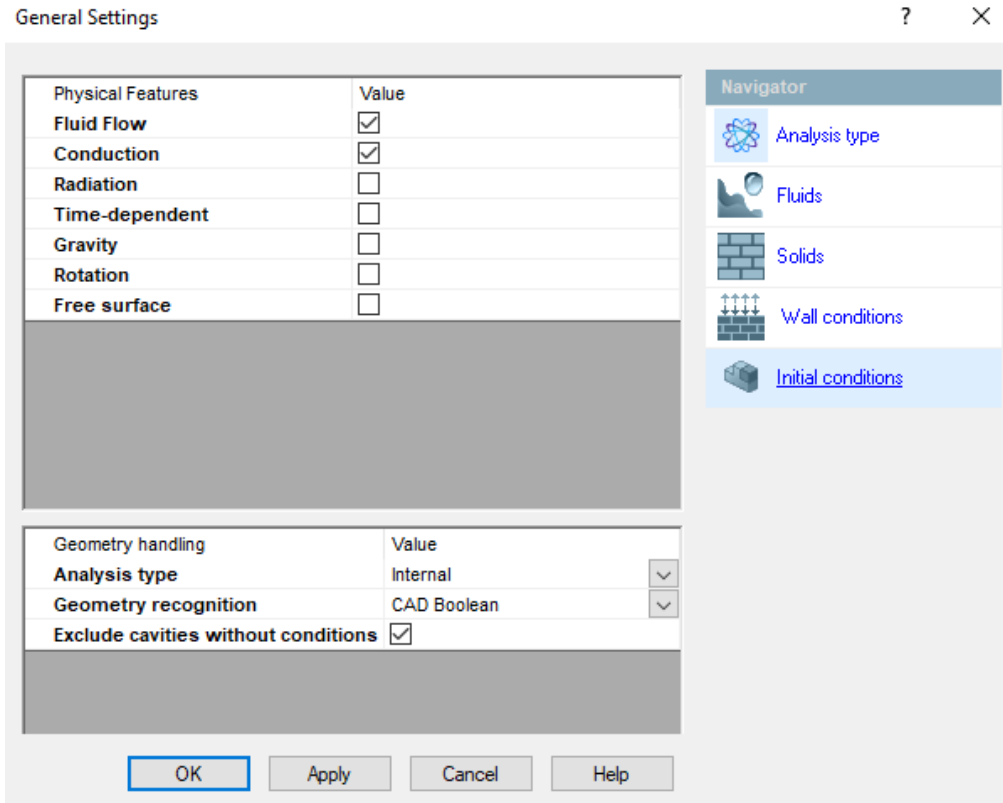
45.1052

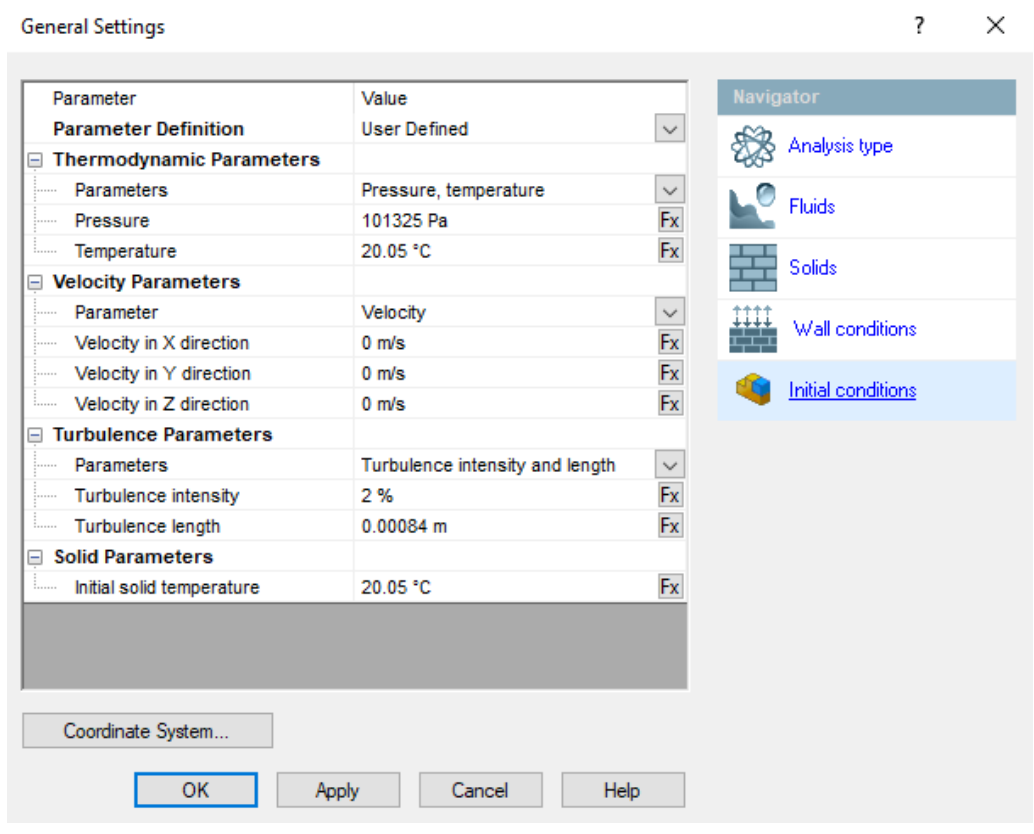
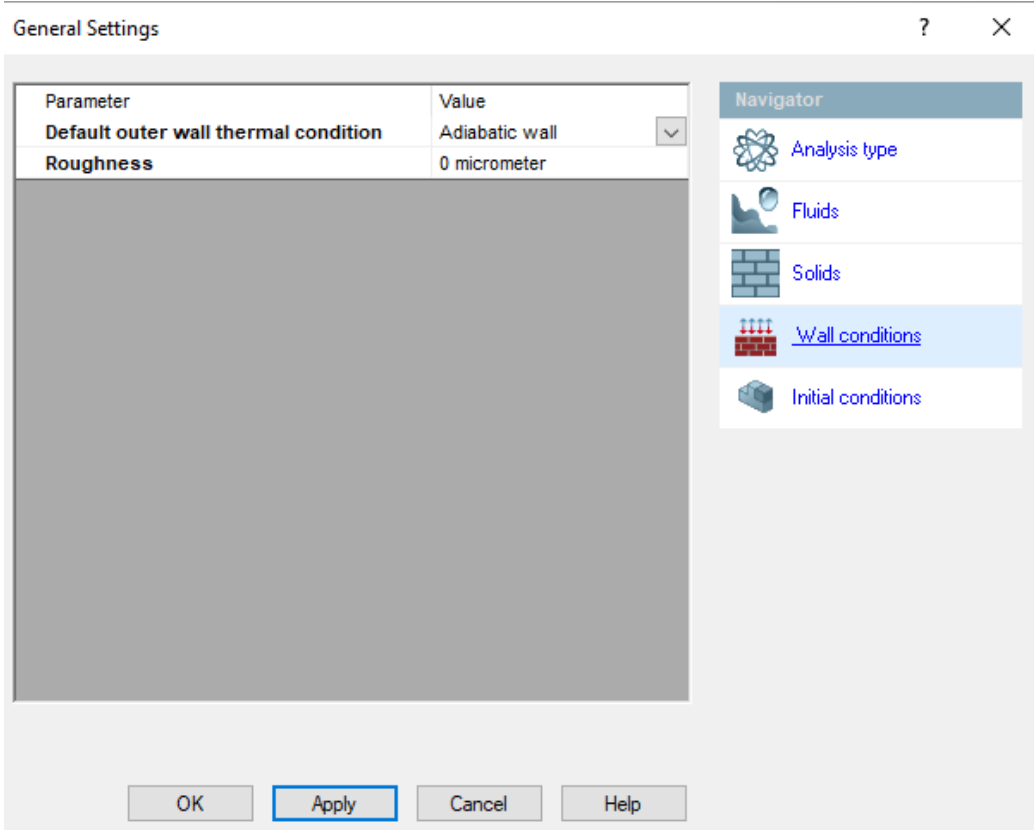
PErrorss =

0.0527

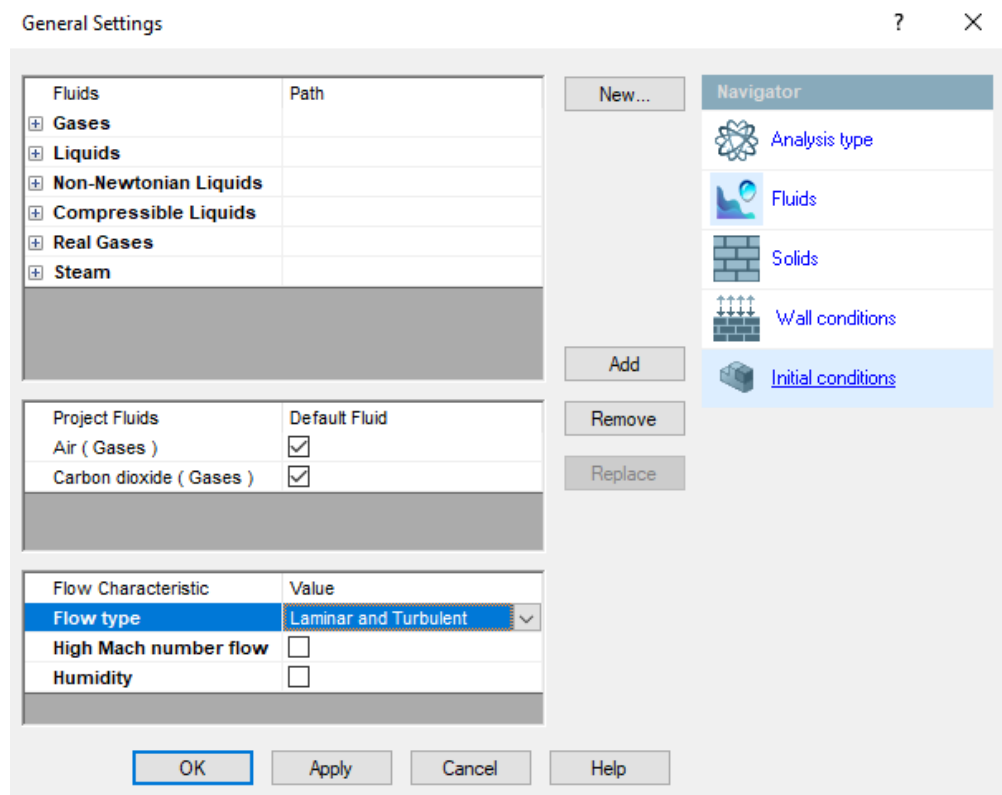
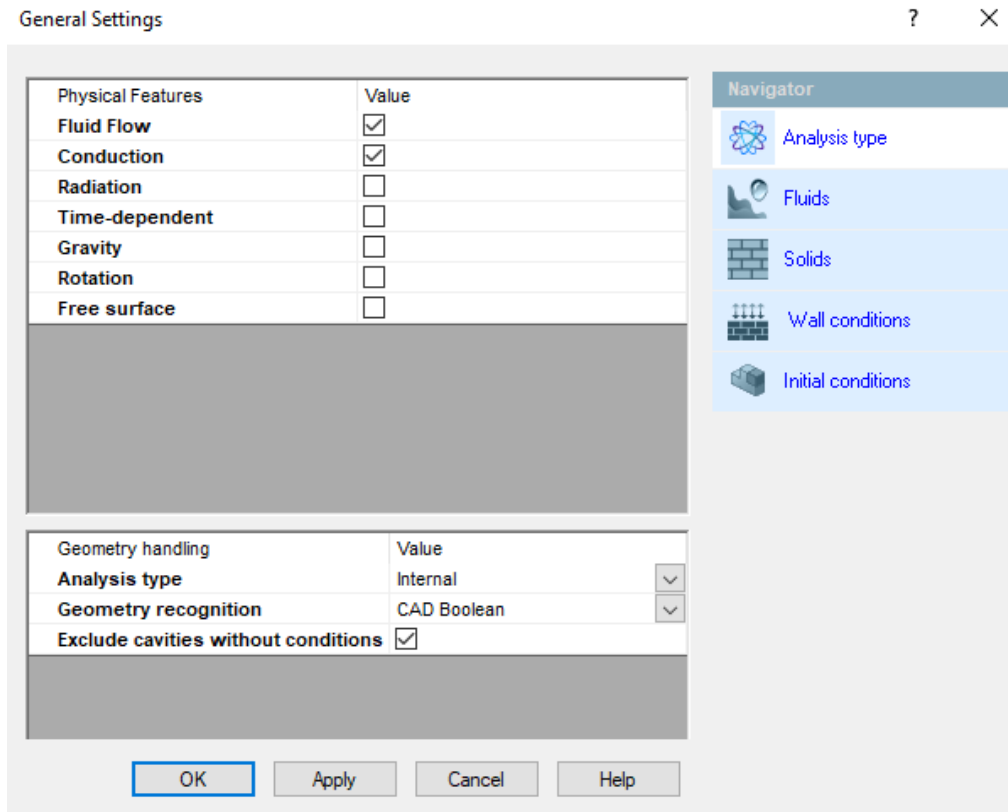
Published with MATLAB® R2023a

K: SolidWorks Flow Simulation Setup for the Validation Study





L: SolidWorks Flow Simulation Setup for the Final Design



General Settings

?

×

Solids	Path
Steel (Electrical Resistance)	Pre-Defined\Alloys
Steel (Mild)	Pre-Defined\Alloys
Steel 5135	Pre-Defined\Alloys
Steel 616	Pre-Defined\Alloys
Steel 9260	Pre-Defined\Alloys
Steel S63198	Pre-Defined\Alloys
Steel Stainless 302	Pre-Defined\Alloys
Steel Stainless 321	Pre-Defined\Alloys
Building Materials	
Ceramics	
Glasses and Minerals	
IC Packages	
Interface Materials	
Laminates	
Metals	
Non-isotropic	
Polymers	
Semiconductors	

Default solid:

Buttons: OK, Apply, Cancel, Help

Navigator

- Analysis type
- Fluids
- Solids**
- Wall conditions
- Initial conditions

General Settings

?

×

Parameter	Value
Default outer wall thermal condition	Adiabatic wall
Roughness	0 micrometer

Buttons: OK, Apply, Cancel, Help

Navigator

- Analysis type
- Fluids
- Solids**
- Wall conditions
- Initial conditions

General Settings






? X

Parameter	Value	
Parameter Definition	User Defined	▼
Thermodynamic Parameters		
Parameters	Pressure, temperature	▼
Pressure	101325 Pa	Fx
Temperature	20.05 °C	Fx
Velocity Parameters		
Parameter	Velocity	▼
Velocity in X direction	0 m/s	Fx
Velocity in Y direction	0 m/s	Fx
Velocity in Z direction	0 m/s	Fx
Turbulence Parameters		
Parameters	Turbulence intensity and length	▼
Turbulence intensity	10 %	Fx
Turbulence length	0.003357 m	Fx
Concentrations		
Solid Parameters		
Initial solid temperature	20.05 °C	Fx

Coordinate System...

OK Apply Cancel Help

Navigator

-  Analysis type
-  Fluids
-  Solids
-  Wall conditions
-  Initial conditions